A 300 FOOT HIGH-PRECISION RADIO TELESCOPE

Volume I

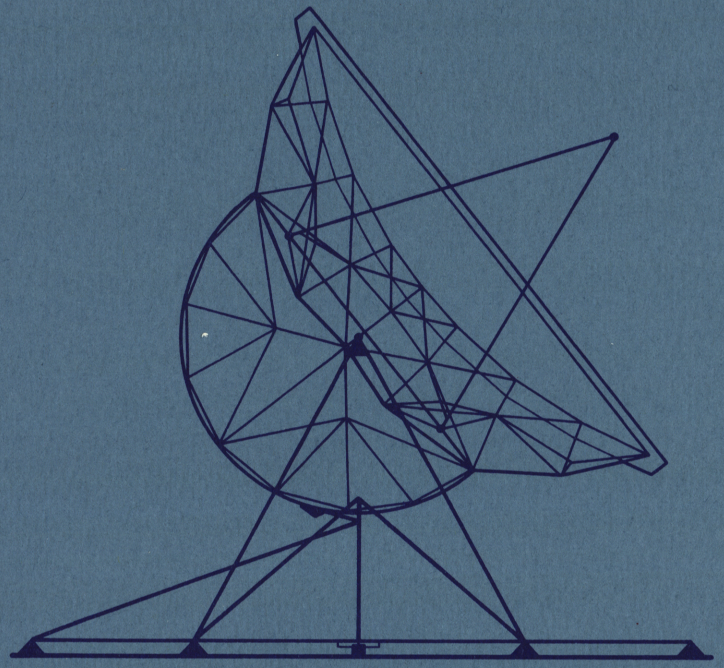

May, 1969

National Radio Astronomy Observatory *
Green Bank, West Virginia

* OPERATED BY ASSOCIATED UNIVERSITIES, INC., UNDER CONTRACT WITH THE NATIONAL SCIENCE FOUNDATION.

Contents

VOLUME I

Chapters 1 - 7

Chapter 1

INTRODUCTION

The need for large fully-steerable radio telescopes has been recognized and generally agreed for many years. A plan by which such instruments might be built was set out in the report of the Whitford Committee (Ref. 1-1). That plan called for the development of two regional instruments, each of about 100 m in size, and the study of the feasibility of constructing a very large telescope.

A part of the NRAO effort to study the largest feasible telescope led to an investigation of the behavior of structures deflecting under gravitational forces, and the design principles used in the presently described 300-ft telescope emerged from these studies.

There are several general parameters which determine the usefulness and applicability of a radio telescope for scientific research.

(1) The telescope should have as large a collecting area as possible so that faint sources may be studied.

(2) The angular resolution should be high so that details of the source structure may be derived.

(3) The telescope should operate efficiently at short wavelengths so that source spectra may be extended and spectral lines occurring at short wavelengths may be studied.

(4) The telescope should have extensive sky coverage so that it may be used efficiently and allow observations of all sources that appear above the horizon.

(5) The tracking capabilities should permit long integration times and also make it possible to study time varying phenomena.

(6) The instrument should be easily adaptable for use at different frequencies and in various modes of operation.

A large, fully steerable parabolic reflector represents an attractive combination of the requirements listed above, and for this reason it has become the basic general purpose instrument in radio astronomy. As new and improved structural and mechanical design methods have been developed, steerable parabolic reflectors have grown in size, improving the sensitivity and resolving power of the telescopes. Whereas only 15 years ago reflectors with diameters of 25 m to 30 m (82 ft to 100 ft) were considered "large", several telescopes with more than twice the diameter are in use today. A 100 m (330-ft) telescope is under construction in Germany, and a 135 m (440-ft) instrument is in the planning stage in the U.S.

The size of a radio telescope is, however, not the only measure of high performance as a scientific instrument, although this assumption is often made. A larger diameter telescope does not necessarily imply better scientific usefulness unless the high frequency limit, which is determined by structural deflections, is improved, or at least retained. The frequencies above 1400 MHz have become more and more important in observational radio astronomy, and it is clear that it is in this region of the electromagnetic spectrum where many of the exciting and rewarding discoveries will be made in the future. Therefore, high-frequency performance should be given high priority in the design of large, general purpose instruments for radio astronomy.

The high-frequency performance of a radio telescope is limited almost entirely by deflections of the telescope structure and the accuracy of its drive system. There are several distinct, although not necessarily independent, limits of the structural performance.

(1) Gravitational deformation of the reflecting surface from its parabolic form when the telescope is moved.

(2) Thermal deflections caused by temperature differences of various parts of the structure.

(3) Wind deflections.

(4) The achievement of tight tolerances in manufacturing or adjustment of the telescope components.

(5) The stress limit when the structure becomes so large that it is not able to support itself in a normal environment.

The implications of some of these limits are illustrated in Fig. 1-1, which shows the relation between the diameter of a radio telescope and the rms surface deviations (or shortest useful wavelength defined here as λ_o = 16 rms). Three structural limits are shown on the graph, together with the performance of several existing and planned radio telescopes. It is clear that a major advance in telescope capabilities could be achieved if the gravitational limit could be eliminated. This is quite possible by designing a structure which retains a parabolic reflecting surface when

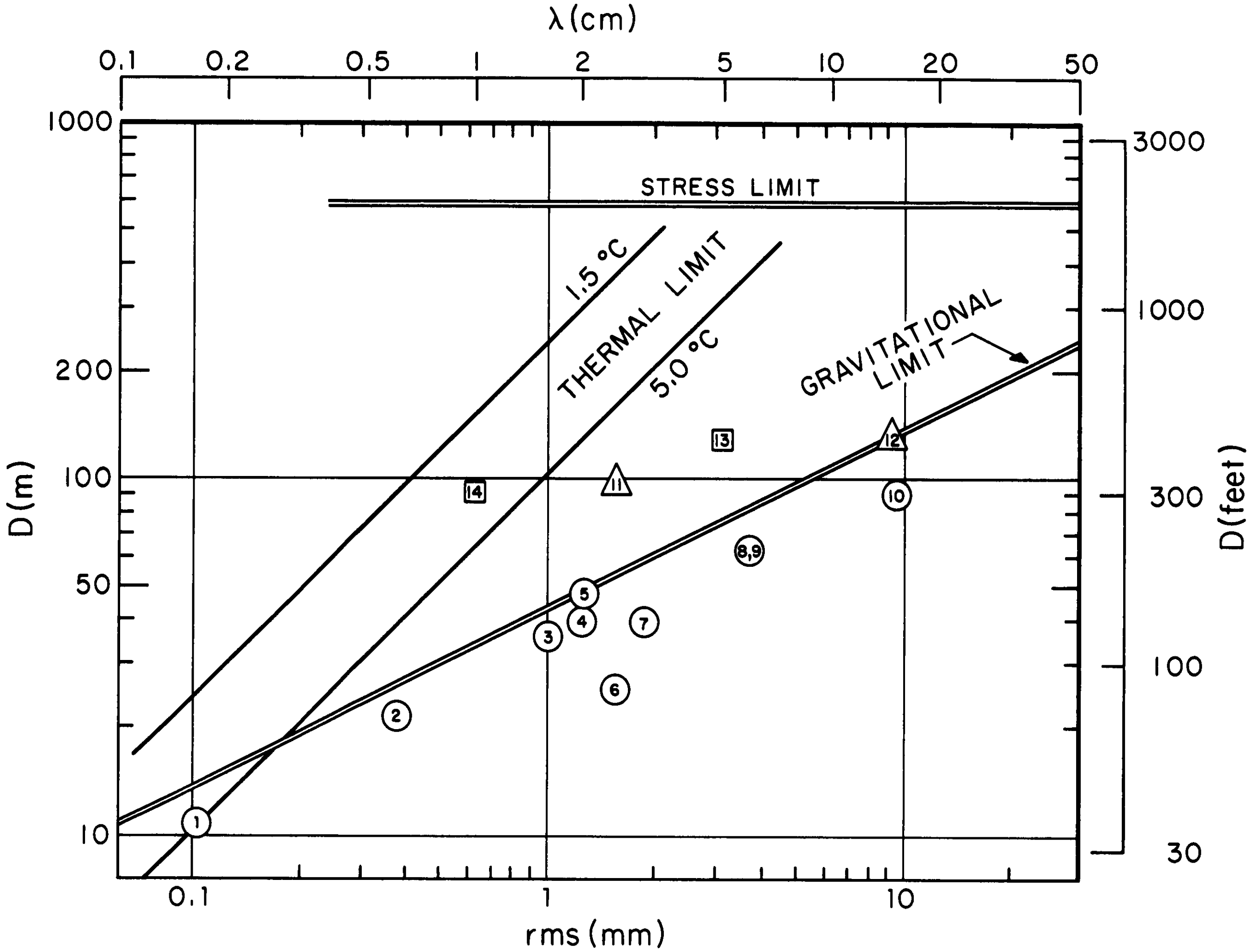

Fig. 1-1. Diameter D and shortest wavelength λ. Three natural limits for tiltable, conventional telescopes.

Existing ○
1. 36-ft, NRAO Kitt Peak
2. 22-m, Lebedev, Serpukhof
3. 120-ft, MIT, Haystack
4. 140-ft, NRAO, Green Bank
5. 150-ft, ARO, Canada
6. Various 85-ft telescopes
7. 130-ft, Owens Valley
8. 210-ft, Parkes, Australia
9. 210-ft, JPL, Goldstone
10. 300-ft, NRAO, Green Bank

Within 1-2 Years △
11. 100-m, Bonn, Germany
12. 450-ft, Jodrell Bank

In Preparation □
13. 440-ft, CAMROC
14. 300-ft, Homologous Design

moved with respect to the gravitational field. The focal length of the paraboloid is allowed to change and its axis need not follow exactly the movement of the reflector support structure. A structural deflection of this type is called homologous deflection, and it is the basis for the telescope design described in this report. This report gives evidence to show that a 91.4 m (300-ft) telescope can be built with an rms surface deviation of 0.7 mm-1.0 mm (depending on thermal conditions), corresponding to a shortest operational wavelength of 1.1 cm to 1.6 cm. The cost for the telescope would be approximately $8 million.

The homology principle and its application to large, high-precision telescope structures are described in detail in Chapters 2 and 3 of this report.

A high-precision telescope of this size will be an instrument capable of very high resolving power. At its shortest usable wavelength the beam width will be of the order of 30 arc sec, and in order to help achieve adequate telescope pointing accuracy, the design includes an optical reference platform which eliminates inaccuracies in the determination of the telescope position caused by the supporting structure.

In Chapter 4 of this report a practical design, including the optical platform, is presented.

The expected performance of the telescope is given in Chapter 5. In Chapter 6 detailed cost figures and schedules are given.

The application of the homology principle is in no way limited to telescopes of the general size and performance described here. By utilization of homologous deflections, it seems both possible and practical to design and construct much larger precision instruments, up to 250 m (800 ft) diameter or more. A scaling of cost and performance of the present design to other diameters is developed and described in Chapter 7.

Appendix 1 to this report contains a collection of design notes and memoranda written during several years of design work, and Appendix 2 contains engineering reports of telescope details made by an outside engineering company.

The specific uses of the telescope, were it in operation today, would include studies of known spectral lines, searches for lines presently unknown, pulsar observations, maps of continuum sources, planetary studies, source counts, etc. These are some of the active areas of today's radio astronomical research where the need for a large, short wavelength instrument is vital.

Future tasks for such a telescope can also be given in broad outline, but experience has shown that such an outline would be incomplete. The growth of this branch of astronomy is so rapid that new discoveries are sure to alter today's views and research emphasis. It is of interest to note that the NRAO 140-ft telescope, which was conceived in the middle fifties and completed in the middle sixties, has made several fundamental contributions to radio astronomy. Some examples of exciting and rewarding discoveries which were made possible with this telescope, and which were totally unanticipated at the time of the design and construction of the instrument, are the detection of excited hydrogen spectral lines, the observation of the galactic magnetic field by the observation of the Zeeman splitting of spectral lines, and the recent detection of the formaldehyde molecule.

The comparative infancy of radio astronomy, our limited understanding of the universe, and, as experience has shown, our "a priori" limited imagination regarding the contents of the universe insure immense dividends from major telescope developments. It is believed that the large, high-precision homologous radio telescope described in this report is such a major development which promises to play a vitally important role in future research in radio astronomy.

REFERENCES

1-1 Whitford Committee, 1964. Report of the Panel on Astronomical Facilities of the National Academy of Sciences' Committee on Science and Public Policy, "Ground-Based Astronomy, a Ten Year Program", National Academy of Sciences, National Research Council, Washington, D. C.

Chapter 2

THE HOMOLOGY PRINCIPLE

A. Homologous Deformations

If a telescope is tilted in elevation, it must deform under its own weight, and this deformation sets a lower limit to the shortest observational wavelength, see Fig. 2-1 and Ref. 2-1. For a conventionally designed 300-ft telescope this "gravitational limit" is about $\lambda_o = 8$ cm. For other diameters, $\lambda_o \sim D^2$. There are three possible ways to overcome this limit.

(1) Servo control of the surface panels, as it was planned for the 600-ft telescope at Sugar Grove.

(2) Surface floating on a system of levers and counterweights, as used with large optical telescopes.

(3) Design of a structure that deforms completely unhindered if tilted, but that has a surface that deforms from one paraboloid of revolution into another, thus yielding an exactly focussing mirror for any angle of tilt. This deformation is termed "homologous" since it deforms one member of a family of surfaces into another member of the same family.

The principle underlying homologous deformations is not new. Several telescopes have been designed with the specification that the rms deformations should be below a certain value; but after the telescopes were built and used, it turned out that their performance exceeded their specifications. Only the deviations of the surface from a best-fit paraboloid of revolution are significant, and these deviations are always less than the structural deformations, since any least-squares fit must diminish the residuals (Refs. 2-1, 2-2, and 2-3).

The task of making the deformations of a telescope more and more homologous can be attacked with a trial-and-error method by gradually changing and improving a design, and good results can be achieved this way (Refs. 2-4 and 2-5). A better approach is to find a rigorous mathematical method for obtaining exact homology solutions within one or two hours on a computer (Refs. 2-3 and 2-4).

The parameters defining the deformation from one paraboloid to the other, such as parallel translations, change of focal length and change of

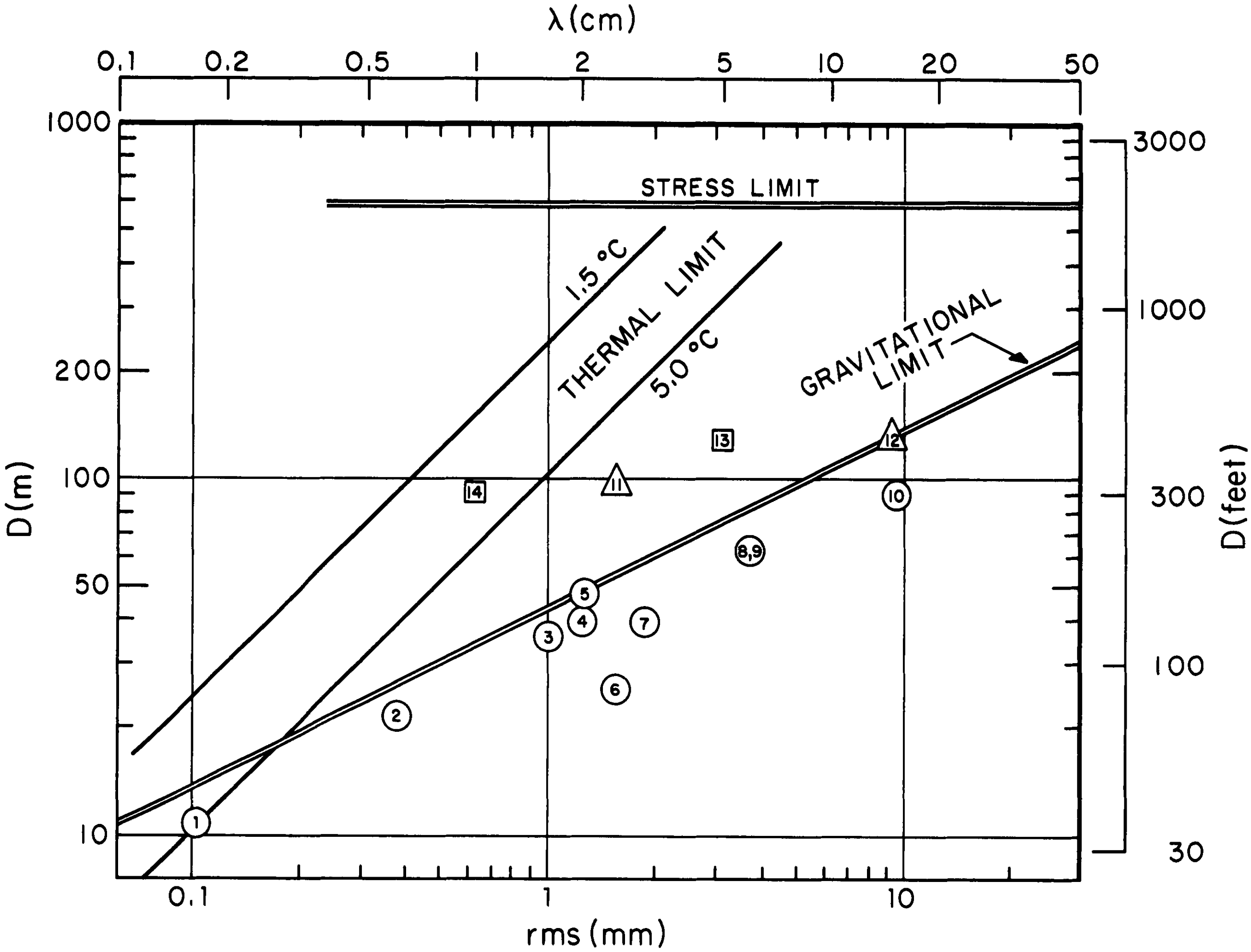

Fig. 2-1. Diameter D and shortest wavelength λ. Three natural limits for tiltable, conventional telescopes.

<u>Existing</u> ○

1. 36-ft, NRAO Kitt Peak
2. 22-m, Lebedev, Serpukhof
3. 120-ft, MIT, Haystack
4. 140-ft, NRAO, Green Bank
5. 150-ft, ARO, Canada
6. Various 85-ft telescopes
7. 130-ft, Owens Valley
8. 210-ft, Parkes, Australia
9. 210-ft, JPL, Goldstone
10. 300-ft, NRAO, Green Bank

<u>Within 1-2 Years</u> △

11. 100-m, Bonn, Germany
12. 450-ft, Jodrell Bank

<u>In Preparation</u> □

13. 440-ft, CAMROC
14. 300-ft, Homologous Design

axial direction, are called "homology parameters." With regard to observations, these changes are not germaine; all existing tiltable telescopes show changes of this kind, and most telescopes incorporate the means to correct for them (e.g., a focal adjustment).

If a telescope is to be designed to have homologous deformations, the design must have four different types of degrees of freedom: (1) the geometrical shape of the structure (coordinates of all joints); (2) the topological description (i.e., specification of the joints that are connected by members, points that are considered surface points, and points at which the structure is held); (3) the cross sections (bar areas) of all members; and (4) the homology parameters. The method solves simultaneously for cross sections and homology parameters, but considers the geometry and topology to be given quantities.

There is a mathematical solution for the homology problem. It has been shown (Refs. 2-2 and 2-3) that homology exists in all elevation angles of the telescope if homology exists in two elevation angles (e.g., at the zenith and at the horizon). Also, homology can be demanded for a finite but otherwise unlimited number of surface points N. Since a paraboloid of revolution is defined by six parameters, there are 2(N-6) conditions to be fulfilled in order to achieve a homology solution. On the other hand, an unconstrained structure with N structural points requires at least 3(N-2) members to maintain its stability. Therefore, a stable homologous structure will have $3(N-2)-2(N-6) = N + 6$ degrees of freedom. Since N is always a positive number, N + 6 is always greater than 0. This means there are more degrees of freedom than conditions to be fulfilled, and a solution must indeed exist.

However, this proof of existence is true for "mathematical solutions", whereas a "physical solution" must demand that all bar areas be positive ($A > 0$) and a "practical solution" finally requires that all areas be above a given minimum, $A \geq A_{sv}$, defined by stability against survival conditions. Although any structure with given geometry must have mathematical solutions, many structures will not have practical solutions, and changes of the geometry will be needed.

For practical applications, the number N of homologous surface points must be large enough so that the deformation of the surface between neighboring points can be tolerated. The larger N, the thinner the surface panels can be.

Three items reduce the final accuracy of a homologous telescope. First, the bar areas should be commercially available. Second, even if the influence of gravity is eliminated by homologous deformations, wind forces still deform the telescope. Third, thermal deformations occur during sunshine, and to a lesser degree also at night from changes in the ambient temperature.

B. The Method

The conditions of homologous deformations lead to algebraic equations of very high order. A direct solution seems impossible, and a linearized iterative method was chosen. One starts with a "first guess" (initial value) for all bar areas, and in each iteration step all bar areas are changed simultaneously in such a way that the deviations of the surface from a best-fit paraboloid of revolution become zero. Since there is a linearized method for a nonlinear task, several iteration steps are required to achieve a given accuracy. To make the task uniquely defined, the method selects (out of all possible homology solutions) that solution which is most similar to the first guess, assuming the first guess to be the most desirable structure, and stable against survival. If wanted, it selects a solution where the homology parameters are as small as possible.

Newton's method is used for finding the zero point of a given function, generalized to n variables (n = number of structural bars plus homology parameters). The function whose zero is wanted is ΔH, the rms deviation of N structural surface points from the best-fit paraboloid of revolution, for both zenith and horizon position. Newton's method then needs the derivatives of ΔH with respect to all bar areas, $\partial(\Delta H)/\partial A$. Generally, the deformation Δx are found from the forces F with the help of the inverse, K^{-1}, of the stiffness matrix, K, as

$$\Delta x = K^{-1} F \,, \tag{2-1}$$

and what is needed for obtaining $\partial(\Delta H)/\partial A$ is the derivative of the inverse stiffness matrix with respect to all bar areas, $T = \partial K^{-1}/\partial A$, which is a tensor of three dimensions and can be obtained as

$$T = \partial K^{-1}/\partial A = -K^{-1}(\partial K/\partial A)K^{-1} \tag{2-2}$$

from the derivatives of the stiffness matrix, $\partial K/\partial A$, again a tensor of three dimensions.

The method of homologous deformations can be applied to all engineering tasks where the deformations themselves do not matter as long as they fulfill certain conditions of similarity. Let a structure be given of a fixed geometry, with p pin joints and m members. Certain deformations Δx_w should fulfill a set of c linear equations:

$$G\ \Delta x_w = g\ . \tag{2-3}$$

These are the "homology conditions." A set of present bar areas A_p gives deformations Δx_p, yielding residuals r according to the relation

$$G\ \Delta x_p - g = r\ . \tag{2-4}$$

The set of area changes dA, needed for changing the present Δx_p into the wanted Δx_w, is given by Newton's method as

$$\frac{\partial(\Delta x)}{\partial A}\ dA = \Delta x_w - \Delta x_p\ . \tag{2-5}$$

Multiplication by G, and the application of eqs. (2-1) and (2-2) then finally yield

$$C\ dA = -r\ , \tag{2-6}$$

where C, to be called the "homology matrix", is defined as

$$C = G\ \{K^{-1}\frac{\partial F}{\partial A} - T\}\ . \tag{2-7}$$

Equation (2-6) contains more unknowns than equation, and an additional condition is needed for defining a unique solution. The present method selects that solution which is most similar to the first guess, demanding that

$$\Sigma(dA/A)^2 = \text{minimum}. \tag{2-8}$$

The combined task of achieving homology according to eq. (2-6) and fulfilling the additional demand (2-8) is solved by the method of Lagrangian multipliers. Since a simultaneous solution of all n variables is wanted, a set of n linear equations must be solved in each iteration step.

What makes this method relatively easy is the fact that the tensor $\partial K/\partial A$ does not depend on the bar areas A; for a given geometry, all elements of $\partial K/\partial A$, and also those of $\partial F/\partial A$, are simple geometrical terms. Furthermore, there is no requirement of large computer storage for tensor $\partial K/\partial A$ or tensor T; their elements are calculated whenever needed.

The method is described in detail in Refs. 2-2 and 2-3. The application to simple telescope structures (N = 9 to 13) gave usually a fast convergence (ΔH decreasing by a factor of 3 or more for each iteration step). The final accuracy depends only on the calculating accuracy of the computer and was $\Delta H = 10^{-4}$ to 10^{-5} in for 300-ft diameter telescopes, and converges only to such solutions where each bar has at least a minimum bar area needed for survival conditions. If no such solution exists, the program prints enough information for finding out which geometrical changes might be necessary for obtaining convergence, or which bars should be omitted. Only one quadrant of an x-y symmetrical structure needs to be calculated.

With the present program it is possible to investigate structures with up to N = 57 equally-spaced homologous points on the total surface, with $p \leq 60$ structural joints and $m \leq 190$ members in one telescope quadrant. On an IBM 360/50 computer, the complete analysis of the original structure takes 20 minutes, and each iteration step takes 80 minutes. Auxiliary programs check the clearance between any two members as well as the angle separating two members at a common joint. Whereas simple structures usually converge on the first try, complicated ones depend much more on the geometry and need many initial tries until convergence occurs.

The survival conditions are 20 lb/ft^2 of snow or ice, or an 85 mph wind (one chance in 100 years) in stow position, with a safety factor of 1.92 below the yield point. The highest wind during observation was chosen as 18 mph (which permits observations at least 75% of the time), where the program calculates the average surface deformation from design (no best-fit used). The homology iterations are stopped when $\Delta H \leq 0.005$ in is reached.

The present structure was iterated to $\Delta H + 0.003$ in. Replacing all calculated bar areas by commercially available pipes from the Steel Manual increased it to $\Delta H = 0.015$ in. The axial and lateral displacements of the focus are about one inch.

REFERENCES

2-1 von Hoerner, S. 1967, "The Design of Large Steerable Antennas," A.J., 72, 35.

2-2 von Hoerner, S. 1967, "Homologous Deformations of Tiltable Telescopes," J. of Structural Division, ASCE, 93, 461.

2-3 von Hoerner, S. 1965, "Calculating Method for Homology Solutions of Telescope Structures," NRAO Report No. 4 (Appendix 1 of this report).

2-4 Rohlfs, K. 1966, "Das Bonner 90 m Radioskop", Sterne and Weltraum, 5, Mannheim, Germany.

2-5 Hachenberg, O. 1968, "Studiem zur Konstruktion des 100-m Teleskops", Beitrage zur Radioastronomie, 1, Bonn, Germany.

Chapter 3

THE TELESCOPE CONCEPT

The telescope employs four unconventional principles: First, homologous deformations as described in the previous section, which practically eliminate the influence of gravity without any extra cost. Second, an optical position reference system that measures the telescope position without any need for accurate foundations and a heavy support structure; it improves the wind-induced as well as the thermal pointing errors by large factors. Third, the surface skin is divided into many small adjustable flat plates, thus removing the accuracy requirement from the manufacturing process to the telescope adjustment process. Fourth, the application of highly automated manufacturing methods is suggested for all structural elements and the surface plates.

A. The Overall Design

The telescope has an altitude-azimuth mount. The dish is held with two elevation bearings on top of two towers, which are moved in azimuth on wheels on a large azimuth track on the ground. The azimuth drive is done with friction wheels.

The dish itself is attached to the elevation bearings by 6 suspension members. The back-up structure of the dish contains a large elevation wheel with bull gear; the elevation drive is mounted, flexible in height, at the center of the supporting structure. A strong pintle bearing on the ground, at the center of the ring, takes up one-third of the vertical dead loads, and all of the horizontal wind forces.

The dish structure (see Fig. 3-1) is divided by "surfaces" into "layers". Between the joints of the reflector surface and those of the sub-surface are the members of Layer 1. Layer 2 lies between the sub-surface and the structure. The octagon is connected to the "antifocus" by the cone members. The fundamental structure of the dish is an octahedron, built from the four feed support legs, the basic square, and four of the eight cone members. Two of the remaining cone members are split-up and broadened in such a way that their outermost chords provide the elevation sheel.

The two towers are tetrahedrons (see Fig. 3-2). Two legs of each tower go down to the azimuth ring and the third leg goes to the central

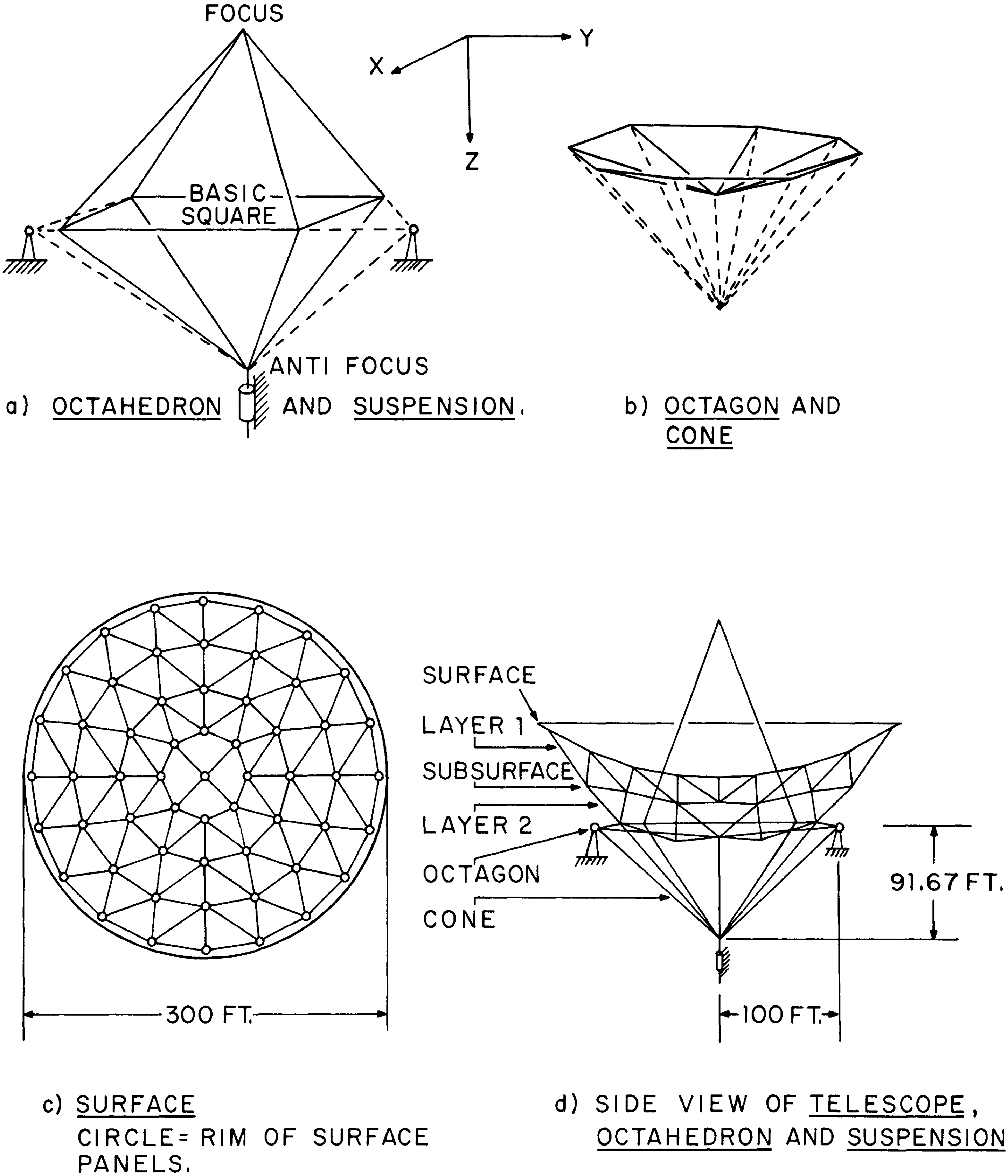

Fig. 3-1. Geometry of the dish structure. The basic structure is an octahedron, held by a suspension from two elevation bearings mounted on top of two towers. This structure has 57 homologous surface points, a total of 149 joints and 646 members.

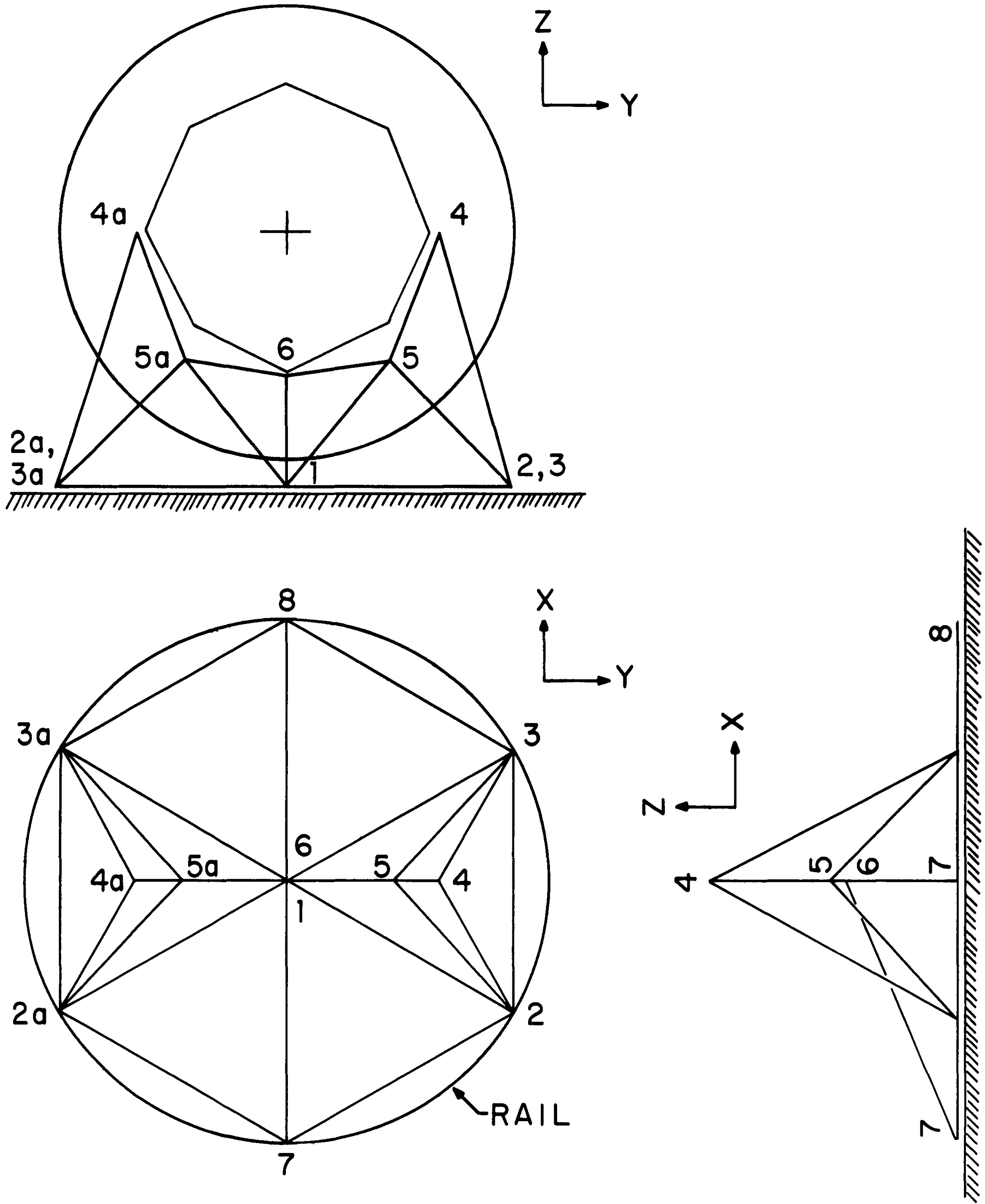

Fig. 3-2. Azimuth towers. Point 1 is a strong pintle bearing, taking up one-third of the total weight, and all horizontal wind forces. The elevation drive is at point 6, the elevation bearings at 4 and 4a. Points 2, 2a, 3, 3a, 7, and 8 drive on track assemblies on a circular track; 2, 2a, 3, and 3a have drive units with friction wheels.

pintle bearing (point 1). This third leg needs a slight bend (point 5) that gives clearance for the dish structure in the horizon or service position. The stiffness of point 6 for the elevation drive is provided by members 6-7 and 1-6. There is no member 6-8, for clearance in the horizon position. Point 8 is added for maximum horizontal stiffness/weight against wind loads. The dish rotates in elevation through a zenith distance from +90° to -45°, and it rotates by ± 360° in azimuth.

B. The Optical Position Reference System

In most radio telescopes the pointing is measured at the axes or drive tracks (too far away from the telescope surface) with respect to some structural elements or rails which are stressed by heavy loads. However, the most logical way is to measure the pointing close to the apex of the reflector and with respect to fixed points on the ground.

The pointing systems of the Parkes and the Goldstone 210-ft antennas have unstressed central pillars reaching from a deep foundation up to the crossing point of both telescope axes. At that point the pillar provides a stable platform from which the telescope orientation is measured. However, leaving a central pillar untouched imposes some awkward structural demands for the design of both the azimuth and the dish structure, and the thermal constancy of the high pillar is difficult to maintain.

A reference platform, located at the crossing of the telescope axes, is optically stabilized with respect to fixed points on the ground.

The system is shown in Fig. 3-3. The platform looks with several small telescopes at light beacons on the ground, and each telescope is provided with four photocells sensing the deviation of the image of the light beacon from its central position in the optical telescope. The platform may rotate about two axes, and a servo system keeps the platform in a stable orientation. From this stable platform, the pointing of the telescope is then measured by conventional encoders.

In principle, three beacons are needed (and only two are required if the telescopes at the platform are replaced by mirrors and if the light beacons are provided with autocollimation telescopes). In practice, however, one should have more than twice as many beacons because the light paths will occasionally be blocked by structural parts. This method does not work in heavy fog or a cloudburst, but then one cannot observe at

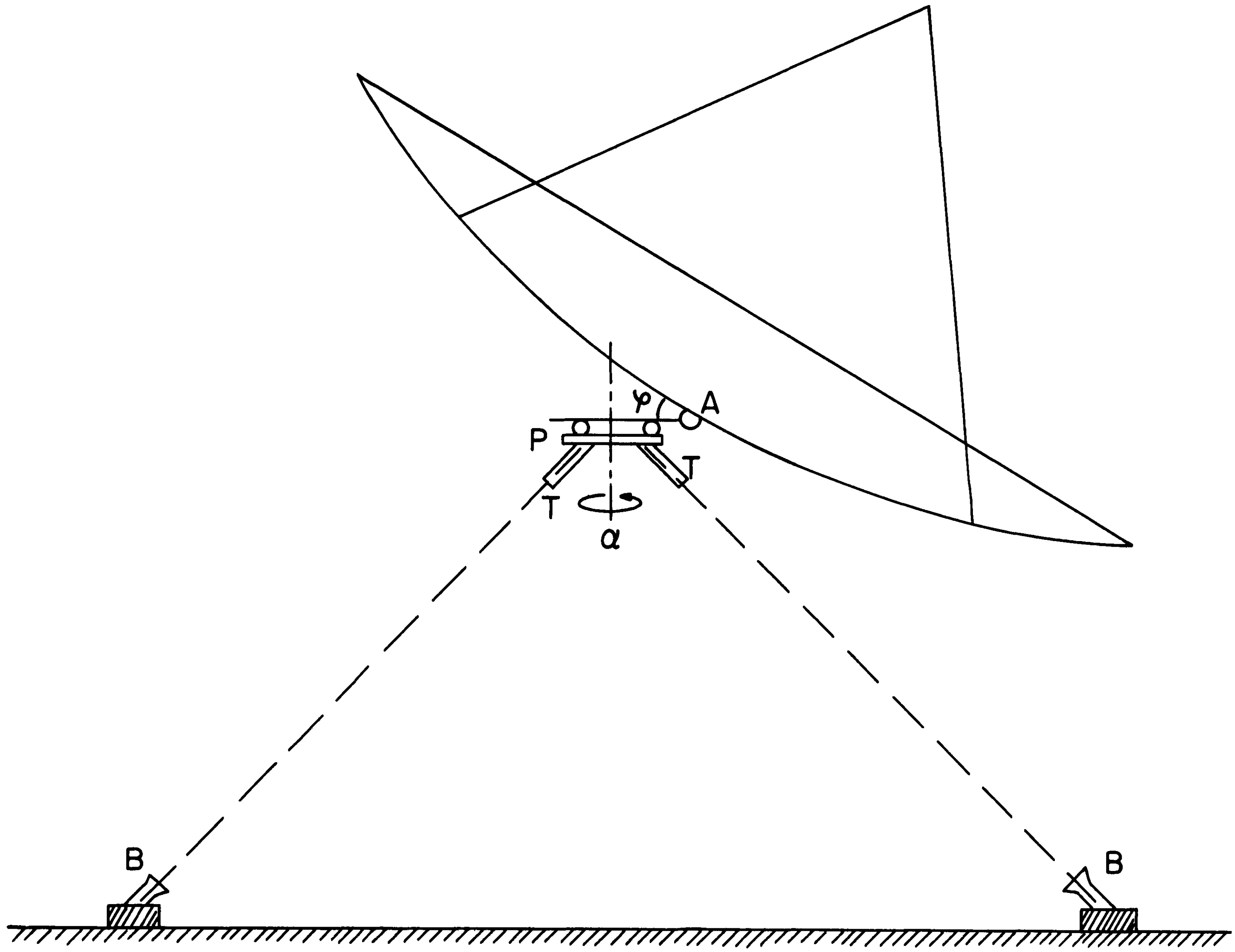

Fig. 3-3. Position measurements by optical means. A small tiltable and rotatable platform P is mounted behind the apex at the crossing of the axes and looks with about six theodolites T to as many optical beacons B fixed at the ground. Three servo motors keep the platform "locked-in" to the beacons; elevation ϕ and azimuth α are then measured between structure and platform. In this way, the position is measured at the optimum point with respect to something unstressed and unmovable. No high accuracy is required for foundations, azimuth rails and elevation ring; also, all slow deformations between apex and ground are eliminated by this technique.

short wavelengths anyway. For work at long wavelengths during exceptionally bad weather conditions, the telescope would have an additional pointing system of conventional type.

The method has two major advantages. First, it keeps the pointing accuracy completely independent of the accuracy of elevation rings and azimuth rails. As far as pointing is concerned, one could as well drive the telescope on a dirt road.

Second, the reference system eliminates all thermal deformations and all wind deformations slower than the servo response time which occurs between the reflector apex and the ground. Using this optical pointing technique, the pointing errors from wind deformations are cut down by a factor of 12, and those from wind deformations by a factor of 4. At the same time, the price of foundations and rails is reduced by a factor of 7.

The final system adopted is shown in Fig. 3-3. The beacons are autocollimated lasers, and the platform carries a 7-sided mirror, with 7 beacons on the ground, a system which gives more than enough redundancy with regard to blocking by structural members. This system yields a pointing accuracy of 3.2 arc sec.

The most elegant method would be to use a gyrocompass and a tilt sensor, without any optical connection to the ground. This is feasible, but it will need some further study regarding its behaviour on a moving telescope shaking in the wind. Thus, the optical system is used in the present design.

C. The Built-up Members

In order to facilitate a fast and accurate structural analysis of the telescope, long, inherently stable built-up members are used (Ref. 3-1). Rectangular building elements pick up 80% more wind force than round pipes (Ref. 3-1) and standard steel pipes are therefore used. The built-up members have 3 main chords (equilateral triangular cross section). This gives smaller ℓ/r ratios and reduces the wind force to $\sqrt{3/4}$ of the effect on a more conventional 4 main chord design. In order to let the bracing contribute to the axial stiffness, double bracing is used (two diagonals for each rectangle) and small triangles were introduced as secondary bracing in order to decrease the ℓ/r ratio of the diagonals. The best compromise between incompatible requirements such as maximum axial stiffness per unit weight, minimum lateral sag, minimum Eular buckling, etc., is a built-up member with parabolic shape of the chords as shown in Fig. 3-4.

The same bar area is used for all chords, battens, and diagonals of one member. The batten/chord ratios were optimized such that for increasing axial loads the chords, battens, and diagonals each become unstable at the same time. The calculated sizes are replaced by their nearest equivalent standard sizes in the Steel Manual.

For each member, an "equivalent bar area" is calculated as

$$A_{eq} = \frac{FL}{E\ \Delta x} \tag{3-1}$$

with F = axial force, Δx = resulting change of length L, and E = modulus of elasticity. With W = total weight of the member, an "equivalent density" is defined as

$$\rho_{eq} = \frac{W}{L\ A_{eq}} \tag{3-2}$$

The analysis regards these members as solid rods of bar area A_{eq} (for stiffness) and material density ρ_{eq} (for dead loads).

Simple approximation formulas have been developed for wind force, stress under various loads, and buckling criteria.

The overall design procedure for the built-up member is the following: First, a structure is developed using the homology program with $\Delta H \leq 0.005$ in, where every member is stable against survival according to approximation formulas. Second, all single calculated bar areas are replaced with standard sizes from the Steel Manual. Fourth, the member program calculates A_{eq} and ρ_{eq} for every built-up member. Fifth, with these changed values, the homology program calculates the final ΔH. Sixth, the stability in survival conditions is checked by an independent engineering firm (Simpson, Gumpertz & Heger).

D. The Surface

The dish structure provides 57 homologous surface points. They form a pattern of 88 triangles, which are approximately equilateral with a length along each side of 43 ft. (see Fig. 3-1). The distances between

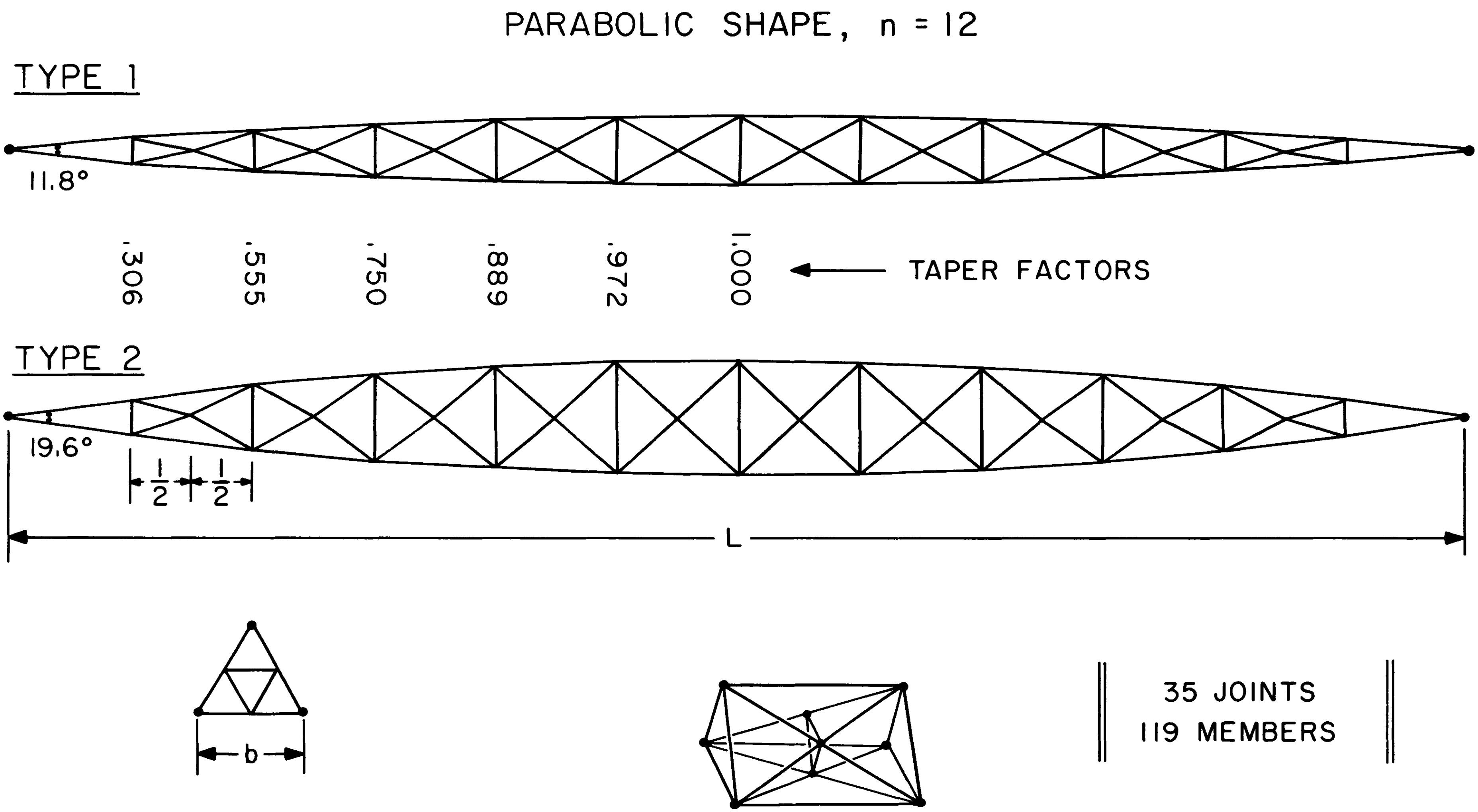

Fig. 3-4. Geometry of built-up members. Type 1 is used for all telescope members and heavy tower members; Type 2 is used for long, lightweight tower members.

neighboring homologous points must be bridged by some additional structure (the "surface panels") which hold the reflecting aluminum skin consisting of smaller pieces (the "surface plates").

1. The surface panels

The surface panels are space frames made from steel pipes. The depth of these panels is defined by their maximum tolerable sag under dead load and wind forces. Since the panels have a considerable total weight, they will contribute to the telescope stiffness: they are rigidly mounted on 57 homologous points. Weight and stiffness of the panels have been analyzed by the STRUDL computer program, and the results were used for replacing the panels in the homology program by fictitious "surface bars" of proper density and bar area.

There are two different possible arrangements of the surface geometry: a radial or a triangular pattern. Dividing the surface with circles and radii gives a radial pattern with rectangular panels and plates. It utilizes the highest number of identical pieces, which eases the manufacturing problems and might lower the price per pound. On the other hand, the triangular pattern of the present design, as shown in Fig. 4-1, yields a specified performance with a minimum amount of steel, although each panel has only 3 identical counterparts (and 4 mirror-symmetrical ones), thus increasing the number of different panel designs needed. With a highly automated manufacturing procedure, the price per pound of both patterns will be the same, and the triangular pattern is best because it is lighter.

2. The surface plates

The surface plates are made from sheet aluminum, supported by aluminum ribs. The plates will be mounted "floating" on the panels by keeping their height fixed but allowing thermal expansion and contraction to occur parallel to the surface. Installation and adjustment of the plates will all be done from above the surface.

Present telescope surfaces usually have large, curved surface plates, but the plates could as well be flat if they were small enough. For a telescope diameter of 300 ft and a shortest wavelength of 1 cm, flat plates can be employed with sizes up to 3 ft long. Experiments have shown that flat plates, cut from sheets as they come from the mill and riveted onto ribs of available channels, are already accurate enough without any further trimming or bending--again because of their small size. Therefore, the use of flat, riveted surface plates of 3.12 ft side length is a practical solution.

The shape of the surface plates will mostly be defined by the panels. The present design uses triangular plates. It will be necessary to use about 18,000 plates, resting on 9,000 adjustment studs, where each stud adjusts one corner each of six different plates. (For comparison: The present NRAO 300-ft telescope has 15,000 adjustment studs.)

The plates must fit accurately, with gaps of only about 1 mm. The procedure will be to weld all studs on the supporting structure and use the measured positions of these studs as input for an automated plate cutter

3. Discussion

The small-sized flat plates seem to be the only way of really ensuring a high precision at low cost. Curved plates cannot be less expensive than flat ones, and the desired flatness is obtained automatically, without any costly trimming or bending, and may easily be checked with a simple straight edge. The precision of the final surface is, therefore, an adjustment problem rather than a manufacturing problem. It would seem that the expense occurred by the few extra weeks that will be required to adjust the surface will more than offset the expense of constructing and checking doubly curved panels. Furthermore, the adjustment can be repeated as soon as better measuring methods are developed later on.

The surface adjustment will start with the location of a reasonable number of key points by using standard optical methods. The intermediate points will then be adjusted relative to the key points by use of templates.

E. Automated Manufacturing of Members, Panels, and Plates

In order to facilitate a very accurate and fast structural analysis used in each iteration step of the homology program, the telescope is designed from long, built-up members. The telescope has 646 built-up members and each member has 219 single pieces of pipe, with 6-8 pipes meeting at each joint at various angles. All connections will be welded. The 88 surface panels are triangles of 43 ft average length, with 1253 single pieces each. In each telescope quadrant, all 22 panels are slightly different from each other.

For the manufacturing, all detailed information will be provided by NRAO in the form of punched cards or tape, and the manufacturer will have automatic machinery that uses punched cards input. Each single piece of pipe of a member or panel is represented by a punched card, numbered in order of decreasing diameter. All pieces are cut, and welded together, in the order of their numbers. An automatic saddle cutter provides both ends of each pipe with saddles fitting the pipes already present at both joints. Each saddle is described by three parameters punched on the card (diameter of the other pipe, angle between the two, angle on periphery). On the average, each pipe end needs 1.5 saddles. In both members and panels, the thick pipes (which are assembled first) provide a complete outer framework, into which the smaller pipes then can be welded with flexible jigs. The total length of a member or panel should be accurate to $\pm$ 1/4 in, but no special accuracy is demanded for the location of all other joints.

A similar procedure is suggested for cutting the triangular surface plates from aluminum sheets. If fully automated cutters are available, NRAO will provide all information on punched cards. If not, 18,000 templates from a Calcomp plotter will be provided.

REFERENCES

3-1 von Hoerner, S. 1966. "The Wind-Area of Members and Space Frames," Report 10.

Chapter 4

THE TELESCOPE DESIGN

A. Introduction

As the evolution of the homology antenna proceeded successfully from definition of a design principle through a theoretical design concept, it was considered advisable by the NRAO management to expend additional effort on the program. This additional effort was planned to proceed in steps whose objectives were to answer the questions: (1) Is a homology design possible? (2) Is a homology antenna concept possible? (3) Is a homology antenna practical? (4) Is a homology antenna economically feasible?

The first question having apparently been answered affirmatively by the development of a computer program which gave a solution answering homology parameters and the second question being answered successfully by the small in house group, additional forces both in house and external to the NRAO organization were assembled and assigned tasks in the completion of the concept development, the development of a telescope design, and the evaluation of the homology antenna.

In July 1968, Systems Development Laboratory was assigned the task of determining the feasibility of and preparing a conceptual design of a position reference system. This assignment was expanded in October 1968 to include the conceptual design of the antenna towers, the azimuth structure, the azimuth trucks and rail system, the elevation and azimuth drives, the elevation and pintle bearing arrangements, and an investigation and evaluation of member design from a fabrication and economic viewpoint. The consulting firm of Simpson, Gumpertz & Heger were retained to review and evaluate the reflector design prepared by NRAO and to prepare a dynamic analysis of the dish tower and azimuth structure. In October 1968 additional NRAO engineering personnel were asked to participate in the evaluation of the antenna feasibility and to review and develop fabrication and erection techniques for the antenna. All of these groups participated in economic evaluation of the antenna or segments of the antenna.

B. The Surface

The general concept of the surface panels was described in Chapter 3, § D. Each panel is a triangle with an average side length of 43 ft. The actual design is shown in Fig. 4-1 for one-sixth of one panel. Each panel consists of 1253 single pieces of pipe. The design of Fig. 4-1 shows a "standard" (or typical) panel, and each actual panel can be derived from this standard by a simple geometrical transformation formula derived for this purpose. Point 51 is the holding point in Fig. 4-1 (a homologous point of the dish structure).

In order to keep the dead load sag low, the panel must have a certain vertical depth, and 10 ft was chosen for this depth. There are axial forces between any two holding points, up to 10 kip, which would give large vertical surface deformations, if the depth of the panel would extend only below the holding points. Thus, in the design of Fig. 4-1 the holding point is placed at half the depth. The remaining vertical deformation from axial loads is sufficiently small.

At their upper surface the panels provide a triangular pattern onto which the adjustment studs are welded that hold the triangular surface plates, see Figs. 4-2 and 4-3.

The triangular plates are made of aluminum sheet (1/8 in; alloy 6061-T6) and have riveted channels under their sides. Plates and ribs are designed for holding a man of 200 lb on any point without permanent deformation. They are stronger than needed for survival, and their gravitational sag is only 0.008 in maximum. The triangular plates have a side length of only 3.12 ft for two reasons: (a) with this size they can be flat instead of curved; and (b) the deviations from flatness, if cut from sheets as they come from the mill, are small enough. Thus, standard available sheets give the wanted accuracy. The total surface needs 18,000 such plates, supported by 9000 adjustment studs (our present NRAO 300-ft has 15,000 adjustment studs).

The design of the adjustment stud is shown in Fig. 4-3. It fulfills five requirements. (1) It never needs a man below the surface. Installing and removing plates and adjusting their height can all be done from above with a combination tool which has been designed for this purpose. The adjustment may be done quickly and in an easy way. (2) After adjustment, everything is tight and no loose or rattling pieces. (3) The leaf-spring connections to the plate corners allow thermal expansion and contraction of the plates, but are extremely stiff for all other movements

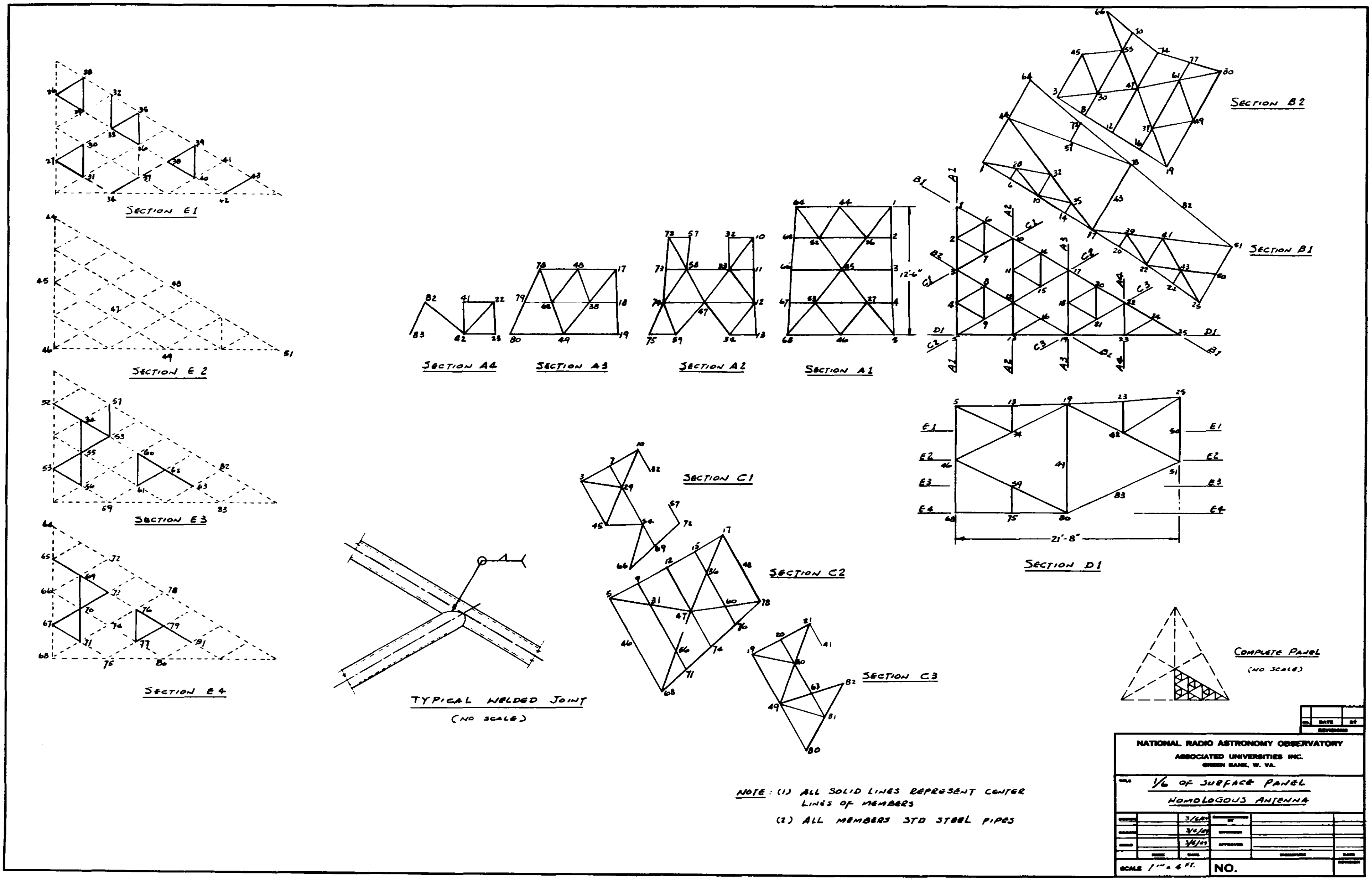

Fig. 4-1. Design of one-sixth of a surface panel.

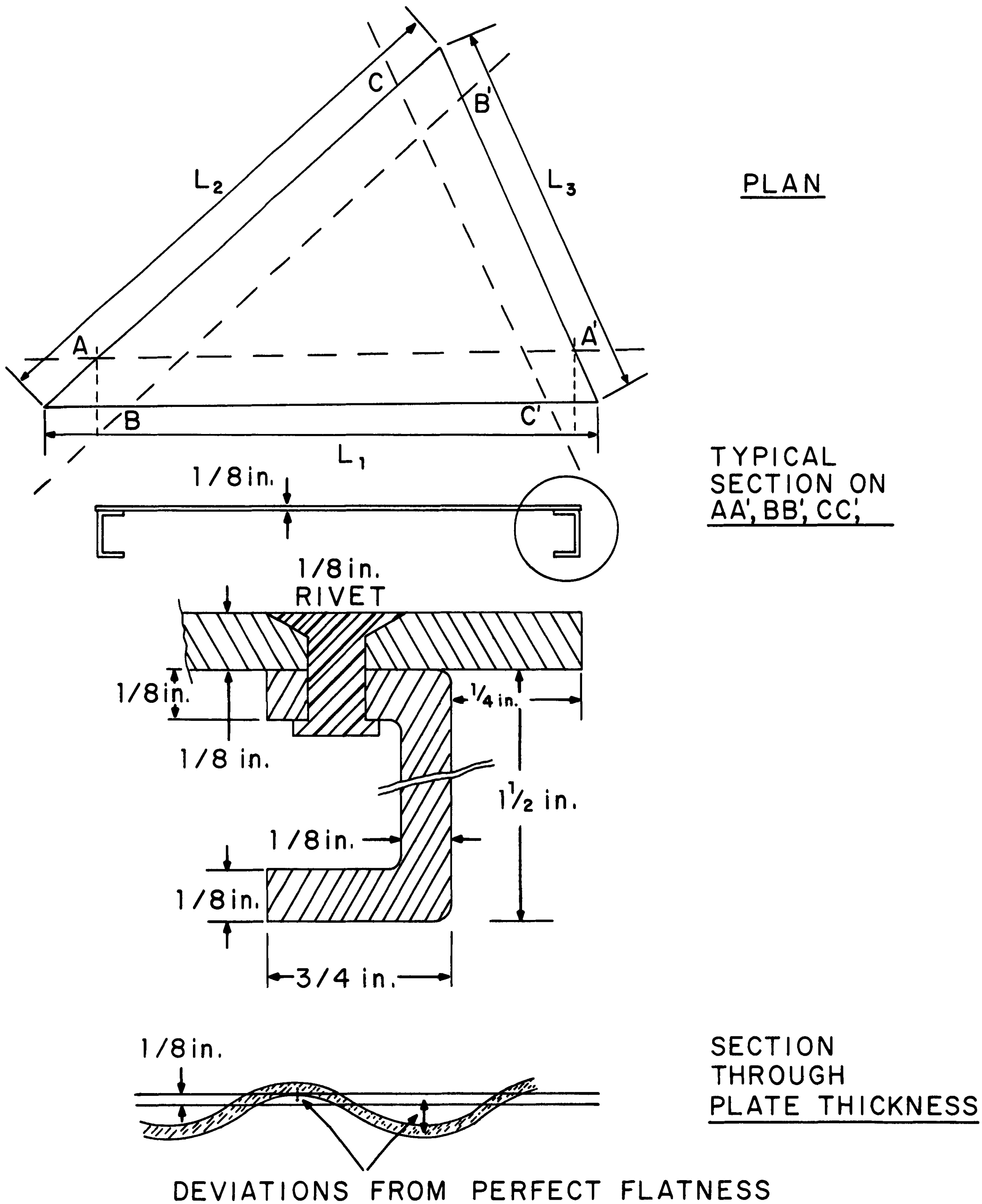

Fig. 4-2. Surface plate with ribs.

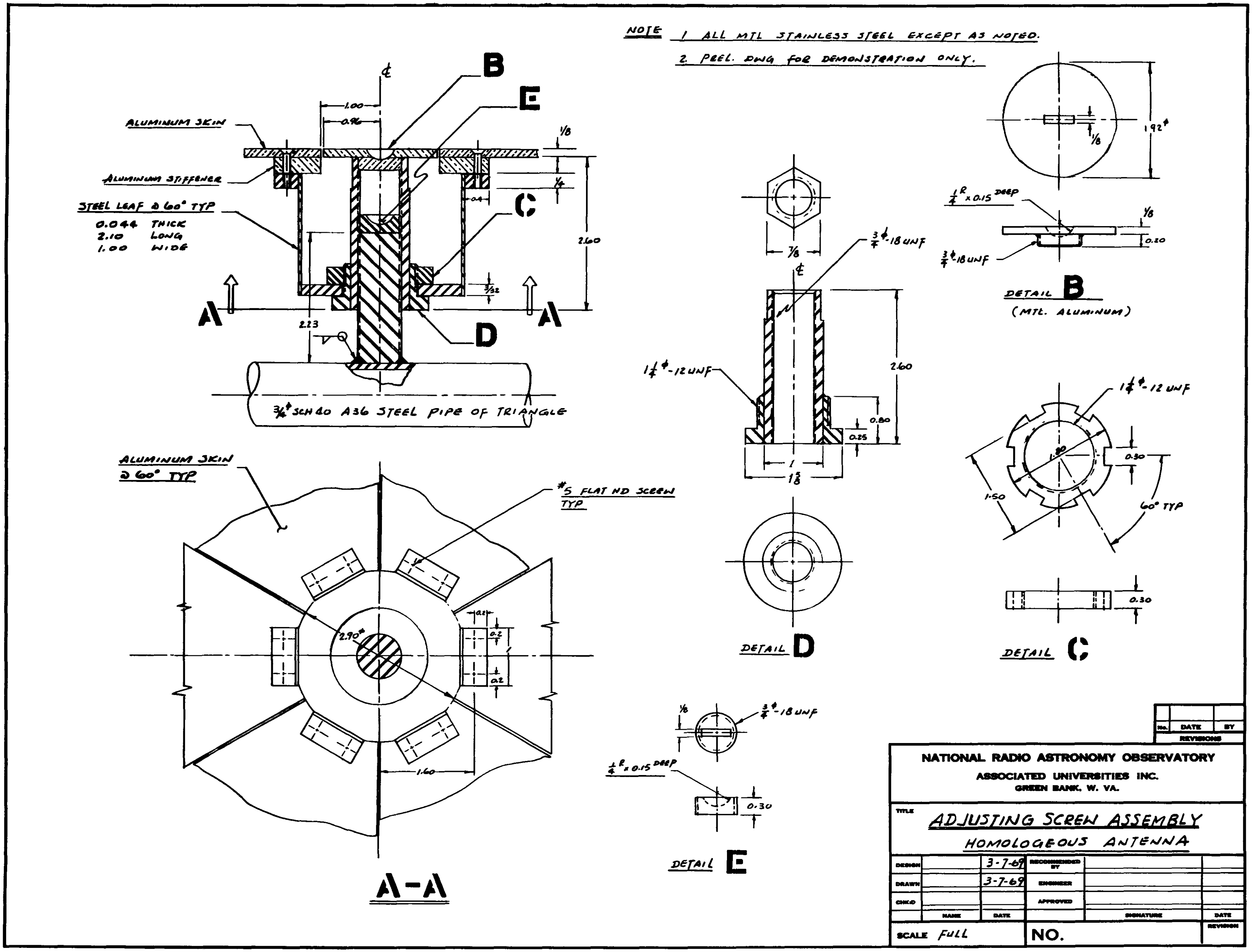

Fig. 4-3. Adjustment stud for surface plates.

or rotations. They hold the weight of a man. (4) After adjustment a lid is screwed on and provides a closed surface. (5) The studs are made from stainless steel, and their final design should make use of as many available standard pieces as possible.

The gaps between two plates, and between the plates and a lid, are about 1 mm, allowing for manufacturing tolerances and thermal expansion. The sum of these gaps is 1/400 of the total surface area.

The total weight of all aluminum plates and ribs is 91 (US) tons, the weight of all surface panels is 213 tons. The weight and stiffness of the panels is represented in the homology program by surface bars with (results of STRUDL analysis)

$$\begin{aligned} A_{eq} &= 3.89 \text{ in}^2 \\ \rho_{eq} &= 0.147 \text{ lb/in}^3 \end{aligned} \tag{4-1}$$

C. The Built-up Members

1. General

The design of both reflector and tower structure consists basically of simple space frames which, for the purpose of simplification and weight savings, make use of relatively long truss members. The conceptual design of these structures is shown in Figs. 4-4, 4-5, 4-6, and 4-7.

As each of the members is subjected to a compression load at one time or another in addition to transverse bending loads due to wind forces, they must have a sufficiently high buckling strength in order to retain stability under maximum load conditions. Furthermore, they must be relatively light and have adequate lateral bending stiffnesses so that their lowest structural resonances are well above the lowest mode of the complete system. These requirements led to the selection of light-weight built-up members.

In the initial structural analyses, built-up members of triangular cross sections with a parabolic shape were found to be more desirable from a functional viewpoint. Two types of members were used, both having the same structural arrangement but different slenderness. Type I was used exclusively in the reflector structure, while the tower structure contained members of both types.

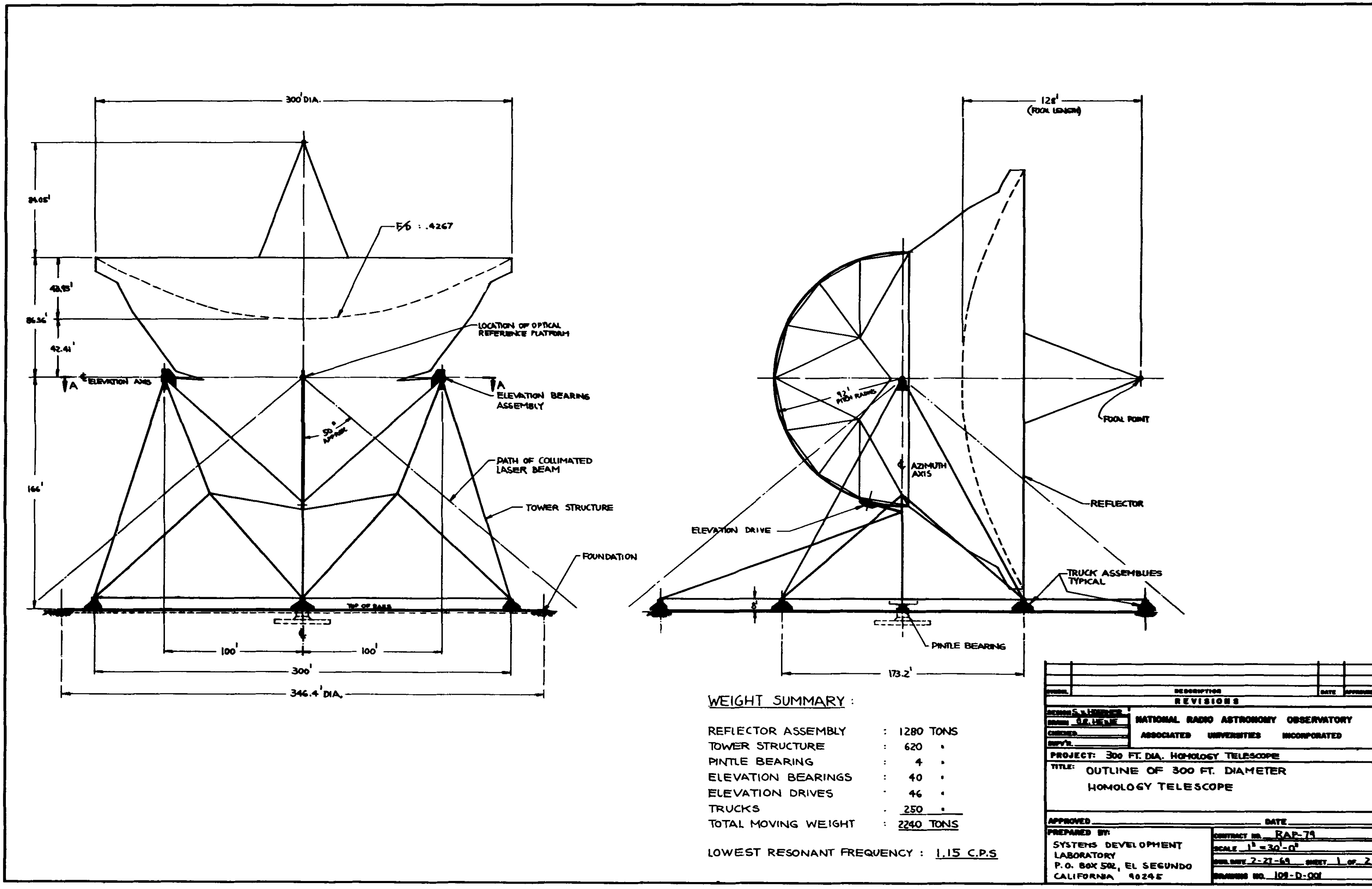

Fig. 4-4. Outline of 300-ft diameter homology telescope.

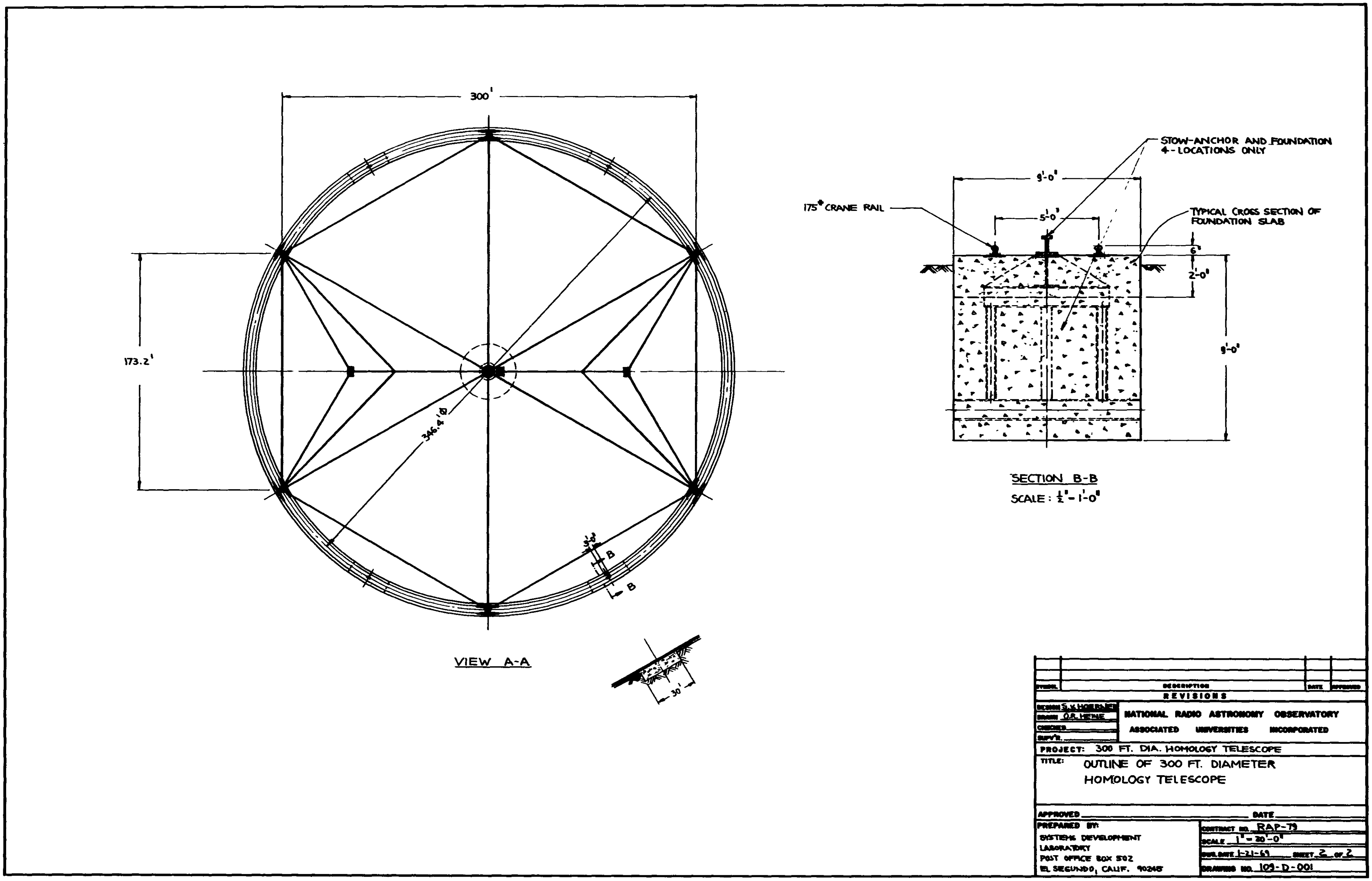

Fig. 4-5. Outline of 300-ft diameter homology telescope.

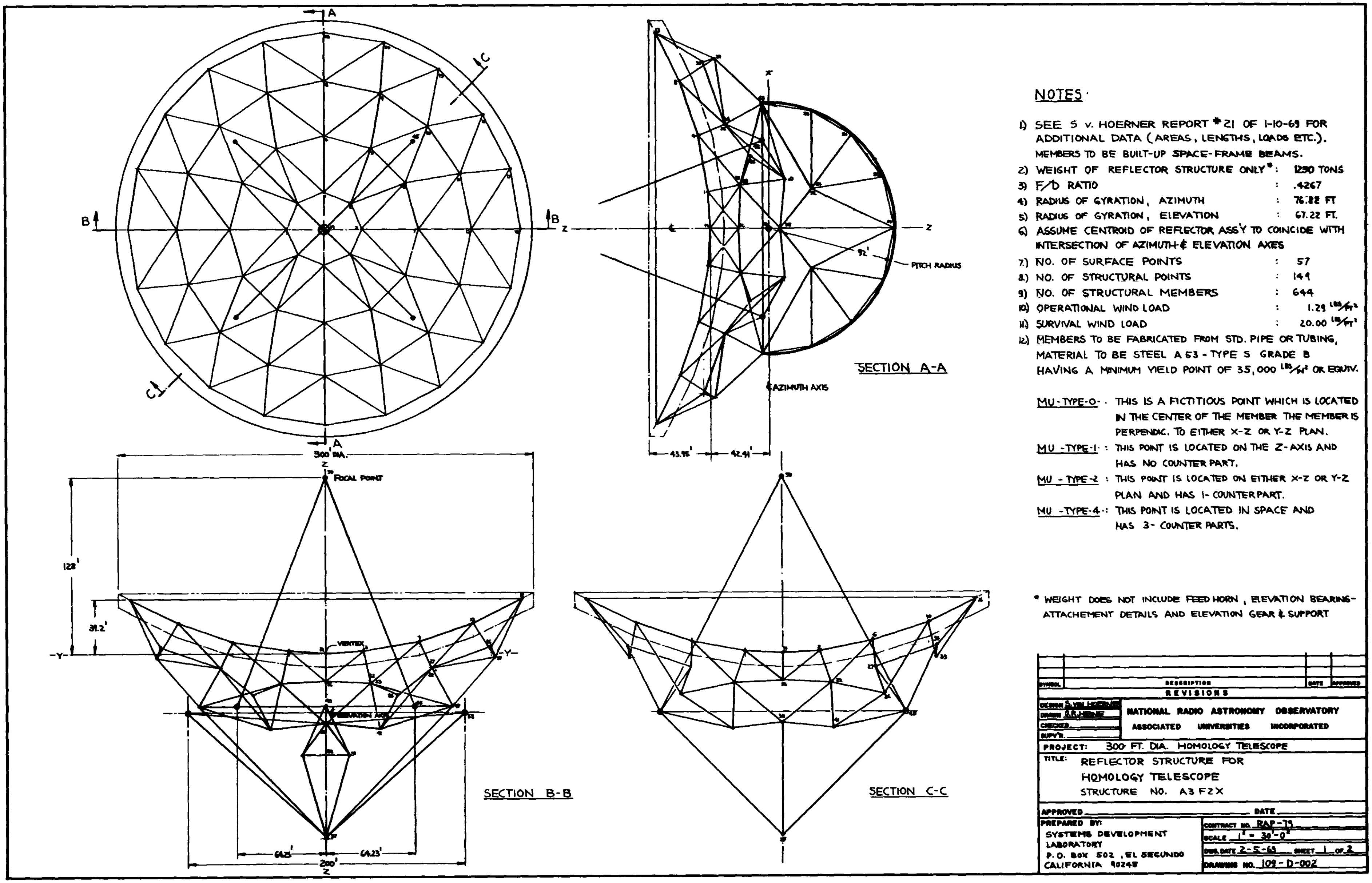

Fig. 4-6. Reflector structure for homology telescope. Structure No. A3F2X.

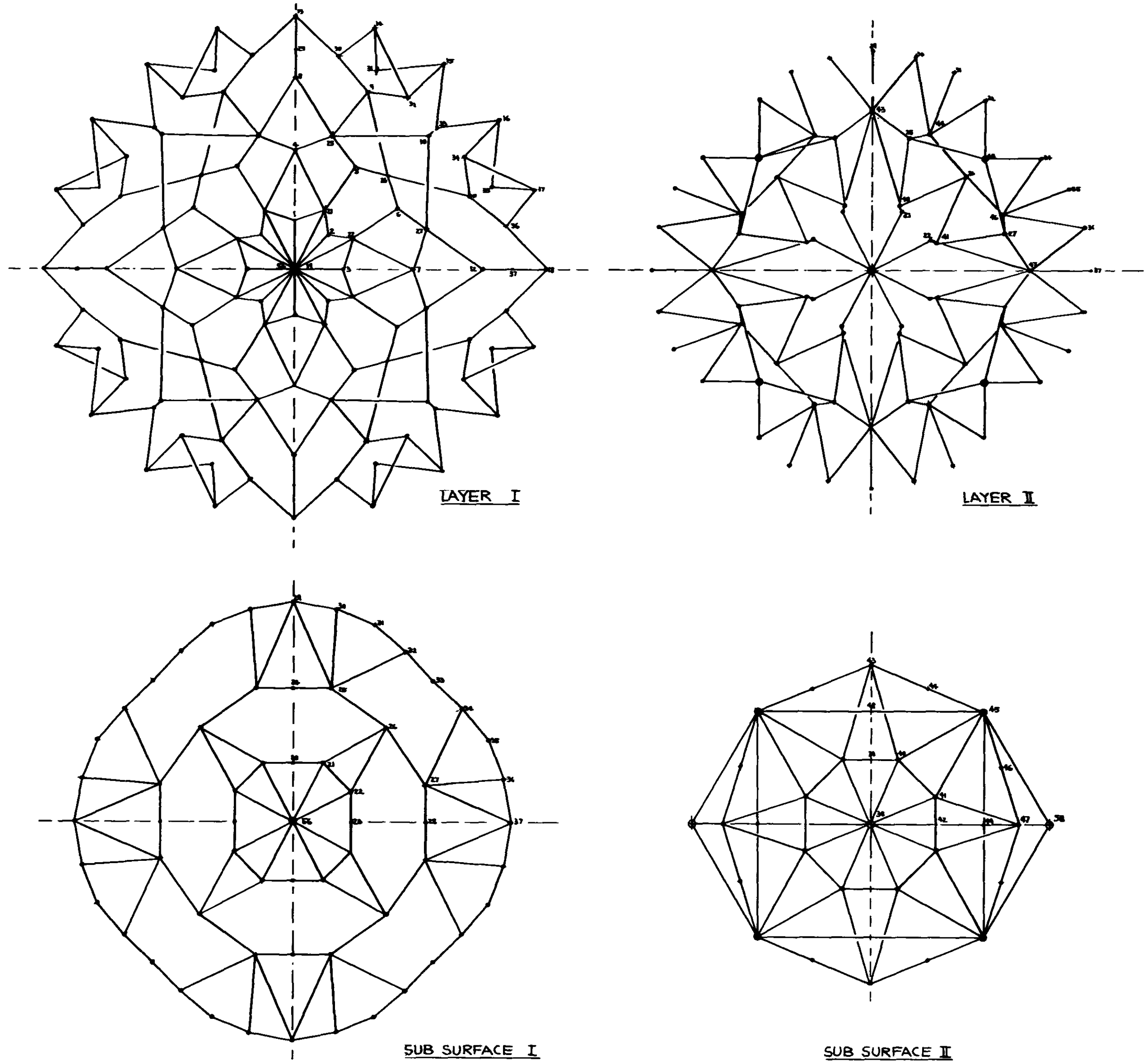

POINT	COORDINATES (IN)			POINT LOAD (KIPS)	MU TYPE
	X	Y	Z		
1	325.00	0.00	-17.19	1714.3	2
2	229.81	229.81	-17.19	3428.6	4
3	0.00	325.00	-17.19	1714.3	2
4	800.00	0.00	-104.17	1714.3	2
5	692.82	400.00	-104.17	3428.6	4
6	400.00	692.82	-104.17	3428.6	4
7	0.00	800.00	104.17	1714.3	2
8	1275.00	0.00	-264.59	1714.3	2
9	1177.95	487.92	-264.59	3428.6	4
10	901.56	901.56	-264.59	3428.6	4
11	487.92	1177.95	-264.59	3428.6	4
12	0.00	1275.00	-264.59	1714.3	2
13	1700.00	0.00	-470.38	1714.3	2
14	1616.80	525.33	-470.38	3428.6	4
15	1375.33	999.24	-470.38	3428.6	4
16	999.24	1375.33	-470.38	3428.6	4
17	525.33	1616.80	-470.38	3428.6	4
18	0.00	1700.00	-470.38	1714.3	2
19	0.00	0.00	0.00	857.15	1
20	390.00	0.00	260.00		0
21	390.00	200.00	260.00		4
22	200.00	390.00	260.00		4
23	0.00	390.00	260.00		0
24	917.63	0.00	123.67		0
25	917.63	245.88	123.67		4
26	630.00	630.00	352.00		4
27	245.88	917.63	123.67		4
28	0.00	917.63	123.67		0
29	1471.18	0.00	85.05		2
30	1432.00	285.00	-64.95		4
31	1321.15	547.24	35.05		4
32	1139.11	761.13	-64.95		4
33	948.19	948.19	35.05		4
34	761.13	1139.11	-64.95		4
35	547.24	1321.15	35.05		4
36	285.00	1432.00	-64.95		4
37	0.00	1471.18	85.05		2
38	0.00	0.00	600.00		1
39	434.22	0.00	650.00		0
40	434.22	179.86	650.00		4
41	179.86	434.22	650.00		4
42	0.00	434.22	650.00		0
43	1071.82	0.00	450.00		2
44	914.86	378.95	450.00		4
45	757.89	757.89	450.00		4
46	378.95	878.95	450.00		4
47	0.00	1000.00	450.00		2
48	757.89	0.00	450.00		0
49	0.00	757.89	450.00		0
50	0.00	0.00	-1536.00		1
51	350.00	200.00	870.00		4
52	350.00	0.00	870.00		0
53	996.38	0.00	860.69		2
54	765.47	0.00	1221.66		2
55	415.12	0.00	1459.53		2
56	0.00	0.00	250.00		1
57	0.00	0.00	1543.16		1
58	0.00	1200.00	0.00		2

SYMBOL	DESCRIPTION	DATE	APPROVED

REVISIONS

DESIGN S. v. HOERNER
DRAWN O.R. HEINE
CHECKED
SUPV'R

NATIONAL RADIO ASTRONOMY OBSERVATORY
ASSOCIATED UNIVERSITIES INCORPORATED

PROJECT: 300 FT DIA HOMOLOGY TELESCOPE

TITLE: REFLECTOR STRUCTURE FOR HOMOLOGY TELESCOPE STRUCTURE NO. A3F2X

APPROVED ____ DATE ____

PREPARED BY:
SYSTEMS DEVELOPMENT LABORATORY
POST OFFICE BOX 502
EL SEGUNDO, CALIFORNIA 90245

CONTRACT NO. RAP-79
SCALE 1" = 30'-0"
DWG. DATE 2-5-69 SHEET 2 OF 2
DRAWING NO. 109-D-002

Fig. 4-7. Reflector structure for homology telescope. Structure No. A3F2X.

The end taper of these members was selected to eliminate structural interference between members connecting at a common joint. Fig. 4-8 shows the structural arrangement of a typical built-up member. As seen from Fig. 4-8, the typical member was divided into twelve panels of equal length, which are crows braced by diagonals connecting at the panel center. These joints in turn are interconnected in such a way that small triangles are formed. The members were optimized with respect to a compromise between the maximum stiffness weight and the maximum axial load weight ratios.

The parabolic outline of the typical members is shown in Fig. 4-9.

The material considered for these members was standard steel pipe A 53, Type S, Grade B, with the following basic characteristics:

$$\begin{aligned} &\text{Density, } \rho, &&= 0.283 \text{ lb/in}^3 \\ &\text{Elasticity, E,} &&= 29\text{x}10^5 \text{ lb/in}^2 \\ &\text{Yield Stress} &&= 35\text{x}10^3 \text{ lb/in}^2 \end{aligned} \tag{4-2}$$

The two types of members used in the present design of the telescope structure had the fixed relationship of bar areas, lengths, and weights listed below.

Member Type	ρ	b_c/L	A_p/A	A_c/A	A_b/A	A_d/A	A_t/A
I Reflector	0.358	0.0557	0.354	0.250	0.0613	0.0650	0.0175
I Tower	0.325	0.0482	0.343	0.287	0.0341	0.0372	0.0200
II	0.381	0.0699	0.364	0.283	0.0684	0.0540	0.0197

where

b_c = length of center batten

ρ = unit density (lb/in^3) of A_c

A_p = area of pyramid bars (in^2)

A_c = area of chords (in^2)

A_b = area of battens (in^2)

A_d = area of diagonals (in^2)

A_t = area of triangles (in^2)

A = equivalent member area (in^2)

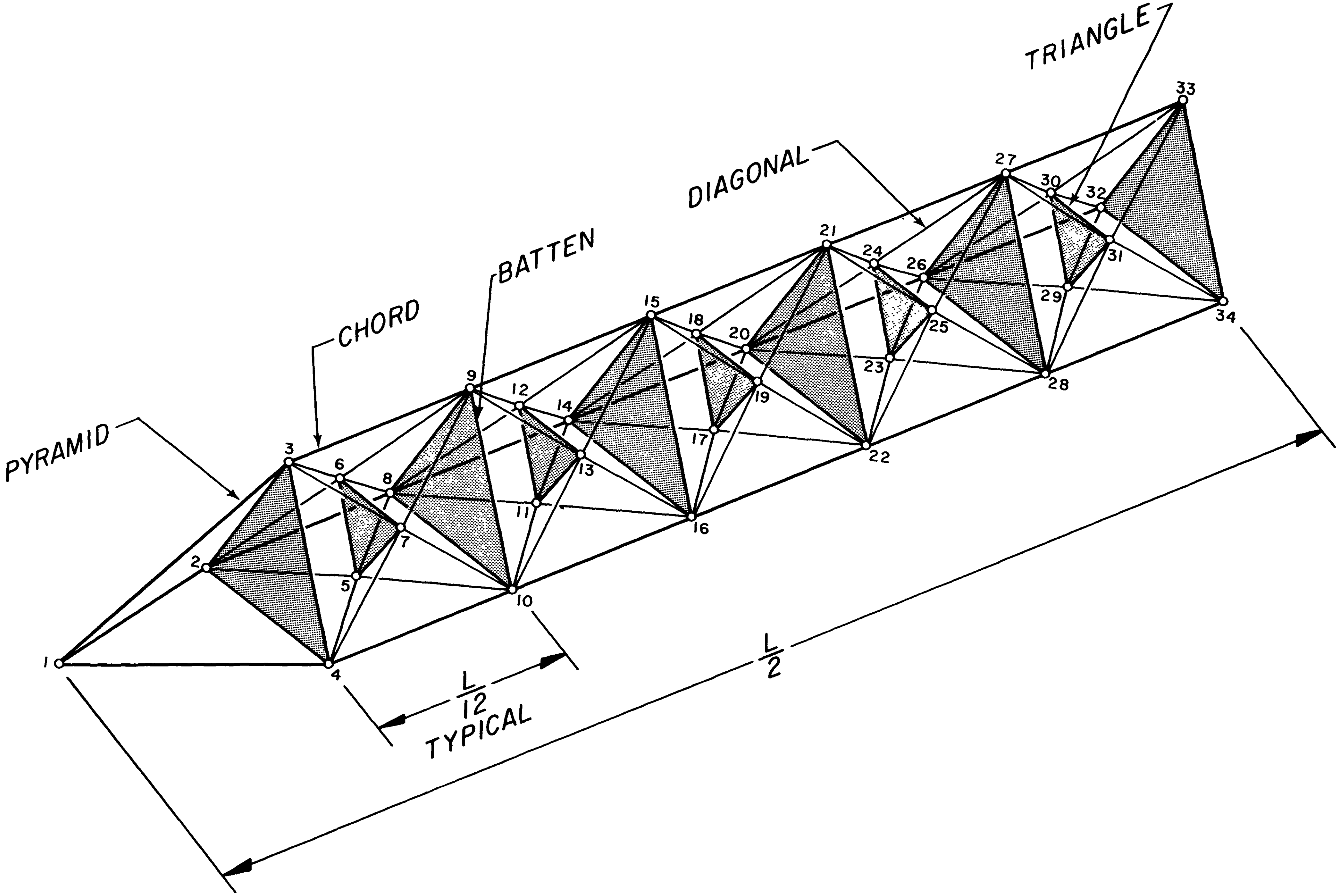

Fig. 4-8. Structural arrangement of a typical built-up member.

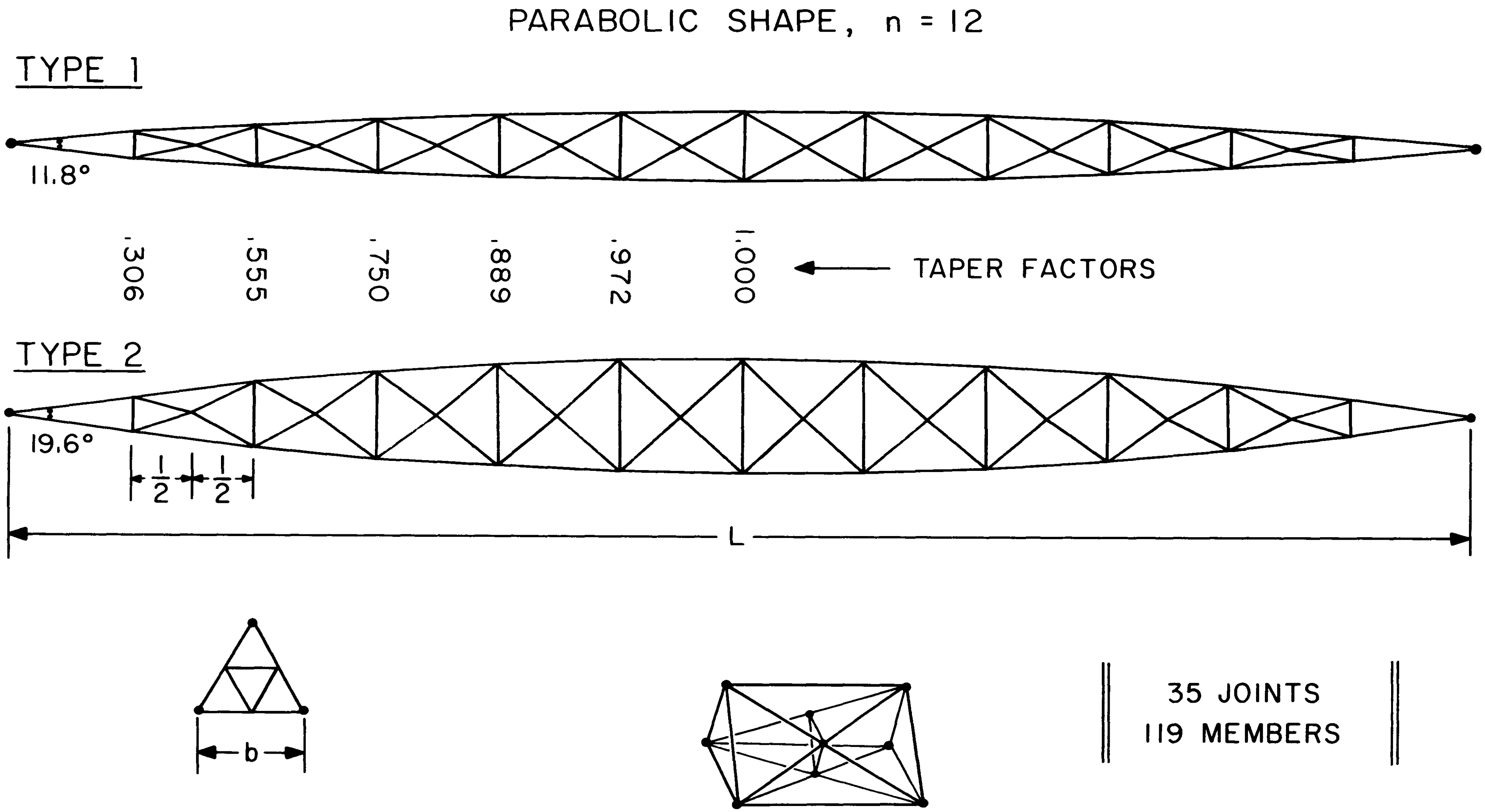

Fig. 4-9. Geometry of built-up members.

2. Other considerations

The foregoing described member design did not take into consideration other limiting factors, which could affect the final best-suited structural configuration from the viewpoint of economy, practicality, and safety against self-excited vibrations.

A study of the sizing of individual members for the tower structure revealed that many secondary bars selected by this method would have been subject to failure due to wind induced, self-excited vibrations through "v. Karman" vortex shedding. It was determined by analysis that the maximum permissible member length should not exceed $L_{max} = 13.92\ D^{1.5}$ (D = outside diameter of tubular member, L = unsupported length) in order to avoid self-excited vibrations, which could lead to fatigue failures, as it was calculated that internal dampening would be insufficient to limit the induced stress amplitudes to remain within the endurance strength of the selected material.

Another limiting factor was found to be a minimum wall thickness which must be maintained in order to assure economy of fabrication and welding. Discussions held with several experienced fabrication firms on this subject indicated that less than a minimum wall thickness of 3/32 in should not be used, since a lesser thickness would require more sophisticated welding techniques, more rigid inspection, and a higher cost. The combination of these two limiting factors resulted in the requirement for increased cross sectional areas of chords, battens, diagonals, and triangles on some members, even when structural tubing which provides a wider selection of areas and diameters is used and the resulting weight increases over the initial configuration was estimated to be as much as 20% in some cases.

This, however, appears not to be a significant design limitation, since it is estimated that a final optimized reflector design will permit the maintenance of presently computed performance parameters without a significant variation from the present estimate.

The built-up members for the tower were not affected by the above considerations as the bar areas, diameters, and lengths of the individual members were found to be within safe limits.

A study of the economy of fabrication of built-up members for the reflector structure indicated that it would be desirable to have a parallel lacing arrangement instead of the previously considered uneven configuration and straight chord members instead of curved ones. This preferred configuration is shown in Fig. 4-10 as compared with the previous configuration shown in Fig. 4-11. This would make it possible to fabricate more than four members of equal configuration, since it would be feasible to manufacture a much greater number of identical one-half members which could be pieced together with inserts of varying length to make up members of equal effective cross sectional areas but varying lengths.

The advantage of this approach would be that the cost of the welding jigs, which is a significant portion of the total cost of the lightweight reflector members, could be amortized over many more units, thereby resulting in a reduced unit cost of the fabricated structure. Fabrication is simplified and manufacturing cost reduced since this approach produces many diagonals and batten pieces of the same length and identical end bevel in each member. This combination of multiple members and multiple pieces within a member makes possible the use of dies and brakes in the fabrication process and substantially reduces time and cost in manufacturing.

3. Members of special design

Some reflector members require a different design effort as their function demands a special treatment. There are three such members which must be individually designed: (a) the feed support legs, (b) the suspension members which support the reflector structure on the bearings, and (c) the central member supporting the optical reference platform.

(a) The feed support legs. The feed support legs must be designed to the following requirements:

(1) They must support the focal structure and a cabin which must be sufficiently large to house the feed elements. This cabin should be at least 10x10x13 ft, and must be surrounded by a "focal structure" which connects the feed legs. This structure must be very stiff in compression, shear, and torsion.

The bottom of the cabin should have a circular opening of at least 5 1/2 ft diameter for the focusing mount to carry the feed and receiver box. The top of the cabin must have an open entrance for men and equipment in the service position (reflector pointed at horizon). One of the cabin walls must provide a horizontal floor in service position, and for convenience

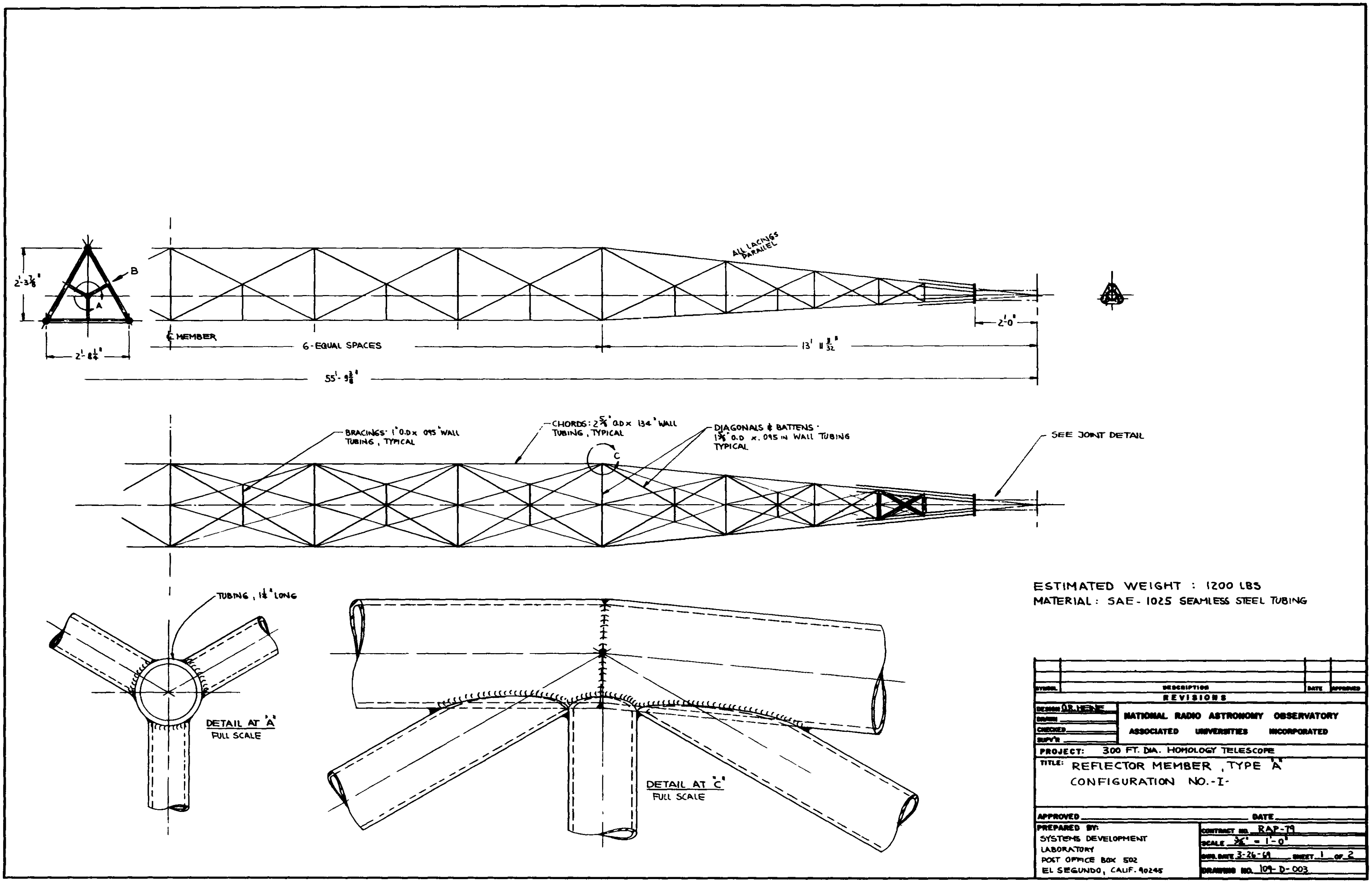

Fig. 4-10. Reflector member, Type A, Configuration No. I.

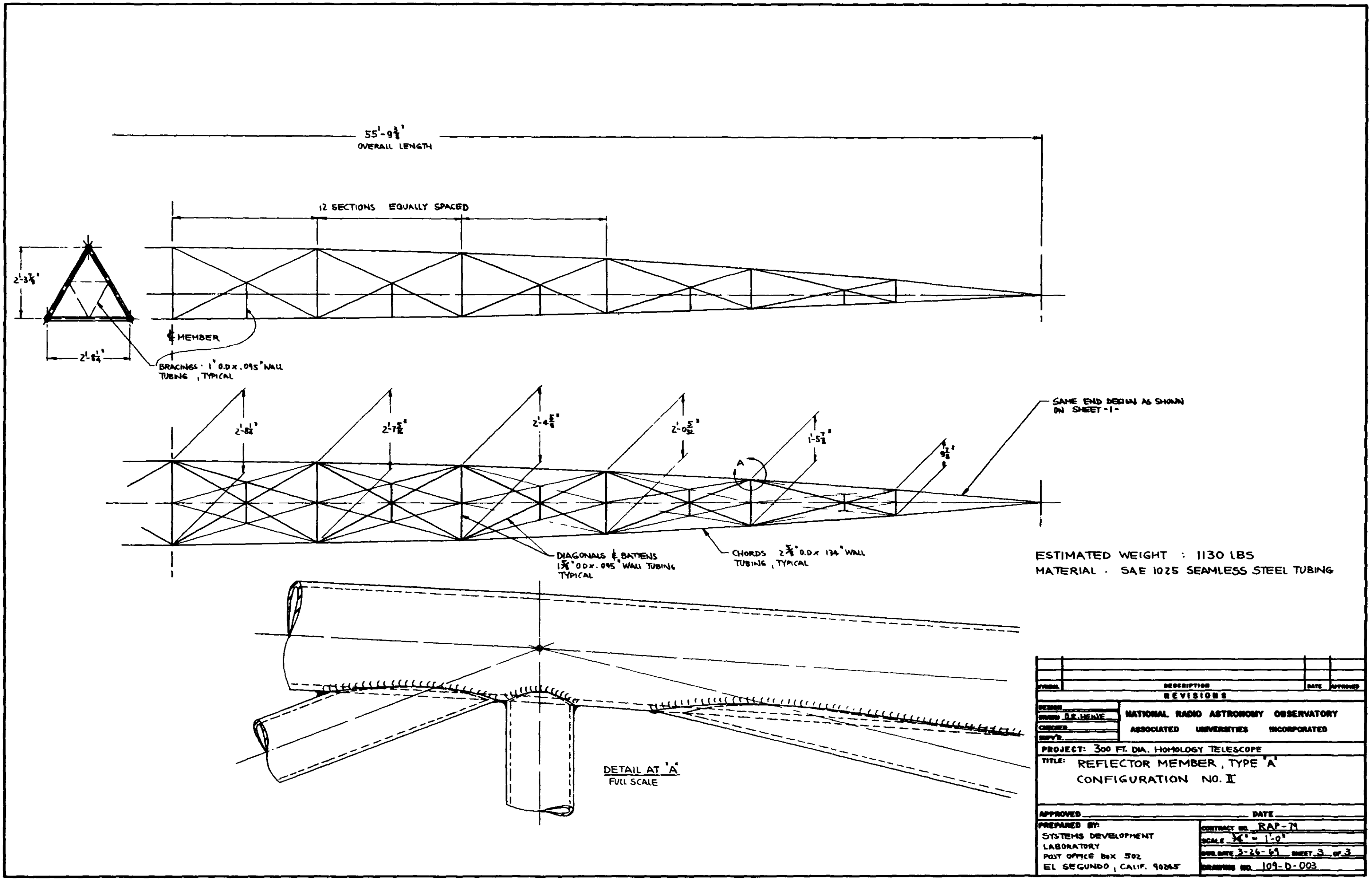

Fig. 4-11. Reflector member, Type A, Configuration No. II.

there should be no door sill in the entrance. With cabin floor and service tower at the same level, equipment can then be rolled conveniently in and out on little carts.

Fig. 4-12 shows a design meeting these demands. The focal structure concept, outside the cabin walls, is the most natural method of connecting the feed legs to each other. For complete stiffness, this structure would need diagonal bracing, in both top and bottom planes of the cabin. These diagonals, however, must be omitted because of the required openings; the diagonals thus should be replaced by two steel plates with large central openings. This focal structure design is stable even if pin joints are used, thus giving maximum stiffness in all directions (not relying on bending stiffness).

The cabin should have double walls with heat insulation and a door at the top. The wall, which is also the service floor, should be made sufficiently stiff.

The following appears feasible:

<u>Plates</u> - A36 steel, 3/16 in thick
<u>Structure</u> - A36 steel, standard pipe, 5 in nominal diameter
<u>Walls</u> - 6061-T6 aluminum, 1/8 in thick (service floor 1/4 in)

The resulting weight would then be 4.15 tons for cabin and focal structure. This would leave 12 tons for receiver, air conditioning equipment, etc., which can be placed inside the cabin.

(2) Another requirement is that the shadow of the legs on the reflector surface be kept at a minimum, while at the same time the legs must be made sufficiently stiff. This can be accomplished by giving the feed legs a rectangular shape so that the depth of the rectangular structure provides for greatest bending resistance and by the application of guy ropes in addition.

These guy ropes must be attached in such a way that the homologous deformation of the reflector structure will not be affected. Fig. 4-13 shows a feasible concept of such a guy rope arrangement.

As can be seen from Fig. 4-13, the feed legs connecting to point 45 should be kept fairly slender in the region below the reflector surface, in order to eliminate structural interference. In the concept shown on this figure, 4 guy ropes are applied parallel to the surface in tangential and radial

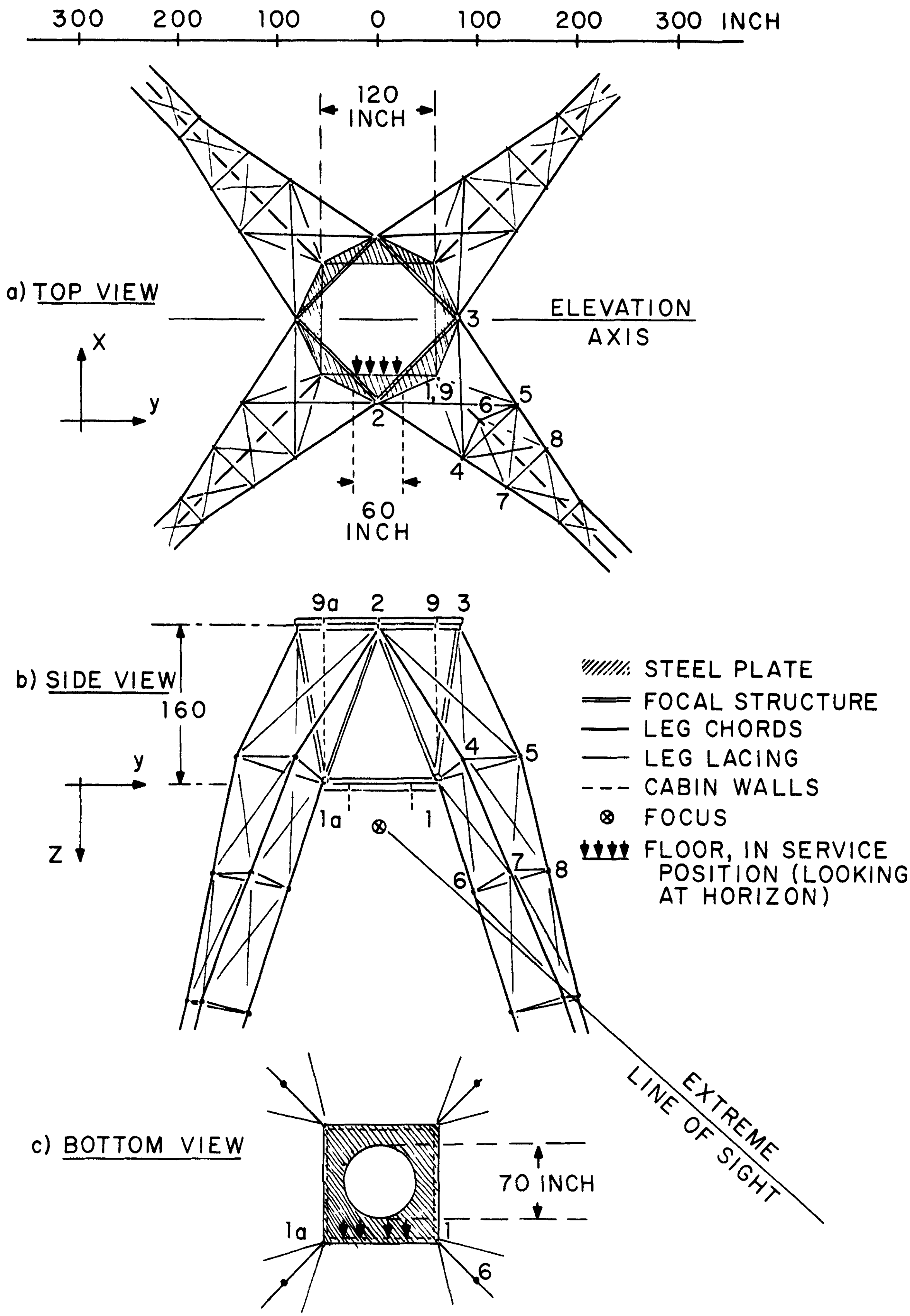

Fig. 4-12. Focal structure and cabin.

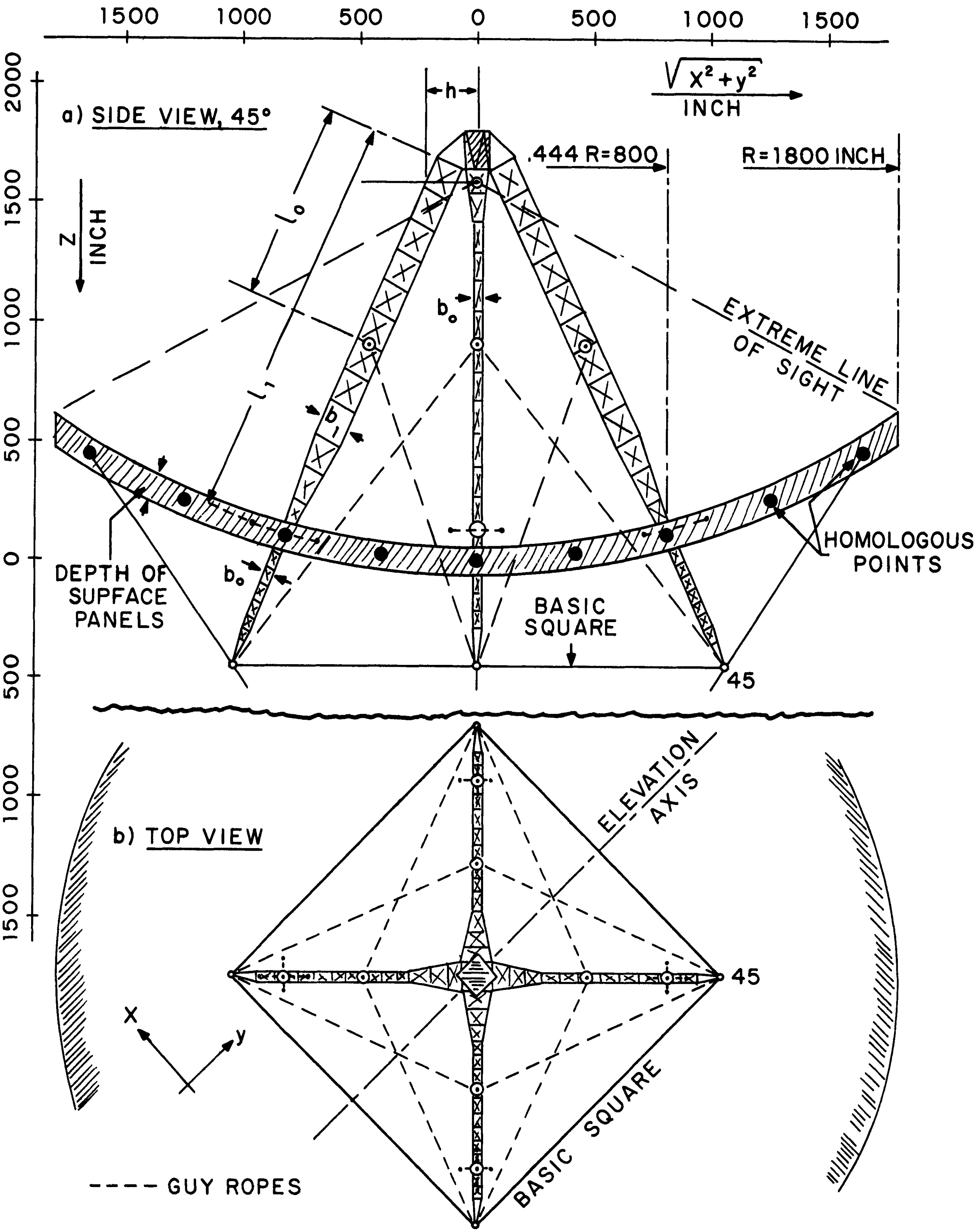

Fig. 4-13. Feed legs and guy ropes.

directions. At one-half the upper length of the feed supports, two additional ropes are attached to point 45. The first guy rope system permits deformation only parallel to the surface, while the second system does not result in any contributing deformations.

Fig. 4-14 shows the combined shadow of the leg on the dish. Part 1 is a parallel strip of width b_o and is due to the blocking of the incident rays. The outer part 2 is due to the blocking of the feed illumination; it begins at the intersection of the leg with the surface, with width b_o, and it widens up toward the rim with a final width αR, with R = telescope radius = 1800 in. The geometry of the design is

$$\alpha = 0.616\ b_o/h + 0.000240\ b_o \ \text{(radians)}, \qquad (4\text{-}3)$$

where h is the horizontal distance of the upper leg chords from the focal point. If f_s is the fraction of aperture* covered by the combined shadow, f_s increases with b_o and decreases with increasing h. In order to determine h if f_s and b_o are given, it is assumed that

$$f_s = 5\% \ \text{(of telescope aperture)}. \qquad (4\text{-}4)$$

For the illumination a parabolic (voltage) taper with pedestal p is assumed.

$$I(r) = 1 - (1-p)\ r^2 \quad \begin{cases} 1 \text{ at center, } r = 0 \\ p \text{ at rim, } r = 1 \end{cases} \qquad (4\text{-}5)$$

with a (power) edge taper of T = -20 log p. For this estimate adopting T = 13 dB yields p = 0.224 and

$$I(r) = 1 - 0.766\ r^2. \qquad (4\text{-}6)$$

The shadow in the outer part is actually curved, but it is replaced by a straight line (which is on the safe side). The intersection of leg and surface is at r = 0.444 (800 in from center); the variation of this value with varying h is neglected. The weighted surface blocking then can be written as

* Weighted with the illumination function.

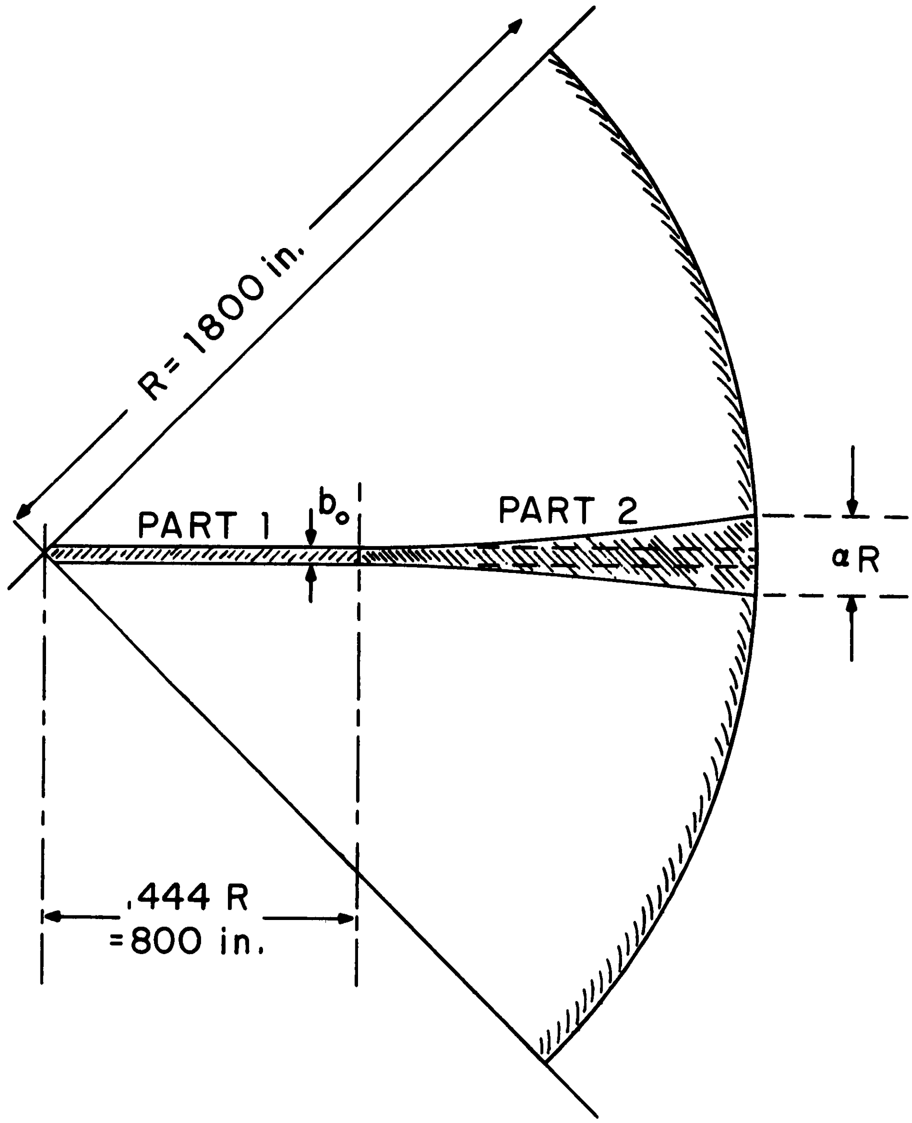

Fig. 4-14. The shadow of a feed leg, and one quadrant of the aperture. Part 1: shadow for incident rays. Part 2: shadow for illumination Width at rim: $\alpha R = 0.616\ b_o R/h + 0.432\ b_o$. Illumination-weighted shadow fraction (of aperture): $f_s = 0.130\ b_o/h + 0.000787\ b_o$.

$$f_s = \frac{\int_0^1 I(r)\,\frac{b_o}{rR}\,r\,d\,r + \int_{0.444}^{1} I(r)\,(\alpha - b_o/R)\,\frac{r - 0.444}{1 - 0.444}\,r\,dr}{\frac{\pi}{2}\int_0^1 I(r)\,r\,dr}\,. \tag{4-7}$$

The evaluation of all integrals yields

$$f_s = 0.130\ b_o/h + 0.000787\ b_o. \tag{4-8}$$

Or, if f_s and b_o are given, h is found as

$$h = \frac{0.130\ b_o}{f_s - 0.000787\ b_o}\,. \tag{4-9}$$

For b_o 30 in is used plus 4.5 in for the chord diameter; thus $b_o = 34.5$ in. Demanding that $f_s = 0.05$, it is found that h = 197 in. Thus, the vertical distance h of the upper chords must be at least about

$$h = 200\ \text{in} = 16.7\ \text{ft}. \tag{4-10}$$

This distance results in 5% area blocking, which gives 10% gain loss (or 0.46 dB). This holds for longer wavelengths ($\lambda > 1$ m) where the build-up feed leg acts as a closed area. For shorter wavelengths, the holes between the lacing will become transparent, resulting in a smaller gain loss of about 6% (0.27 dB). A further increase of h does not help much. For example, demanding that $f_s = 4\%$, h = 350 in = 29 ft is required, resulting in a very awkward design.

(b) The suspension members. The three types of suspension members, supporting the reflector on the elevation bearings, are listed below, with L = length, A_{eq} = equivalent bar area (of a solid rod of same stiffness), S_m = maximum stress in any telescope orientation, 1/r = slenderness ratio of single chord if 12 segments were used. The last column mentions the problem which makes a special design necessary.

Type	Points	L Inch	A_{eq} si	n	S_m ksi	1/r	Problem
a) Side support	45-58	878	150	4	9.4	10	Small angle with 45-46 at 45
b) Down support	57-58	1609	360	2	6.0	11	Small angle with 47-57 at 57
c) Center support	38-58	1206	100	2	11.2	17	Must cross 47-57 without touching

All these members have very large bar area and small 1/r ratio, which means they should have fewer than 12 segments. And unlike the normal members, they should have rectangular cross section (not triangular), and should be made from heavy standard sections (not pipes). Since the support has only little influence on homology, no exact values of A_{eq} and no special types of lacing are required, thus all details are left to the design engineer. The bar area should meet the above requirements within $\pm$ 30%, say, and the lacing should have as little weight as possible. With respect to the problems listed above, the following suggestions are made:

(1) The side support splits in two parts (up and down) at least toward point 45; such that its upper and lower parts leave enough clearance for the end of member 45-46 in between, Fig. 4-15a.

(2) The two down supports join in a horizontal piece which holds point 57 from underneath, Fig. 4-15b.

(3) The center support is split in two parts (right and left) all the way through, with a clearance of at least 60 in in between for member 47-57, Fig. 4-15c.

(c) Central member supporting the optical reference platform. If a reference system with gyro compass and tilt sensor could be used, the system could be mounted at the vertex of the surface and no special design would be needed for member 38-57. But at present, it is not established that this system would work, and thus an optical system is considered.

The optical reference platform must be located exactly at the crossing of the two telescope axes, which means in the center of the center support 58-58a. The system needs around it, in the lower hemisphere, as much clearance

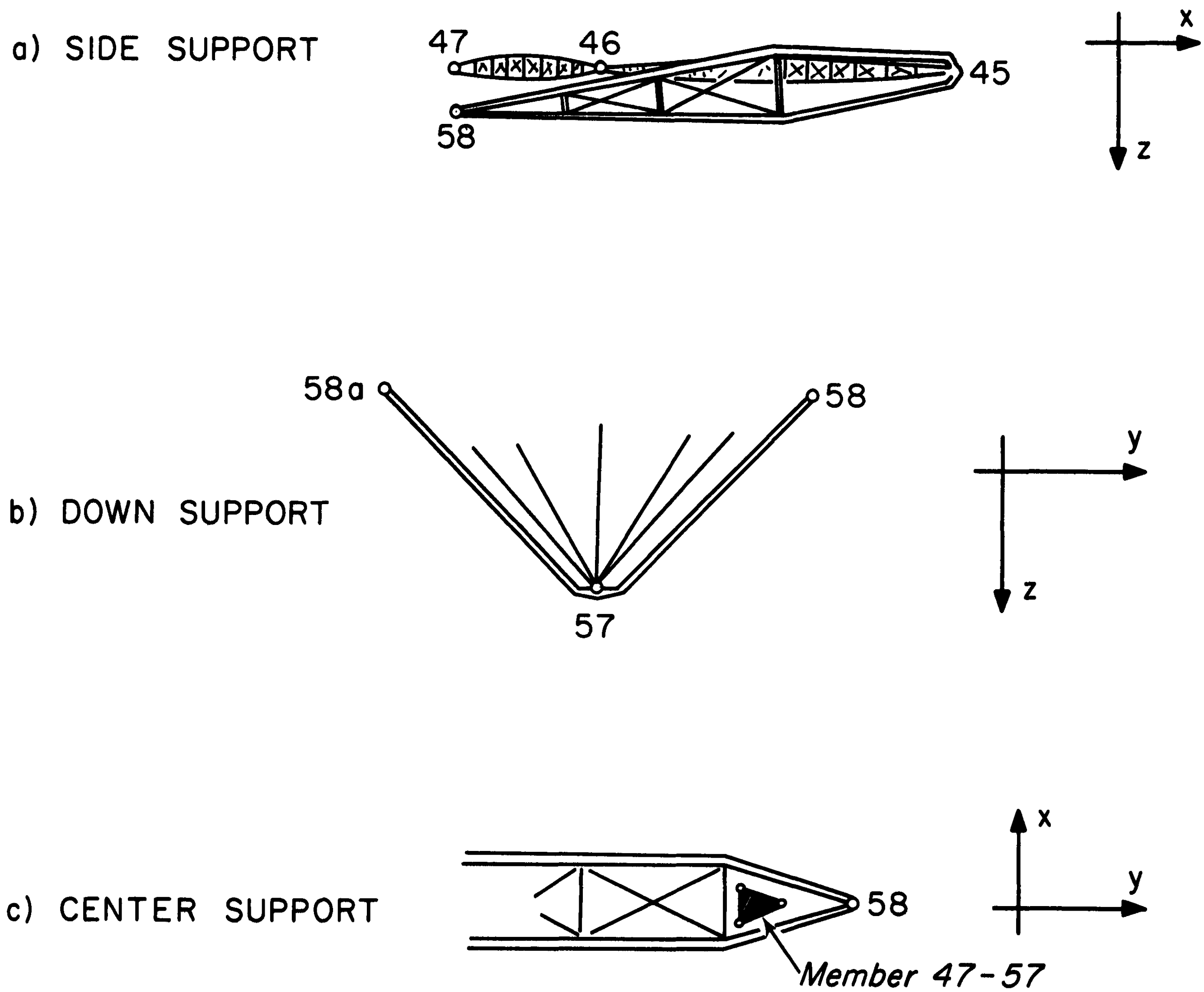

Fig. 4-15. Suggestions for suspension members.

as possible (blocking of light rays). For this purpose the member 38-57 should be divided into two parts. The lowest part, 57-59, should be a normal built-up member. The upper part should be a quadratic pyramid upside-down, with its top at point 59 and its base supplied by the widely split-up center support 38-58. The four sides of the pyramid could be single standard pipes, of say 10 in diameter. If the base of the pyramid has a side length of 110 in, the shadow of these pipes would then coincide with the shadow of four cone members (46-57) and would be of the same width too, thus giving no additional shadow.

Point 38 carries a maximum downward load of 340 kip (stow position, 20 lb/ft^2 of snow, plus dead loads). If that should be too much to be taken up by the beam action of the center support (38-58), an additional point 61 above 38 would be needed, at the top of another pyramid, connected to all four points 60 and to 38. Structurally, this can be done, since 38 has no upward member along the Z-axis, and since all its horizontal members (to 21, 22, 40, and 41) leave 38 at azimuth angles of 22.5° and 67.5°, whereas member 60-61 leave 61 at 45°.

If possible structurally, it would be best if the reference platform, with respect to all torsional deformations, could follow the movements of the telescope members (38-21, 22, 40, and 41) and not that of the support (38-58). But since the difference will be only small, no emphasis is placed on this demand.

Since the platform must be right on the elevation axis, point 38 must be somewhat above it, giving enough clearance for the elevation movement of the platform. A possible arrangement of central member, platform, and center support is shown in Fig. 4-16.

D. The Reflector Structure

1. General

In May 1969 the design of the 300 ft diameter reflector for the homology telescope has approached such a degree of completion that prediction of achievement of desired performance characteristics during the course of the final design can be made with confidence.

The philosophy leading to the homology concept and the computing technique applied are described in Chapters 2 and 3 and are not repeated here. This chapter defines primarily the basic physical design of the reflector

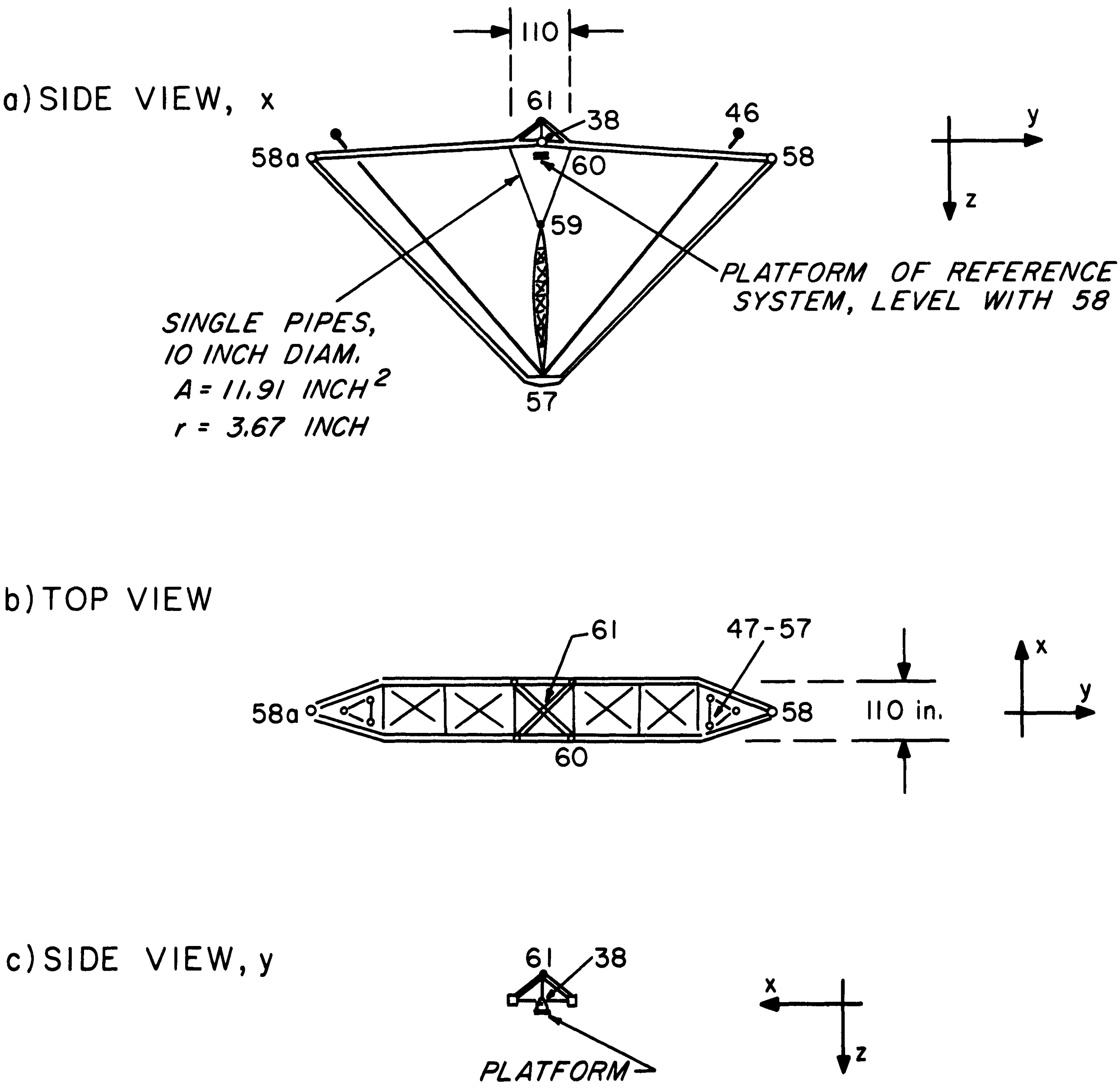

Fig. 4-16. Central member (38-57) and optical reference platform.

structure and lists the results of a comprehensive computer analysis. A dynamic analysis of the reflector structure has been performed by Simpson, Gumpertz & Heger, in addition to the basic static-homology-design analysis. The results of this dynamic analysis, in which the dynamic behavior of the reflector structure, independent of the tower structure, is investigated, are also shown in this chapter.

The structural configuration of the reflector is shown in Figs. 4-6 and 4-7, which are attached to this report.

2. Applied design constants

Focal length	: 128 ft
Diameter of reflector	: 300 ft
Number of surface points	: 57
Number of structural points	: 149
Number of built-up members	: 644
Weight of reflector	: 1170 tons*
Wind load during operational condition	: 1.29 lb/ft^2
Wind load during survival condition	: 20.00 lb/ft^2
Maximum dead load at surface points	: 3428.60 lb
Maximum snow or ice load on surface	: 20.00 lb/ft^2
Modulus of elasticity	: 29x10 lb/in^2
Specified yield strength	: 33x10 lb/in^2
Density of material	: 0.283 lb/in^3

3. Coordinates of member joints

Due to the symmetry of the reflector, only one quadrant of the structure was analyzed. Weight factors used are in the last column of the following table and are defined as follows:

MU = 0	A ficticious point, located in the middle of a member. Member perpendicular to either X-Z or Y-Z plan.
NU = 1	This point is located on the Z-axis and is unique, without a counterpart.
MU = 2	The point is located on either X-Z or Y-Z plan and has one counterpart,

* Final estimate is 1280 tons including gear and feed assembly.

MU = 4 Located in space this point has three counterparts. The following table contains the coordinates of member joints in one quadrant. A mirror image of this quadrant forms a complete reflector structure.

4. Built-up member details

The conceptual design of the built-up members is described in detail in Chapter 4, § C.

The following tables list the results of the homology computer analysis and includes detailed information on cross-sectional area and length for each built-up member. Location of the members may be seen in Figs. 4-6 and 4-7.

Some members will have to be modified in accordance with considerations outlined in Chapter 4, § C, paragraphs 2 and 3, and the reflector design will be repeated until all special requirements are met.

5. Results of dynamic analysis

The reflector structure was analyzed as a frame model in the zenith pointed position. The elevation bearings were assumed to be infinitely rigid in X-Y and Z-direction but free in rotational direction. The elevation drive was assumed to be infinitely rigid in tangential direction, but free in radial and perpendicular directions.

The frequencies thus computed are given in the table below, and the corresponding normalized modes are reported directly from the computer output.

Mode No.	Frequency C.P.S.	Mode Description
1	2.58	Rocking in X-direction
2	2.62	Rocking in Y-direction
3	3.61	Symmetric expansion
4	2.76	Rotation about Z-axis
5	3.61	Vertical along Z-axis (up and down)

6. Member joints

The design of the member-joints will be such that maximum joint flexibility is assured, while sufficiently low stress levels in the member ends must be maintained. Each joint must be individually analyzed and designed to deal with the imposed moments and loads; thereafter the joint stiffnesses must be determined for inclusion in the final homology analysis.

So far the effect of joint stiffnesses have not been included in the homology analysis or the dynamic analysis of the reflector structure. It is estimated that the joint stiffness will have little, if any, effect on the homologous deformations as the built-up members are relatively long and slender and have small moments of inertias in the vicinity of the joints.

Fig. 4-17 shows the proposed concept of a typical member joint and end connection detail. As can be seen, it is proposed that these joints be prefabricated and that the members be fitted and either welded or bolted to the joints during erection at the site.

Several joints, such as joint No. 45, will have to be of a special design to facilitate the desired function or to avoid structural interference.

E. <u>The Tower Structure</u>

1. <u>General</u>

The concept of the tower structure was selected on the basis of specified wind deformations, stability during survival load conditions, and desired dynamical behavior at lowest possible weight.

In addition, the tower structure should be able to accept stresses resulting from the vertical and horizontal irregularities of the azimuth turntable during rotation around the pintle bearing, which constrains the tower structure in both lateral and radial directions, without imposing undue strain on the reflector structure.

The conceptual design shown in Figs. 4-4 and 4-5 fulfills these requirements at a minimum weight since the design includes long, pin-ended, built-up members which are similar to the reflector members. The advantages of this type of design are: First, this approach is economical with respect to the stiffness-weight as well as maximum force-weight ratios, and second, the analysis of this structure can be broken down into two independent parts. The tower structure can be analyzed, considering each built-up member as a single rod with given area and density while the built-up members can be analyzed separately.

As can be seen from Figs. 4-4, 4-5, and 4-18, the tower base forms a symmetrical hexagon whose corners are the suspension points for four drive trucks and two auxiliary trucks. The structural members connecting at

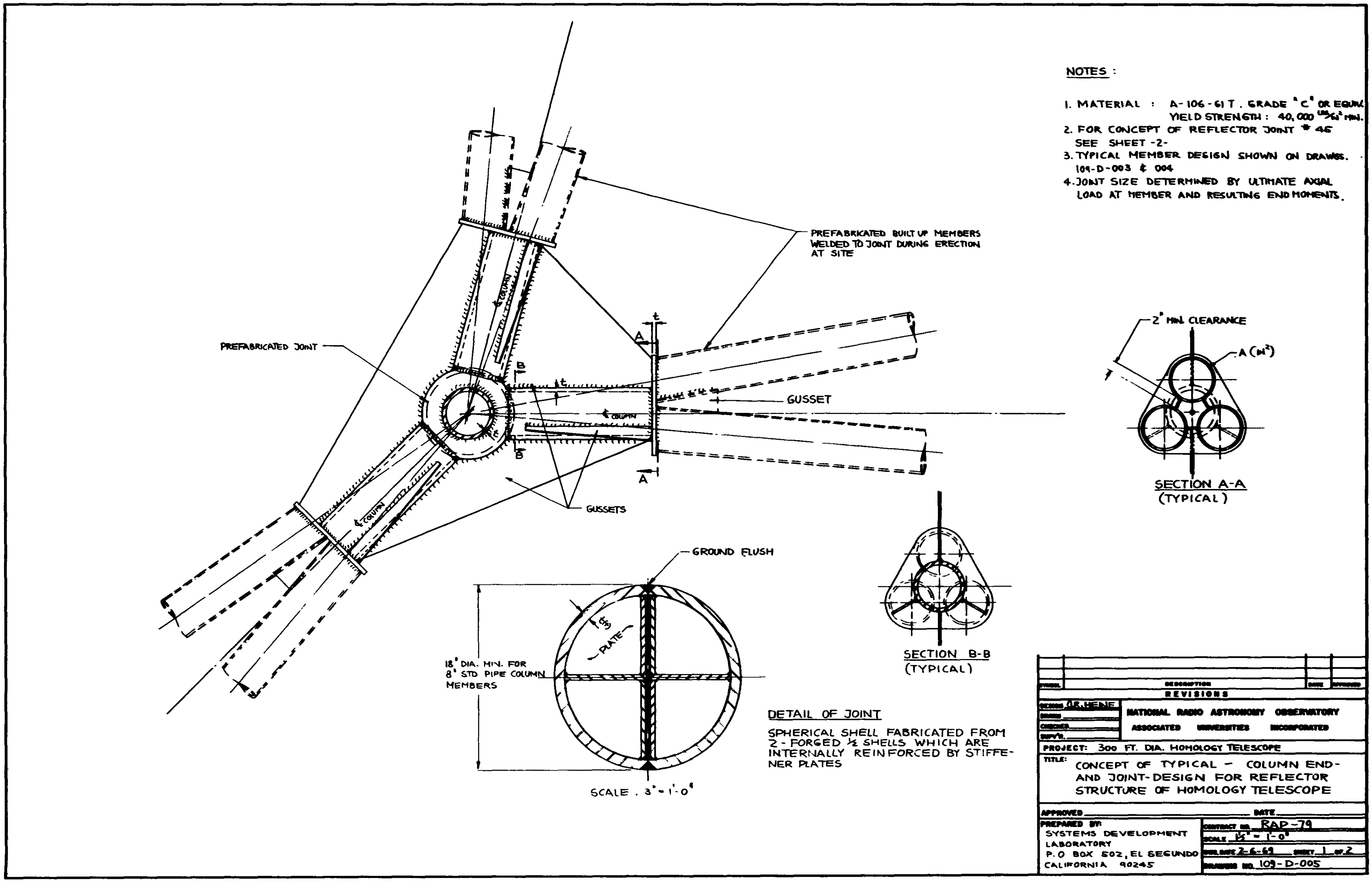

Fig. 4-17. Concept of typical column end and joint design for reflector structure of homology telescope.

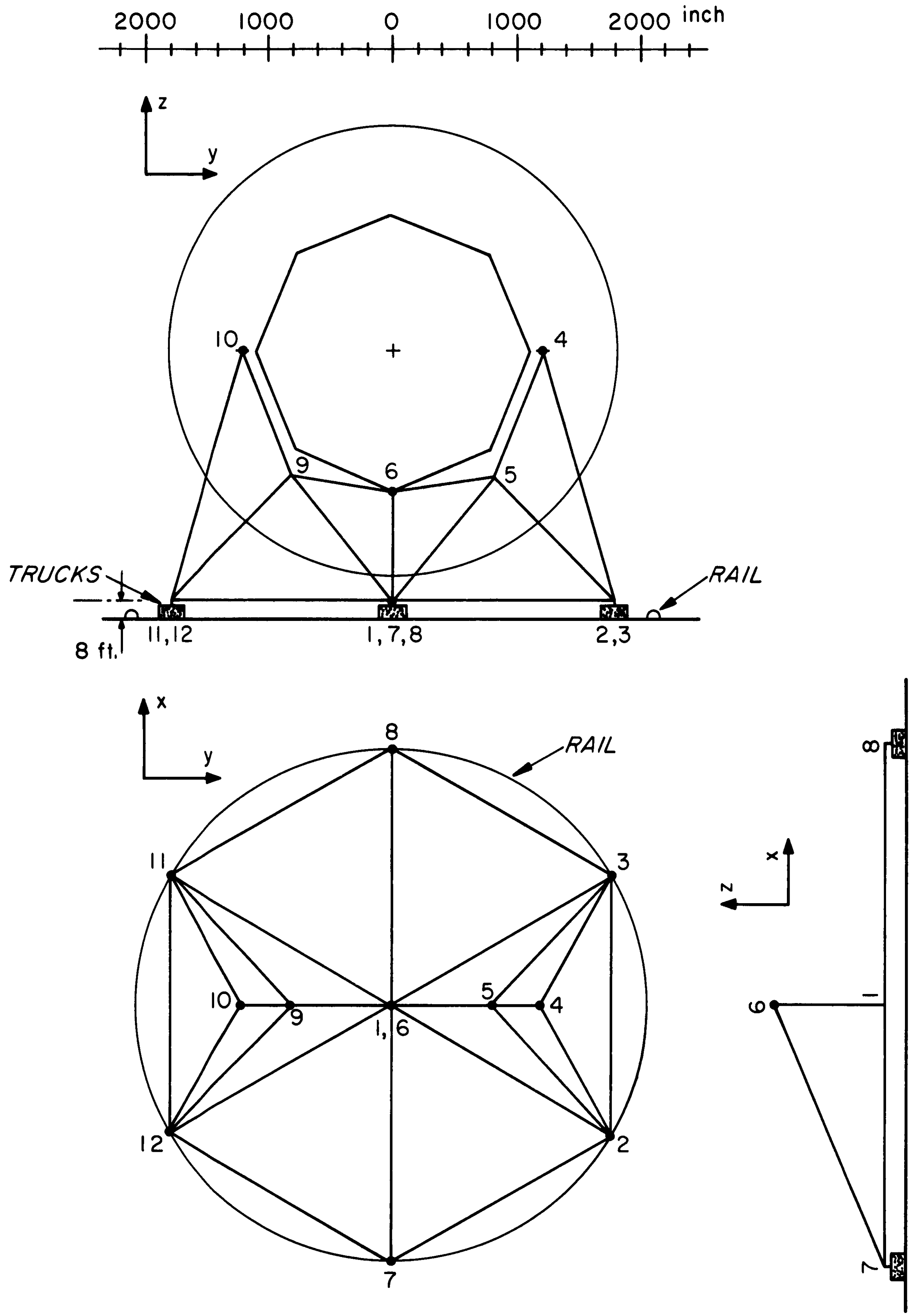

Fig. 4-18. Tower geometry.

point 8 in Fig. 4-18 have only one purpose, that is to reduce the maximum horizontal loads in the base plane during survival conditions since joint 8 cannot accept vertical loads.

Actually these members and joint 8 could be eliminated, which, however, would increase the maximum loads in the remaining base members during survival conditions and would require that these members be made somewhat heavier. It may be more economical to make the tower structure heavier and to eliminate three built-up members plus one supporting truck at the same time. The alternative configurations will be reviewed in the detail design stage and a final decision arrived at.

2. Geometry of the tower structure

The geometry of the tower structure is shown in Fig. 4-18, and the coordinates are given in the following table:

Coordinates (in)			
Joint	X	Y	Z
1	0	0	0
2	-1039	1800	0
3	1039	1800	0
4	0	1200	1896
5	0	650	875
6	0	0	736
7	-2078	0	0
8	2078	0	0
9	0	- 650	875
10	0	-1200	1896
11	1039	1800	0
12	-1039	-1800	0

3. Built-up member details

The conceptual design of the built-up members for the tower structure is described in detail in Chapter 4, § C. Nominal bar areas, lengths, and types are shown in the following table.

POINT	COORDINATES X	Y	Z	POINT LOADS	MU
1	325.000	0.0	-17.192	1714.30	2
2	229.810	229.810	-17.192	3428.60	4
3	0.0	325.000	-17.192	1714.30	2
4	800.000	0.0	-104.167	1714.30	2
5	692.820	400.000	-104.167	3428.60	4
6	400.000	692.820	-104.167	3428.60	4
7	0.0	800.000	-104.167	1714.30	2
8	1275.000	0.0	-264.587	1714.30	2
9	1177.946	487.921	-264.587	3428.60	4
10	901.561	901.561	-264.587	3428.60	4
11	487.921	1177.946	-264.587	3428.60	4
12	0.0	1275.000	-264.587	1714.30	2
13	1700.000	0.0	-470.377	1714.30	2
14	1616.796	525.329	-470.377	3428.60	4
15	1375.329	999.235	-470.377	3428.60	4
16	999.235	1375.329	-470.377	3428.60	4
17	525.329	1616.796	-470.377	3428.60	4
18	0.0	1700.000	-470.377	1714.30	2
19	0.0	0.0	-0.0	857.15	1
20	390.000	0.0	260.000	0.0	0
21	390.000	200.000	260.000	0.0	4
22	200.000	390.000	260.000	0.0	4
23	0.0	390.000	260.000	0.0	0
24	917.630	0.0	123.670	0.0	0
25	917.630	245.878	123.670	0.0	4
26	630.000	630.000	352.000	0.0	4
27	245.878	917.630	123.670	0.0	4
28	0.0	917.630	123.670	0.0	0
29	1471.178	0.0	35.050	0.0	2
30	1432.000	285.000	-64.950	0.0	4
31	1321.148	547.237	35.050	0.0	4
32	1139.113	761.131	-64.950	0.0	4
33	948.193	948.193	35.050	0.0	4
34	761.131	1139.113	-64.950	0.0	4
35	547.237	1321.148	35.050	0.0	4
36	285.000	1432.000	-64.950	0.0	4
37	0.0	1471.178	35.050	0.0	2
38	0.0	0.0	600.000	0.0	1
39	434.223	0.0	650.000	0.0	0
40	434.223	179.861	650.000	0.0	4
41	179.861	434.223	650.000	0.0	4
42	0.0	434.223	650.000	0.0	0
43	1071.820	0.0	450.000	0.0	2
44	914.856	378.946	450.000	0.0	4
45	757.891	757.891	450.000	0.0	4
46	378.946	878.946	450.000	0.0	4
47	0.0	1000.000	450.000	0.0	2
48	757.891	0.0	450.000	0.0	0
49	0.0	757.891	450.000	0.0	0
50	0.0	0.0	-1536.000	0.0	1

51	350.000	200.000	870.000		0.0	4
52	350.000	0.0	870.000		0.0	[illegible]
53	996.382	0.0	866.692		0.0	2
54	765.474	0.0	1221.664		0.0	2
55	415.124	0.0	1459.526		0.0	2
56	0.0	0.0	250.000		0.0	1
57	0.0	0.0	1543.164		0.0	1
58	0.0	1200.000	471.136		0.0	2

BAR	POINT	NU	L	AREA
1	1- 2	4	248.74	5.00
2	1- 4	3	482.90	2.50
3	1- 5	4	550.32	5.00
4	1-21	4	347.94	3.85
5	1-56	3	420.73	2.36
6	2- 3	4	248.74	5.00
7	2- 5	4	500.91	5.00
8	2- 6	4	500.91	5.00
9	2-19	4	325.45	5.00
10	2-21	4	321.53	1.92
11	2-22	4	321.53	2.71
12	2-56	4	420.73	6.62
13	3- 6	4	550.32	5.00
14	3- 7	3	482.90	2.50
15	3-22	4	347.94	2.36
16	3-56	3	420.73	1.42
17	4- 5	4	414.11	5.00
18	4- 8	3	501.36	2.50
19	4- 9	4	637.69	5.00
20	4-21	4	583.71	3.65
21	4-25	4	355.25	3.70
22	5- 6	4	414.11	5.00
23	5- 9	4	518.47	5.00
24	5-10	4	566.45	5.00
25	5-21	4	514.12	2.51
26	5-25	4	355.25	2.52
27	5-26	4	514.72	12.88
28	6- 7	4	414.11	5.00
29	6-10	4	566.45	5.00
30	6-11	4	518.47	5.00
31	6-22	4	514.12	2.90
32	6-26	4	514.72	13.82
33	6-27	4	355.25	4.09
34	7-11	4	637.69	5.00
35	7-12	3	501.36	2.50
36	7-22	4	583.71	4.19
37	7-27	4	355.25	11.87
38	8- 9	4	497.48	5.00
39	8-13	3	472.20	2.50
40	8-14	4	659.65	5.00
41	8-25	4	582.16	11.78
42	8-29	3	358.15	1.09
43	9-10	4	497.48	5.00
44	9-14	4	486.15	5.00
45	9-15	4	585.45	5.00
46	9-25	4	526.40	14.52
47	9-26	4	837.02	4.18
48	9-30	4	381.54	2.46
49	9-32	4	340.60	2.67
50	10-11	4	497.48	5.00

51	10-15	4	525.69	5.00
52	10-16	4	525.69	5.00
53	10-25	4	762.18	6.30
54	10-27	4	762.18	7.60
55	10-33	4	306.81	2.12
56	11-12	4	497.48	5.00
57	11-16	4	585.45	5.00
58	11-17	4	486.15	5.00
59	11-26	4	837.02	3.82
60	11-27	4	526.40	18.11
61	11-34	4	340.60	3.19
62	11-36	4	381.54	3.17
63	12-17	4	659.65	5.00
64	12-18	3	472.20	2.50
65	12-27	4	582.16	7.96
66	12-37	3	358.15	1.16
67	13-14	4	531.88	5.00
68	13-29	3	554.81	2.24
69	13-30	4	563.40	2.69
70	14-15	4	531.88	5.00
71	14-30	4	506.24	4.49
72	14-31	4	585.96	1.83
73	14-32	4	669.44	5.35
74	15-16	4	531.88	5.00
75	15-31	4	680.22	2.28
76	15-32	4	526.18	4.40
77	15-33	4	663.71	2.28
78	16-17	4	531.88	5.00
79	16-33	4	663.71	2.56
80	16-34	4	526.18	5.22
81	16-35	4	680.22	2.81
82	17-18	4	531.88	5.00
83	17-34	4	669.44	3.93
84	17-35	4	585.96	2.45
85	17-36	4	506.24	3.46
86	18-36	4	563.40	3.23
87	18-37	3	554.81	2.07
88	19-21	4	509.61	1.76
89	19-22	4	509.61	2.61
90	19-56	1	250.00	4.25
91	20-21	2	200.00	3.09
92	21-22	4	268.70	1.77
93	21-26	4	500.96	1.81
94	21-38	4	554.71	4.35
95	21-40	4	393.02	4.76
96	21-43	4	735.51	5.39
97	22-23	2	200.00	4.38
98	22-26	4	500.96	1.92
99	22-38	4	554.71	10.70
100	22-41	4	393.02	7.05

101	22-47	4	669.48	4.64
102	24-25	2	245.88	5.77
103	25-26	4	531.43	5.57
104	25-29	4	612.15	2.99
105	25-30	4	549.26	8.28
106	25-32	4	591.71	3.19
107	25-40	4	717.68	2.70
108	25-43	4	436.72	10.41
109	25-44	4	352.43	2.95
110	25-45	4	627.83	11.92
111	26-27	4	531.43	3.87
112	26-40	4	574.25	2.39
113	26-41	4	574.25	2.29
114	26-44	4	392.14	3.65
115	26-46	4	366.89	5.18
116	27-28	2	245.88	9.81
117	27-34	4	591.71	3.03
118	27-36	4	549.26	4.89
119	27-37	4	612.15	3.88
120	27-41	4	717.68	4.24
121	27-45	4	627.83	16.32
122	27-46	4	354.53	5.30
123	27-47	4	416.81	24.96
124	29-30	4	304.56	1.53
125	29-45	3	575.91	2.93
126	30-31	4	301.76	1.85
127	30-43	4	690.02	9.89
128	30-44	4	735.82	4.07
129	31-32	4	298.14	1.82
130	31-44	4	604.63	2.41
131	32-33	4	285.38	4.43
132	32-44	4	679.36	5.45
133	32-45	4	640.71	11.66
134	33-34	4	285.38	4.27
135	34-35	4	298.14	2.26
136	34-45	4	640.71	15.01
137	34-46	4	692.04	17.87
138	35-36	4	301.76	1.48
139	35-46	4	629.32	2.15
140	36-37	4	304.56	1.85
141	36-46	4	761.49	10.26
142	36-47	4	730.08	13.37
143	37-47	3	627.85	3.77
144	38-40	4	472.65	24.22
145	38-41	4	472.65	21.72
146	38-51	4	485.18	5.54
147	38-57	1	943.16	10.97
148	38-58	3	1206.90	58.62
149	39-40	2	179.86	6.65
150	40-41	4	359.72	7.20

151	40-43	4	692.01	15.50
152	40-45	4	692.01	7.71
153	41-42	2	179.86	4.76
154	41-45	4	692.01	11.60
155	41-47	4	626.46	6.46
156	43-44	4	410.17	49.47
157	43-51	4	858.73	22.76
158	43-53	3	423.47	15.67
159	44-45	4	410.17	31.88
160	45-46	4	397.81	81.96
161	45-48	2	757.89	12.11
162	45-49	2	757.89	40.53
163	45-50	4	2256.77	23.88
164	45-57	4	1530.95	59.26
165	45-58	4	877.67	154.35
166	46-47	4	397.81	41.11
167	47-57	3	1481.56	30.81
168	51-52	2	200.00	4.73
169	51-53	4	676.62	17.66
170	51-54	4	579.90	21.32
171	51-55	4	625.92	21.35
172	51-57	4	784.63	31.80
173	53-54	3	423.47	25.10
174	54-55	3	423.47	33.89
175	55-57	3	423.47	48.97
176	56-21	4	438.41	2.14
177	56-22	4	438.41	3.14
178	57-58	3	1609.11	180.00

Member Details			
Member	A_n	L	t
1-2, 1-12	75	2078	2
1-3, 1-11	70	2078	2
1-5, 1-9	140	1090	1
1-6	30	736	1
1-7	100	2078	1
1-8	30	2078	2
2-3, 11-12	30	2078	2
2-4, 12-10	130	2230	2
2-5, 12-9	35	1780	1
2-7, 12-7	40	2078	2
3-4, 11-10	130	2230	2
3-5, 11-9	35	1780	1
3-8, 11-8	30	2078	2
4-5, 10-9	140	1146	1
5-6, 9,6	30	657	1
6-7	100	1950	1

where:

A_n = effective bar area (in^2)

L = member length (in)

t = member type

The computed weight of the tower is approximately 620 tons.

4. Member joints

The member joints for the tower structure in general will be similar in design to the joints of the reflector structure described in paragraph 6, Chapter 4, § D.

F. The Trucks and Bearings

1. The trucks

The foundation and track concept finally adopted as the best suited consists of 175 lb/yd heat treated crane rail supported on a reinforced concrete slab, having rail centers of approximately 5 ft.

The truck assembly contains eight double-flanged, 36 in diameter "rim toughened" crane wheels arranged in pairs at 4 ft distance in pivot mounted bogies. The bogies are mounted in side frames connected by a transom structure containing a torque tube.

The load is transferred into the transom structure by means of a saddle arrangement, having a spherically shaped bearing contact area. The load is evenly divided among all eight wheels as a result of the structure arrangement of the truck assembly. The truck dimensions are 15 1/2 ft x 6 3/4 ft x 7 1/2 ft height and the assembled weight is estimated to be 45 tons. Four wheels of the truck are independently driven by means of spur gear trains connecting to the axle. Each bogie contains a pneumatically released, spring applied braking arrangement exerting a brake force on each wheel. The trucks are designed to take both upward and downward loads.

The maximum upward loads however can only be taken in designated stow positions containing an anchor arrangement. Due to the equalizing arrangement, rail surface contour variations will not cause significant wheel load variations.

Four such truck assemblies will be required under the tower structure to support the weight of the telescope structure and the loads generated by wind forces and dynamic forces. Two additional trucks with reduced load capacity will be required to provide for auxiliary support. The four drive wheels on each truck will have sufficiently high contact loads, even under "drive to stow" condition to generate the required traction. There will be no need for counterweight since the number of wheels is kept to a minimum, resulting in sufficiently high wheel rail contact loads and since upward loads can be taken in the stow position during survival load conditions. The use of a concrete slab, which permits attainment of a short wheel base, results in a maximum vertical stiffness of the truck assembly/rail/slab/soil combination.

The truck concept is shown in Fig. 4-19.

2. <u>The pintle bearing arrangement</u>

Lateral loads on the telescope structure due to wind or other external forces will be reacted by a central pintle bearing arrangement; the rails will not be subjected to any horizontal load. The bearing arrangement is required additionally to support part of the dead load and vertical wind forces.

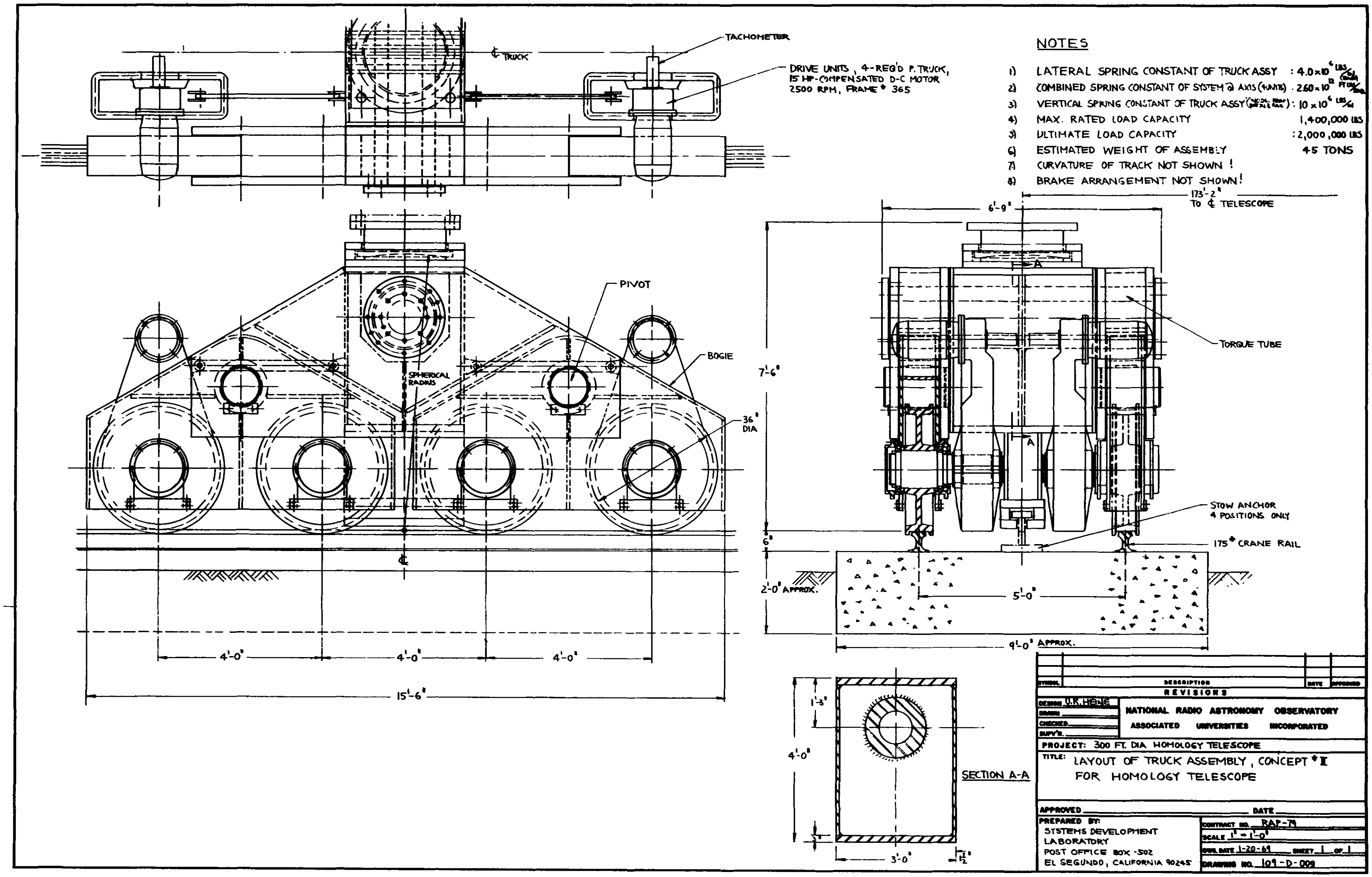

Fig. 4-19. Layout of truck assembly, concept No. II, for homology telescope.

It is calculated that the maximum loads on the pintle bearing will be about $1.6x10^6$ in lateral direction and $2.5x10^6$ lbs in the vertical direction during survival load conditions.

Since the azimuth turntable plane does not require a high degree of accuracy in respect to wobble or tilt (the reference system provides an accurate base from which the pointing position is controlled), a fair amount of angular misalignment can be tolerated. The bearing arrangement must therefore be self-aligning in order to minimize strain in the tower structure which could affect the accuracy of the telescope. In order to meet the above three demands, the application of a spherical roller thrust bearing, capable of supporting simultaneously both thrust and radial loads, will be required. The type of bearing must be axially preloaded, which can be accomplished by means of a self-aligning cylindrical thrust bearing and suitable clamping device.

It is possible to arrange this combination bearing in such a way that their centers of alignment rotation coincide. This type of bearing arrangement must be force lubricated and provisions for this can easily be made. The bearing assembly should contain a hollow kingpin through which power, signal, and control cables can pass.

Fig. 4-20 shows the envisioned pintle bearing arrangement, including foundation and housing. The housing can be jacked up against the telescope structure so that the required dead load can be imposed on the bearing arrangement.

3. <u>The elevation bearing arrangement</u>

Both the tower mount and the reflector structures are relatively flexible and care must be taken that the connection between the two structures will not impose structural deformation due to its own rigidity on the reflector, for obvious reasons.

An effective flexible bearing arrangement which will permit equal sharing of the loads on either side of the elevation axis without introducing large moments into the reflector structure or towers is attained by mounting two self-aligning spherical roller thrust bearings so that their center of spherical curvature coincides on either tower side. This setup, which is axially preloaded, permits simultaneous acceptance of both radial and axial loads while eliminating radial or axial play and permitting misalignments due to mounting inaccuracies or load flexures.

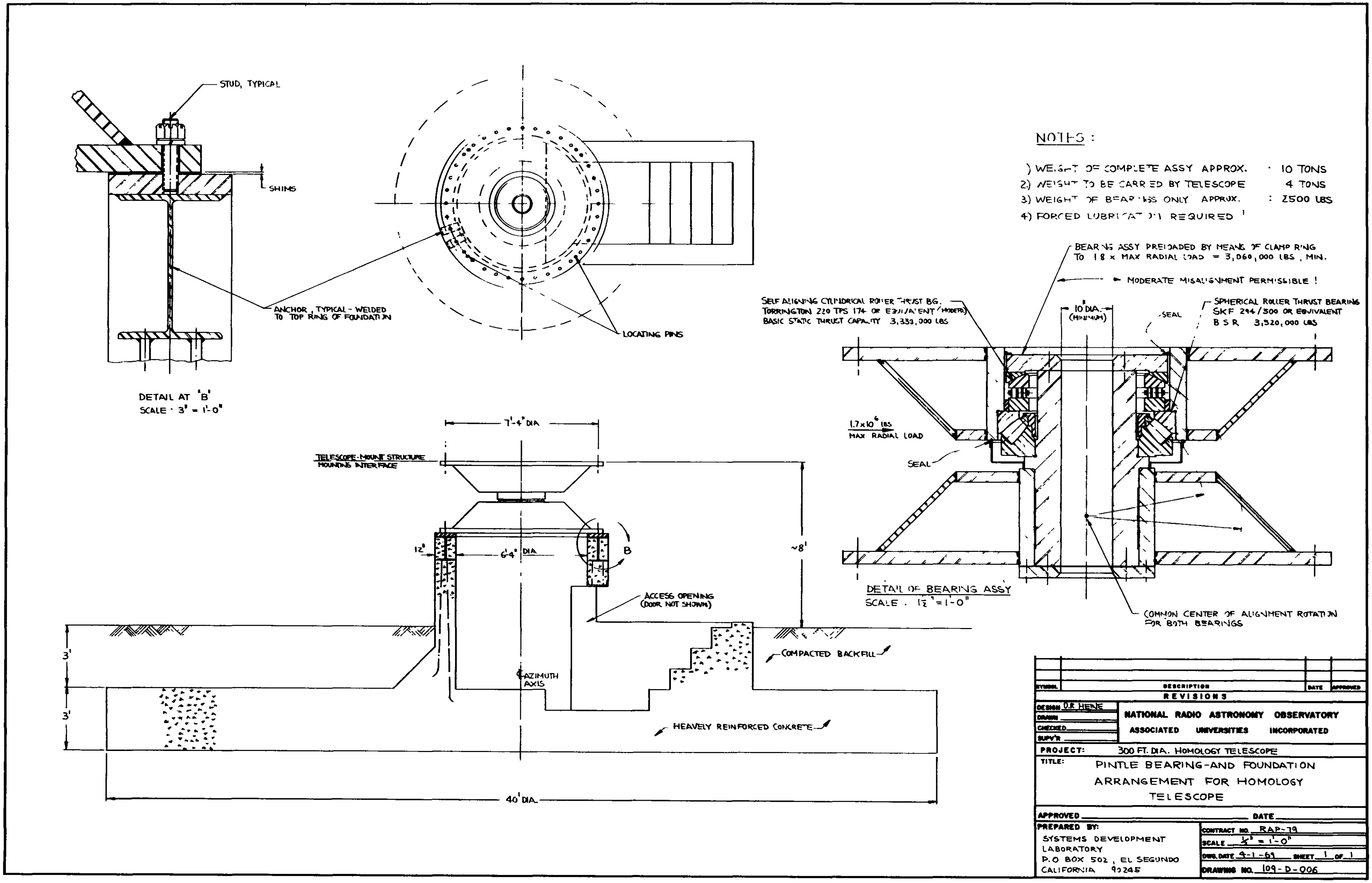

Fig. 4-20. Pintle bearing and foundation arrangement for homology telescope.

Each of the two elevation bearing arrangements can take loads in any direction and will share any such imposed loads. An outline of this concept is shown in Fig. 4-21.

G. The Foundation and Track

1. Turntable base

Originally two circular concentric standard railroad tracks (4 rails) supported on wood ties with gravel ballast were thought to be the most suitable turntable base. It was proposed to mount the telescope structure on heavy-duty gondolas (with suspension springs removed) running on these standard railroad tracks. The concept was found to be impractical primarily due to the length of the gondolas which required the application of unusually long, heavy and relatively flexible walking beams for the formation of a suitable truck assembly.

A second concept proposed the use of standard railroad truck assemblies (consisting each of 2 axles, 4 wheels, journal boxes, side frames, and bolsters) and positioning 8 units each as closely as possible together (4 on each track) to form the base for a truck assembly. This resulted in a more manageable overall truck size with relative short walking beams, which could be made sufficiently stiff.

An analysis of the obtainable foundation and truck stiffness indicated that this scheme would be suitable for the intended purpose and a subsequent dynamic analysis of the complete telescope structural system showed that the flexibility of this turntable arrangement would affect the lowest system resonance only to a permissible degree.

At the same time the feasibility of another concept utilizing a single (2 rails only) track consisting of 175 lb/yd heat-treated crane rails supported on a 2 ft thick by 9 ft wide reinforced concrete slab was investigated and was subsequently found to be superior in performance and lower in cost.

The configuration permits the application of fewer wheels per truck due to the higher load capacity of the uniformly supported crane rail and wider crane wheels as only eight 36 in diameter crane wheels are required against thirty-two 38 in diameter heavy-duty railroad wheels per truck assembly.

This reults in shorter, more compact, lighter and yet stiffer truck assemblies which were found to be also less costly due to the simplification

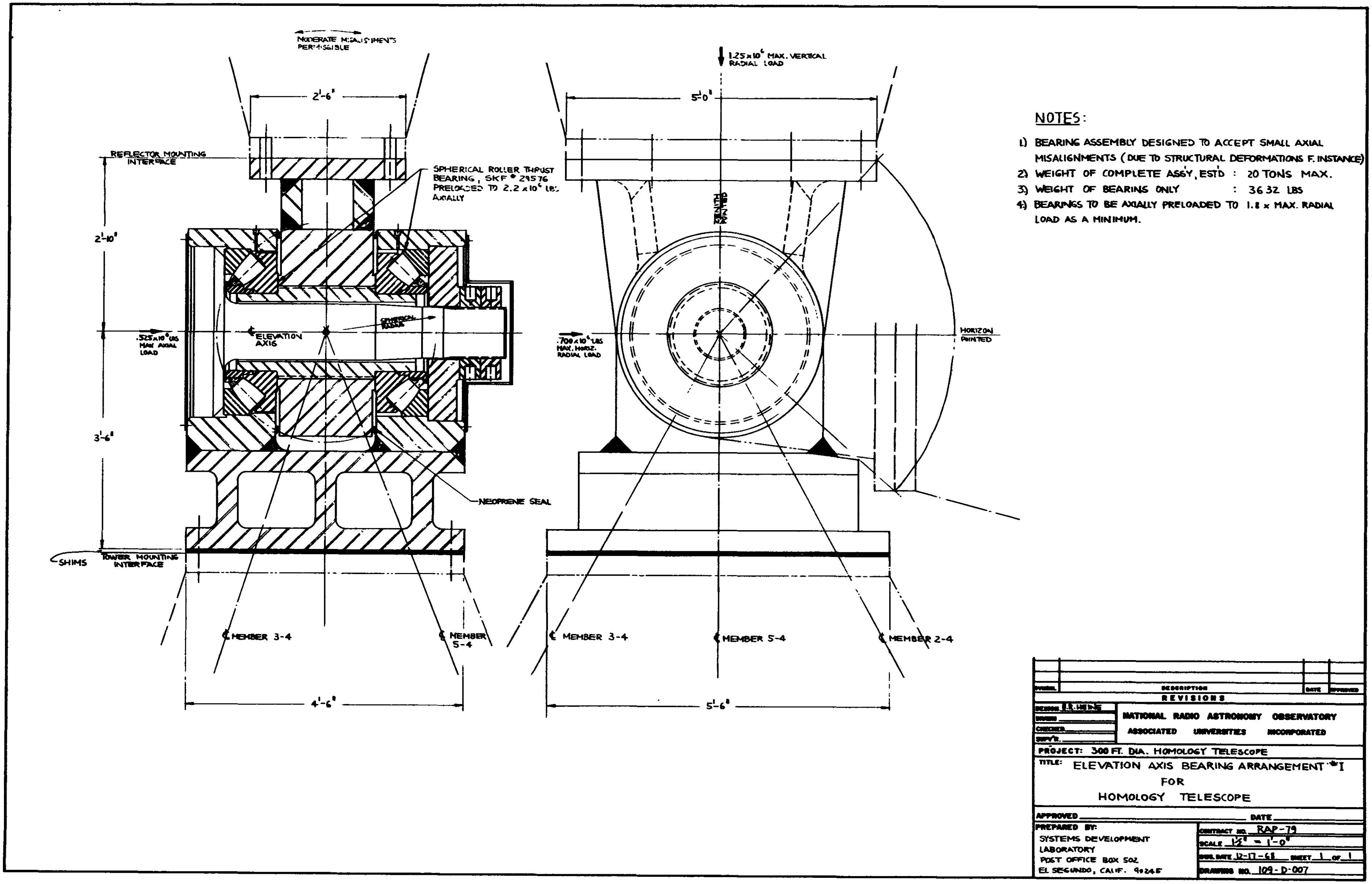

Fig. 4-21. Elevation axis bearing arrangement No. 1 for homology telescope.

of the truck design. A dynamic analysis of the complete telescope system indicated furthermore that the lowest systems' resonance would be about 10% higher over the resonance obtainable with the railroad track concept.

Additionally, it was found that there would be a number of reasons why the concrete slab-crane rail turntable base concept would be preferable to the railroad track concept. They are as follows:

1. Reduced truck maintenance.
2. More accurate rail surface contour.
3. Fewer mechanical components.
4. Shorter, more manageable truck dimensions.
5. Improved drive wheel traction.
6. Reduced friction losses and surface wear.
7. Stow anchors are feasible.
8. Simplification of installation of single track rails.

Because of the improved performance characteristics and reduced cost, the concrete slab-crane rail concept has been selected as the best suitable turntable base configuration for the homology telescope.

2. Pintle Bearing Foundation

The basic requirements for the pintle bearing foundation are that it be designed to react the imposed vertical and lateral loads and that it provide for suitable mounting of the pintle bearing assembly and for easy access below the kingpin so that cabling and instrumentation (coarse encoder) located at the kingpin can be serviced.

Achievement of any set stiffness number is not an important requirement as the bearing has self-aligning features and the flexibility of the pintle bearing arrangement will not contribute significantly to the dynamics of the system. Thus the design requirements for the pintle bearing foundation are straightforward. The proposed foundation shown in Fig. 4-20 consists basically of a circular reinforced concrete base of about 40 ft diameter and 3 ft thickness buried below 3 ft of compacted back-fill. A circular central housing extends above the surface and is provided with an access opening.

A stress analysis of this configuration showed that the proposed dimensions are resonable and that stability is assured.

H. The Drive and Control System

1. Dynamic requirements

The corner frequency of random wind gusts was determined by the Naval Research Laboratory (Ref.4-1) and others to be around 0.33 cycles/sec. In order to correct the pointing error due to structural and mechanical deflections caused by this disturbance, the drive-control system of the telescope must be designed to respond to these perturbations. Thus it is obvious that the frequency response of the telescope drive system should be equal to or higher than the frequency of disturbance.

To avoid dynamic performance limitations, it is necessary that the lowest mechanical resonance of the system occurs at an appreciably higher frequency than the desired closed loop system frequency response. A good practical rule is to design the system so that the lowest natural frequency occurs at a frequency of at least three times the desired frequency response of the system. Hence the homology telescope should be designed to have a lowest system resonance of at least 1.0 cycles/sec. Servo analyses so far performed, considering a lowest resonance of 1.0 cycles/sec and feasible control component parameters, indicate that a 0.40 cycles/sec closed loop bandwidth appears feasible and that the desired pointing accuracy can be attained.

To date rigorous dynamical analyses by computer have been made, and indications are that achievement of a minimum resonant frequency of 1.0 cycles/sec is entirely feasible.

2. The reference system

The purpose of this system is described in Chapter 3 of this report. It consists basically of the following elements:

(1) A 2-axis (asimuth and elevation) reference platform mounted at the axis intersection of the homology telescope behind the vertex of the reflector.

(2) Seven laser autocollimators and quad cell detectors located on the ground and arranged along a circle outside the azimuth track.

(3) A precision, 2-axis shaft angle encoding system.

(4) A 2-axis retransmission system to provide processed feedback signals to the drive system of the telescope.

(5) A collimator selector system for sequence selection to assure continuity of operation regardless of structural blocking of the optical collimation beam.

(6) A servo system to control the position of the reference platform which must remain fixed in both north-south and gravity deflection regardless of the position of motion of the telescope.

The function of the reference system is described as follows:

(1) Description. There are at least three types of optical systems commercially available which could be successfully used in this application for azimuth reference.

(i) An optical beacon tracking system by "Kollsman Instrument Corporation" (Fig. 4-22).

(ii) A laser autocollimation system by "Keuffel and Esser" (Figs. 4-23 through 4-26).

(iii) A laser auto-reflector system by "Davidson Optronics, Inc."

(a) Description of the "Kollsman" system. The Kollsman system consists of optical trackers, which are rigidly attached to the reference platform and an equal number of beacons, which are positioned on the ground. These beacons project a light beam onto the optical trackers located on the platform; the trackers furnish electrical signals proportional to the azimuth angle by which the tracker axis departs from the line-of-sight between tracker and beacon. The beacon trackers actually have quadrature cells and thus could detect Az and El errors simultaneously.

The linear range of either axis output is approximately $\pm$ 30 sec for a 1 sec accuracy and saturates at approximately $\pm$ 60 sec.

The platform must be slaved (by servo control) to these signals and must be located at the intersection of azimuth and elevation axes of the radio telescope. This point of intersection, however, does not remain fixed in space, but subject to eccentric and vertical motions due to load flexure of the supporting structure or unevenness of the telescope azimuth turntable, which results in slow heave motions during rotation of the telescope. These heave motions are estimated to be $\pm$ 1.0 in, which makes a simultaneous Az-El reference impossible because the beacons would eventually lose their targets.

Thus the beacon trackers can, therefore, be designed to generate linear azimuth output only.

(b) The "Keuffel and Esser" or "Davidson Optronics" system. These two systems use the same technical approach and comparable hardware. A better and also less expensive approach is to utilize a "laser autocollimation" system for both azimuth and elevation reference.

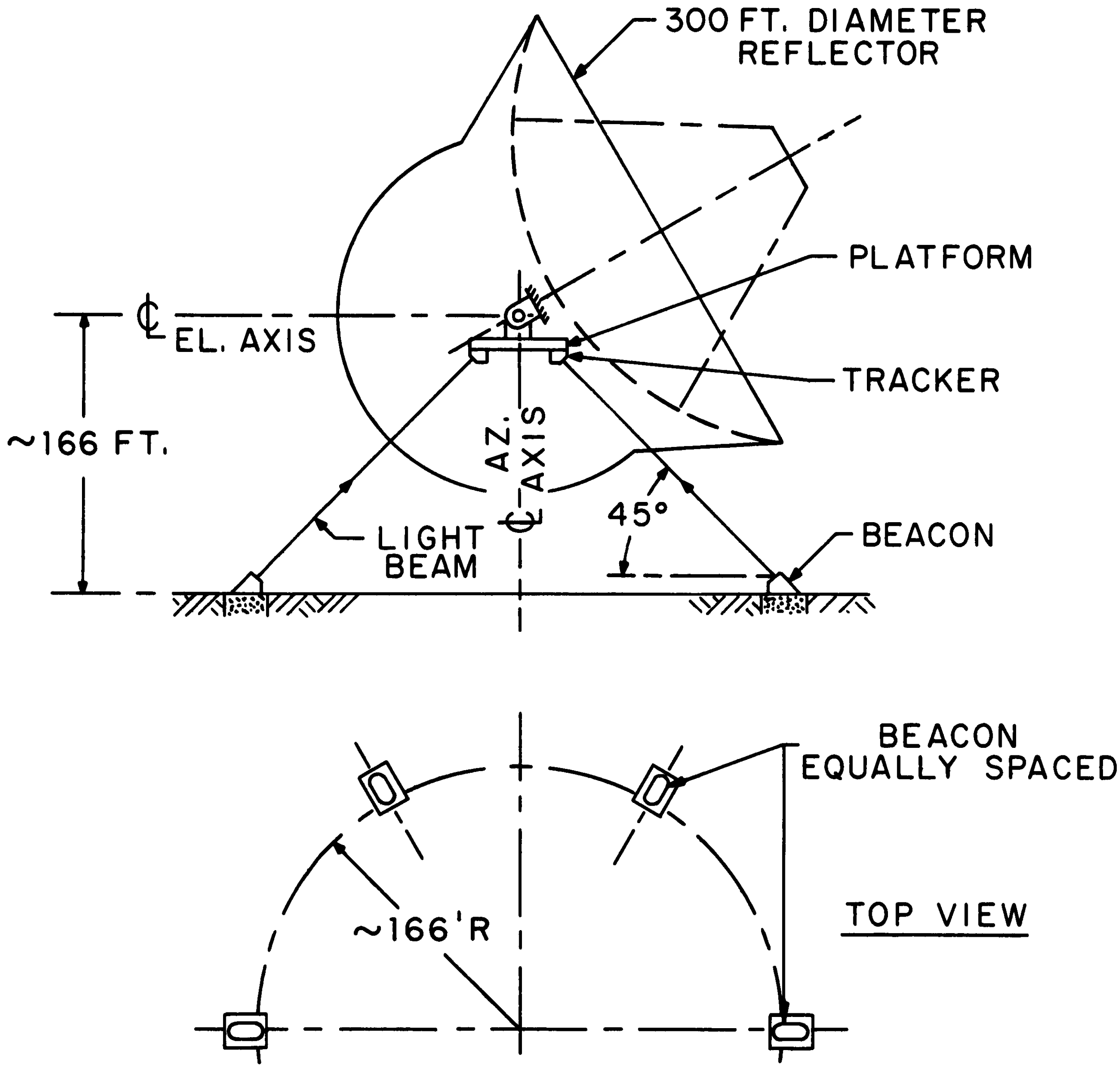

Fig. 4-22. Reference platform with Kollsman system.

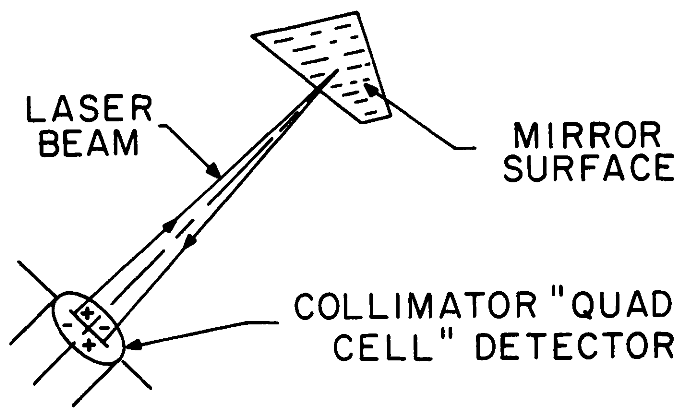

Fig. 4-23. The "Keuffel and Esser" or "Davidson Optronics" System.

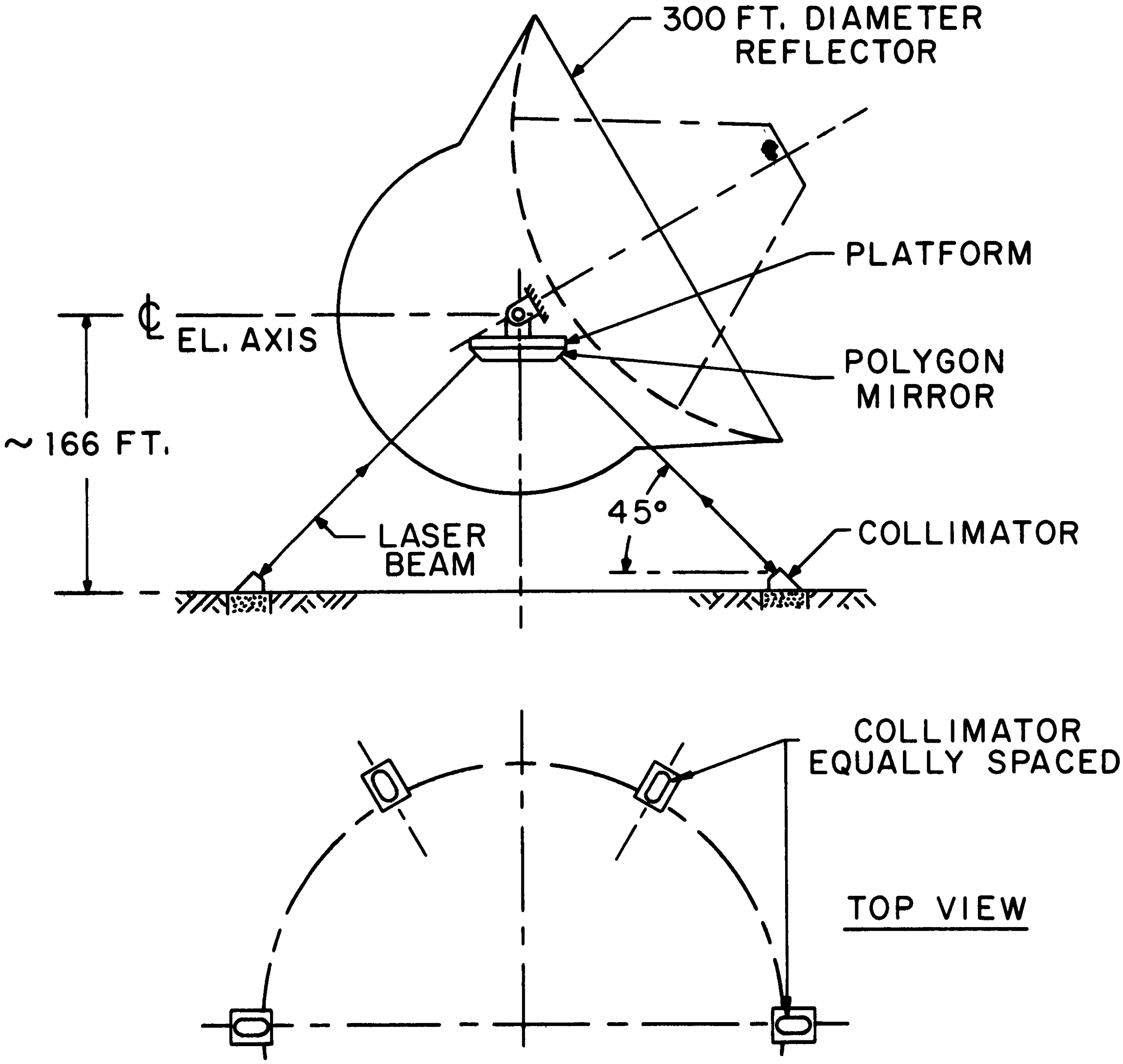

Fig. 4-24. Reference platform autocollimating system.

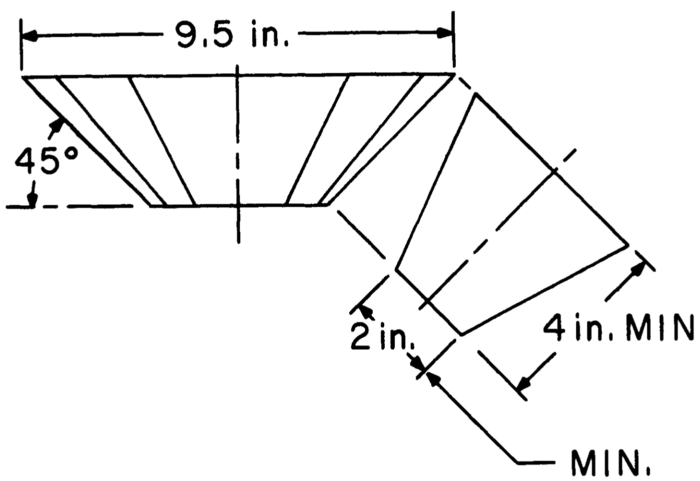

Fig. 4-25. System characteristics.

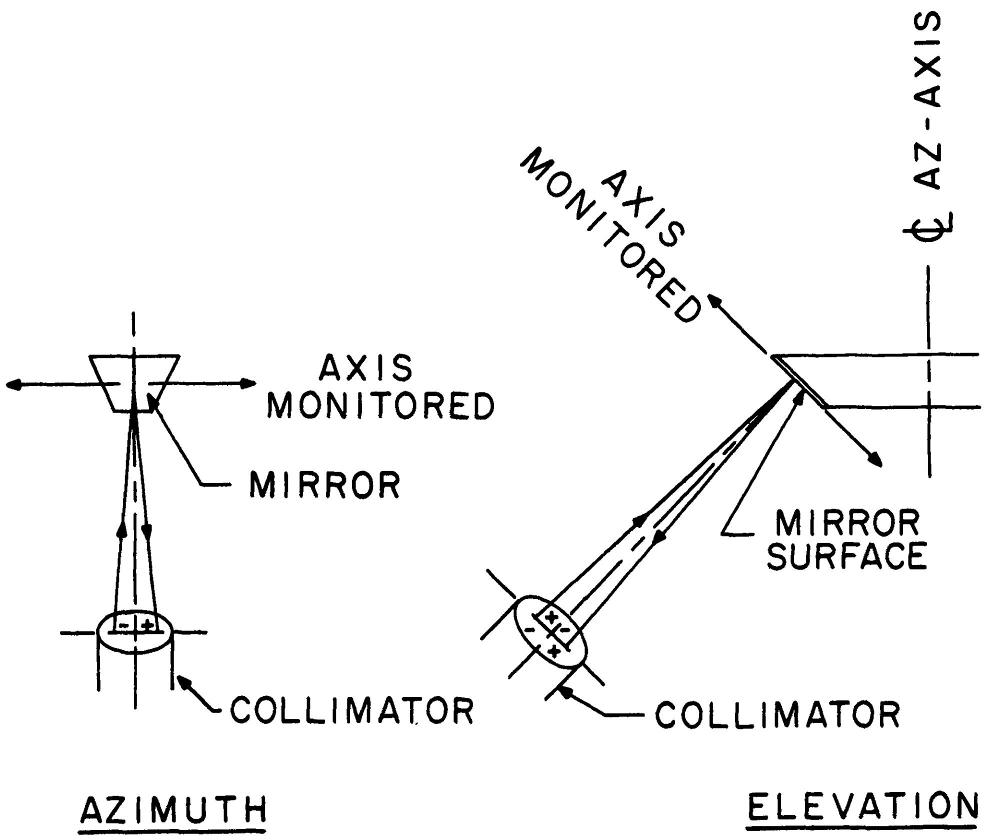

Fig. 4-26. Schematic of collimator.

This instrument functions as follows. Narrow modulated laser light beams are generated by laser tubes located on the ground and are reflected each by a perpendicular mirror surface of a "polygon" mirror located on the azimuth axis of the reference platform. The reflected laser beams are then projected on quad cell detectors which are located at the points from which the laser beams originate.

Since it is easily possible to get large enough flat mirror surfaces, deviations from the theoretical Az-El axes intersection point can be tolerated without losing the targets, resulting only in insignificant position errors.

These systems have the following operating characteristics.

(c) Systems characteristics

(1) Because of beam modulation the system is not affected by sunlight or other light interference.

(2) System hysteresis is less than ± 0.30 arc sec.

(3) System accuracy is better than ± 0.50 arc sec at a range of ± 10 arc sec; output saturates after ± 25 arc sec.

(4) Maximum distance between light source and mirror is 300 ft.

(5) Frequency response is 50 C.P.S. min as measured from in. to output.

(6) There is cross talk between the two axes output if simultaneously operated; thus, selective interrogation must be applied.

The multiple side reflecting mirror (optical polygon) would be specially made in one piece and would have the following typical characteristics.

The present state-of-art limits alignment of sides to a tolerance of 5 arc sec; however, each side can be calibrated and the error of each side can be determined with respect to a reference side. The 5 arc sec error can thus be reduced to approximately ± 0.50 arc sec by application of proper compensation methods.

(d) Collimator. Azimuth and elevation signals can be generated by the same mirror by successively interrogating the collimator once for one axis and subsequently for the other axis. This will tend to minimize signal interference (cross talk) between the axes.

The high frequency response (50 C.P.S.+) of the instrument permits high interrogation and storage rates.

Only mirror surfaces offset to the elevation axis can be utilized for feedback and reference purpose; the side coinciding with the El axis will, of course, not generate any signals as a function of platform tilt.

Each individual collimator/mirror will have a different tilt servo loop gain characteristic in elevation; a collimator programming matrix must thus be applied in order to correct the individual gain for the selected mirror in-phase signal component.

(e) Selection of collimation sequence. If there would be no blocking of the light paths, a single autocollimator/mirror would suffice for this application. However, since the telescope structure rotates around the reference platform during tracking operation, blockage of the beam would occur from time to time as part of the structure crosses the light path. Thus, multiple autocollimator/mirror elements are required to assure that at least one unit is unobstructed and operational, in order to assure continuity.

Hence, the free collimator/mirror combination must be selected either by memory or by method of sensing (change in light intensity for instance during begin of blockage). There are two approaches for collimator sequence selection based on memory data as to which collimator can clear the structure and operate in a certain range.

Both azimuth and elevation data will be needed for the programming of successive selections.

Approach No. 1. This approach makes use of mechanical memory and consists of one azimuth and one elevation instrument servo; both are slaved to the respective reflector motion.

Each instrument servo would contain a mechanical cam for each autocollimating station. The cams would be made adjustable over the full telescope travel range. A dial indicator, mechanically coupled to the cam shaft would indicate the respective axis position, thus making the calibration of the unit independent from the digital read-out devices of other equipment. Both instrument servos would make use of the synchro transmitters which are located on the platform axes, after proper buffering. It is estimated that a selection reference position accuracy of $\pm$ 0.50° and repeatability will be satisfactory for this purpose.

Fig. 4-27 shows the servo approach for the collimation matrix.

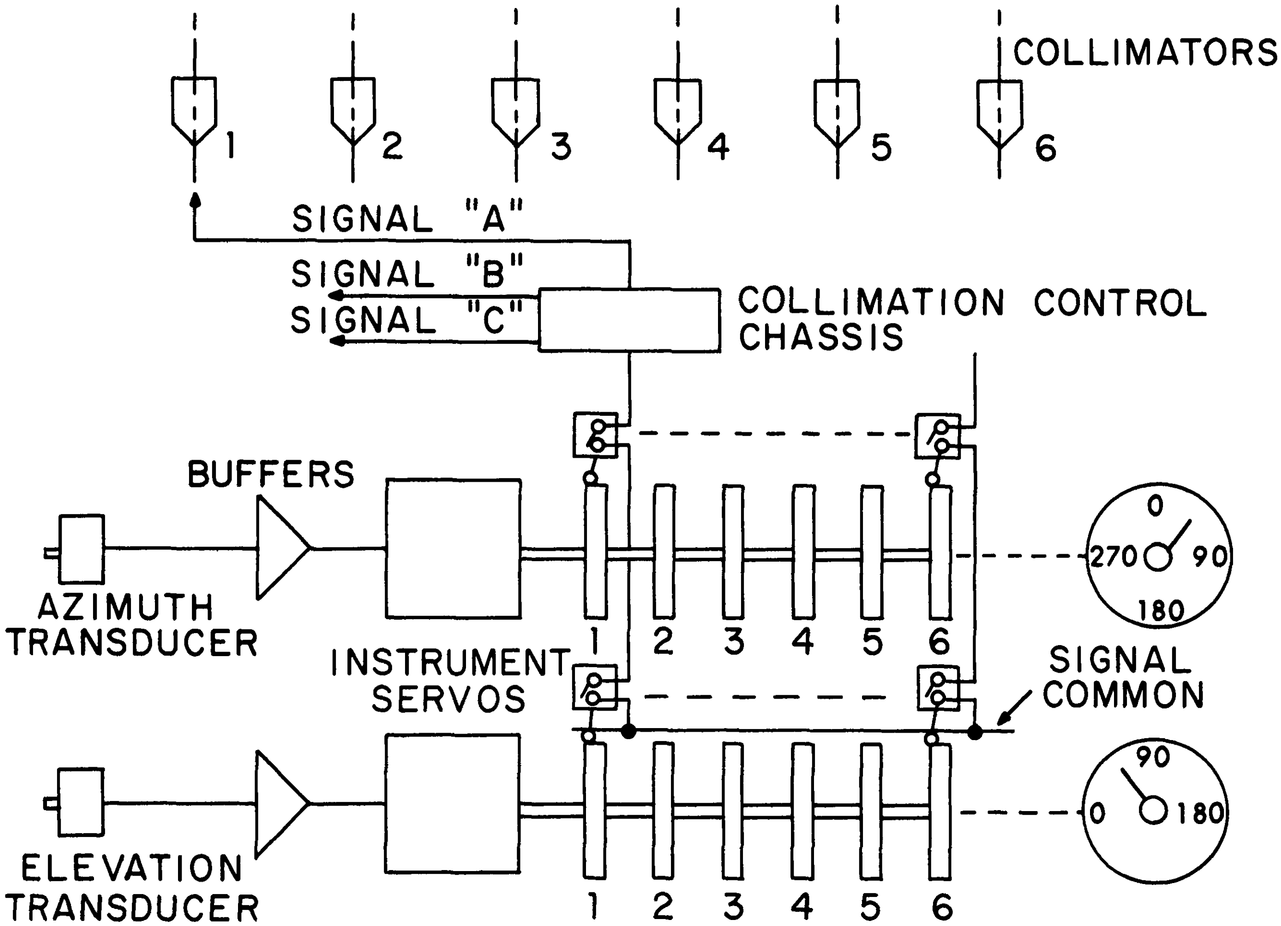

Fig. 4-27. Servo approach for collimation matrix.

Signal "A" switches the respective collimator on. Signal "B" corrects the azimuth axis for the indexing error of the precalibrated mirror. Signal "C" compensates the elevation tilt servo loop based on the in phase value of the selected mirror. The advantages of this approach are:

(1) Ease of adjustment.

(2) Flexibility.

(3) Non-volatile memory in case of power failure, power transient or noise.

Approach No. 2. Another approach is logic programming of the collimator selection. For a resolution of 1°, 9 bits of position information have to be gated in logic programming. With 9 bits of information from each axis, a total of 18 bits are needed for each of the collimator positions defining range.

This required digital information is derived from the nine most significant bits of each axis; this data is already available in the system and needs only be buffered for this use. Fig. 4-28 shows the logic approach for the collimation matrix.

Explanation of Fig. 4-28. Gated 9 bits of azimuth and elevation provide position No. 1. Similar gating defines position No. 2. Between these positions collimator No. 1 can operate. The memory module prevents transients or bit noise from effecting the matrix and is reset only if another range is satisfied.

Collimation control chassis and signals A, B, and C are identical for either approach 1 or 2.

(f) Environmental considerations. Three factors are of main concern: temperature variations; reflection and refractions; and change of refraction due to turbulence or temperature gradients in the air.

a-a) Temperature variations. Temperature gradients within the collimators or polygon mirror will cause dimensional distortions resulting in positional errors. In order to eliminate this error source, it will be necessary to maintain a selected constant temperature for either component. It is estimated that a local ambient temperature of + 130° F controlled to ± 1/4° F will satisfy this requirement.

b-b) Reflections and refractions. In order to protect the polygon mirror or the collimator from the environment, either unit will have to be

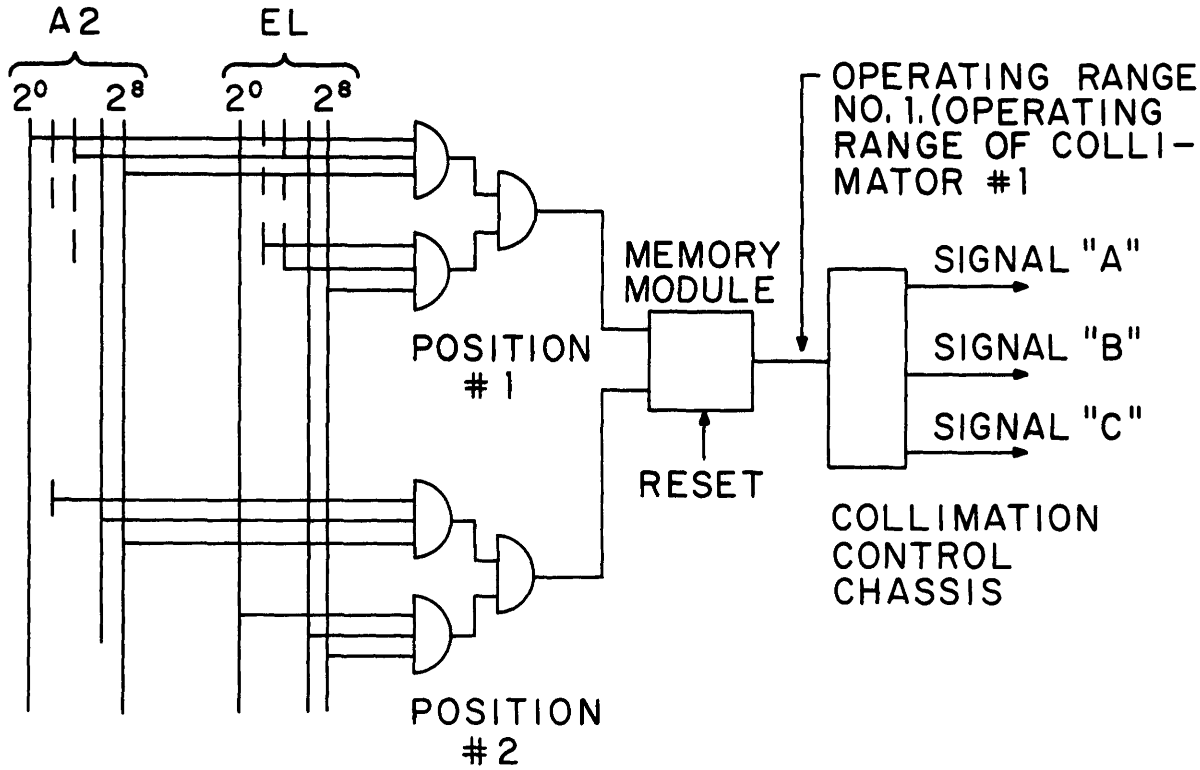

LOGIC APPROACH FOR COLLIMATION MATRIX

The main features of this approach are:

a) It is downstream in the signal path; hence, any upstream failures in the subassemblies will render this system non-operative. This could cause shutdowns and difficulty in trouble shooting.

b) Even though highly reliable "solid state" components can be used, its component population is high, which results in decreased overall reliability.

c) This system is more noise sensitive and the memory is volatile in nature, i.e., can be lost due to power failure or transients.

Fig. 4-28. Logic approach for collimation matrix.

enclosed. These housings must have window openings for passage of the laser beams. These should be quartz windows so as to minimize reflection of the laser beam. The windows must furthermore be installed perpendicular to the optical path for minimization of beam refraction errors due to errors in parallelism of the quartz window surfaces.

c-c) Change of refraction. Since both the projected and reflected beams have almost identical paths, their refractions will be almost the same and would be insignificant.

Only the change in refraction as a function of air temperature will produce errors; for the distance considered, however, these errors should be insignificant. Air turbulence is not a problem either since the beam travels at the speed of light.

(g) Gravity reference system. There are two types of gravity sensing instruments which could be utilized for elevation angle reference purposes. They are a pendulous vertical sensor by "Kearfott" and a bubble-type tilt meter by "Ideal-Aerosmith." Only the Kearfott sensor application is described here. The advantages of application of a gravity sensing device over optical reference are that blocking is eliminated and that the accuracy of the instrument would not be affected by rain or snow, etc. However, if an optical system is required anyway for azimuth reference, then the elevation reference may as well be optically also. But if it should be feasible and practical to utilize a gyro compass for azimuth reference, the elevation reference system must then be gravitational. Such a platform could be installed right behind the vertex of the parabolic reflector, which would improve the pointing reference of the radio telescope still further.

(i) Kearfott - "Pendulous Vertical Tilt Sensor". This instrument, as the name implies, utilizes a precision pendulum for the detection of the gravity. The pendulous element is suspended in a viscous fluid and the output is sensed electromagnetically (Hz pickoff). For this application, a custom made, high performance unit will be required. In order to achieve sufficiently high response, the length of the pendulum is kept shorter and the fluid less viscous than for standard precision units. The model considered for this application is Kearfott #C 70-1815 002, since at present the autocollimation system is proposed a complete description of the gravity system will not be presented. Appendix 2, Report H79-7, Section 3, of this report contains complete coverage of the gravity system.

(h) Platform System Description. The foregoing described the basic instruments which can be used for fixing the platform in both azimuth and elevation directions. Since the platform, as implied, must remain fixed in space while the telescope reflector moves about the azimuth and elevation to track a radio source, it is obvious that the platform should move in the opposite direction relative to the rotating structure at exactly the same speed. This is accomplished by using the amplified error signal generated by the position sensors for feedback purpose to drive a null seeking platform servo system. The position between the platform and the telescope reflector is detected on the platform by means of a readout transmitter; the transmitted position is then received by a receiver on the ground and the signal is there digitized.

At the same time the position readout signal which is initially in analog form is re-transmitted to the telescope drive servo for position correction of the telescope, if a digital comparison between the position command by the computer and the actual position should indicate a telescope position error.

The applicable block diagram for this system is shown in Fig. 4-29. For a description of the instrumentation proposed for the position indicating system, functioning and capabilities of these instruments, reference is given to Appendix 2, Report H79-7.

(i) Servo requirements. The platform positioning servo characteristics should closely fit the required overall dynamic performance and error budget considerations. To cope with the disturbances due to wind gusts, structure, travel, etc., the servo loop should have a high natural frequency (at least two octaves higher than the perturbation frequency). The open loop gain of the feedback control system should be high enough to operate within the $\pm$ 1 arc sec dead band required by error budgeting.

a-a) Drive: The required drive should be able to position the following loads:

Azimuth. Weight: Approx. 60 lbs

Inertia: 0.09 $lb/ft/sec^2$

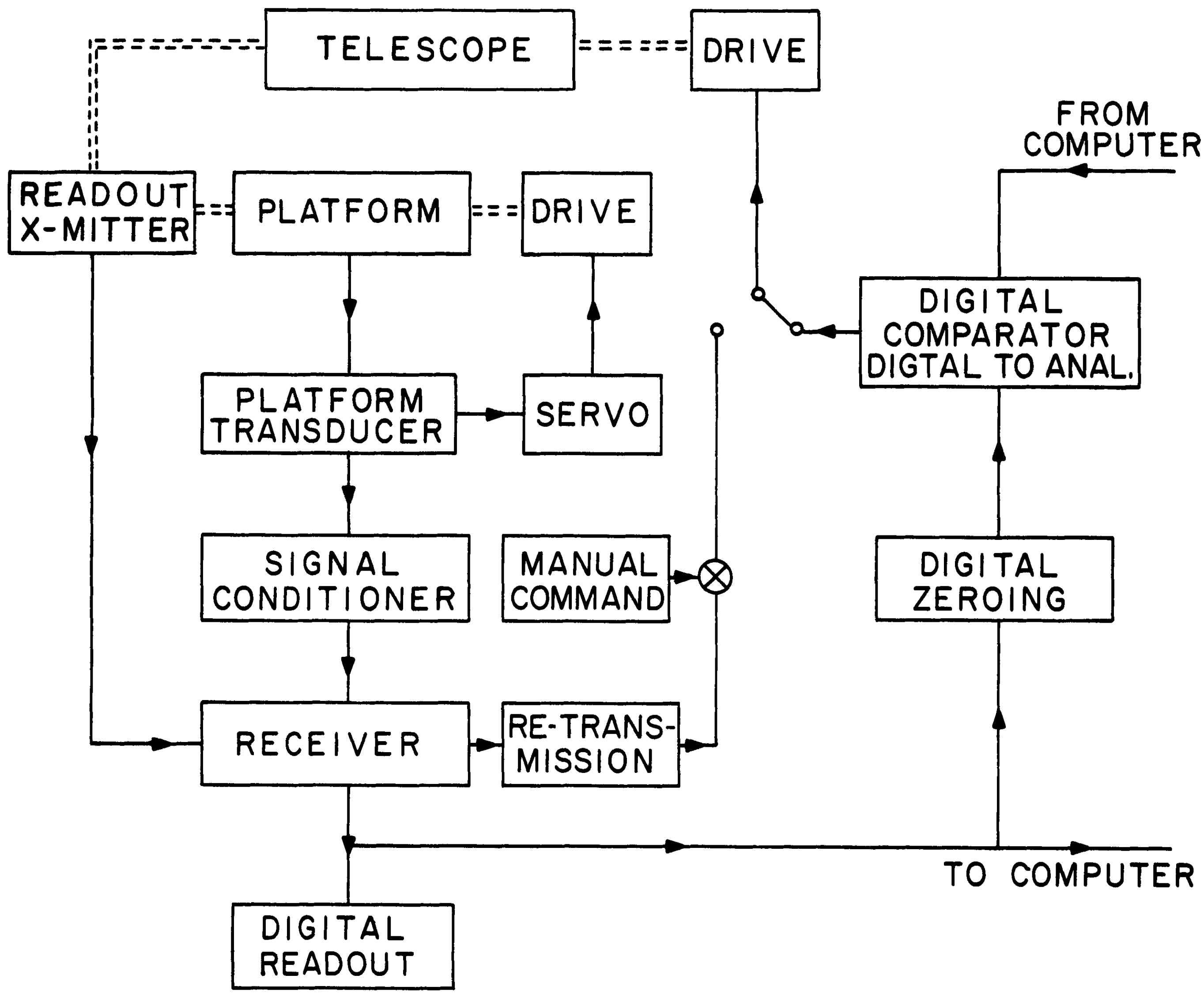

Fig. 4-29. Reference platform system block diagram (typical, either axis).

Elevation: Weight: Approx. 69 lb

Inertia: 0.23 lb/ft/sec^2

It appears possible that these loads can be reduced during the final design by as much as 30% for increased servo bandwidth.

As the elevation axis also carries the azimuth axis full weight, the elevation axis performance requirements are more difficult to meet (worst case). The frictional torque on this axis is approximately 70 oz-in, if commercially available bearings are used. State-of-the-art components, techniques and alignment methods can reduce this to 25 oz-in.

b-b) Performance. The performances of the selected hardware and techniques are discussed below:

The "Inland" servo (torque) motor T-5730 which produces 7 lb/in of torque fits the loading conditions best. The hysteresis requirements dictate an open loop gain of 435,000 volts/radian. This high gain, in turn, makes it necessary to use lead-lag compensation techniques for stable operation.

The suggested compensation can give a closed loop bandwidth of 50 radians/sec which compares very favorably with the estimated 6-8 radians/sec antenna structural natural frequency and 2-4 radians/sec of perturbance inputs.

In any event, the relative high closed loop bandwidth dictates use of lightweight, low inertia components; thus, the proposed application of the polygon mirror is ideally suited for this requirement.

c-c) Error budget estimate. The following error budget estimate appears feasible for the before described instrument systems and components:

Sensor errors		
Basic error, including linearity and hysteresis	:	$\pm$ 0.10 arc sec
Interface errors, due to small temperature differentials in the mirror ($\sim$ 0.25° F)	:	$\pm$ 0.40 arc sec
Platform servo errors		
Servo loop hysteresis error	:	+ 1.0 arc sec
Dynamic lag error	:	Negligible

<u>Readout instrumentation errors</u>	
Inductosyn transducer readout error	: ± 1.2 arc sec
Inductosyn digitizing electronics error (digitizing accuracy can be ± 1 count)	: ± 0.30 arc sec
Inductosyn hysteresis error due to shaft and coupling wind-up	: ± 0.20 arc sec
<u>Error due to cabling</u>	
Temperature effect error, on 500 ft long transducer transmission cable	: ± 0.50 arc sec
Drift error (10 kHz carrier is used)	: Negligible
Total worst case sensor loop error (Items 1 and 2 combined)	: ± 1.5 arc sec
Total worst case readout instrumentation error (Items 3 and 4 combined)	: ± 2.2 arc sec

Combining the two worst case components result in the following:

Worst case peak to peak error	: ± 3.7 arc sec
Root-sum square error (combining each error component)	: ± 1.7 arc sec
Root-sum square error (combining worst error of sensor loop and readout instrumentation)	: ± 2.6 arc sec

The above applies for both azimuth and elevation references. It is believed that a ± 3.0 arc sec rms system accuracy is well within the state-of-the-art at the present time.

Allowing 4 arc sec rms error for the telescope drive system and structural deformations in the reflector structure, secondary reflector, support legs, etc., it appears feasible that a 5 arc sec RMS pointing accuracy of the radio telescope is obtainable with the application of this system, providing the above dynamic telescope drive system accuracy can be achieved.

(j) Mechanical configuration. The mechanical configuration of the reference platform is shown in Fig. 4-30.

As can be seen, the platform consists basically of a hollow tubular member (1), which is mounted on bearings and is free to rotate with a "U"-shaped base (2). The axis of this tubular member is mounted level and coincides with the elevation axis of the radio telescope. The rotor of a torque motor (3) is attached to one end of the tubular member, while the stator (4) is mounted to the base. On the same end is mounted an inductosyn unit (5) via a flexible coupling (12). The tubular member supports the polygon mirror (6), which is attached to a hollow azimuth shaft (7). The axis of this azimuth shaft is held perpendicular to the elevation axis and coincides with the azimuth axis of the telescope. This shaft is running on precision bearings (8) and is also driven directly by a torque motor (9). A readout transmitter arrangement (10) is incorporated on the shaft and in the shaft housing, and an inductosyn transducer (11) is coupled to the shaft via the bellows coupling (12).

The entire rotational portion of the platform assembly is covered with a "fiberglass-polyurethene" sandwiched housing (13), which has window openings containing quartz windows (14), through which the laser light beam is projected onto the mirror (6).

Fig. 4-30 shows provisions for mounting of tilt sensor (15), acclerometer (16) and rate gyro (17), which are "alternatives" only. The "optical only" platform will not have these instruments and hence the elevation shaft would not have the cutouts required for the accommodation of the gravity sensing system instruments.

The "U"-shaped mounting base (2) is also covered with insulation (18) to eliminate temperature distortions in this structure. A twist cable (19) passes through tubular member (1) and is designed to allow rotation about the El-axis through $\pm$ 45°.

The entire platform assembly is kept at a constant temperature of + 130° within an accuracy of $\pm$ 1/4° F by means of built-in, controlled circulating air heating units (not shown).

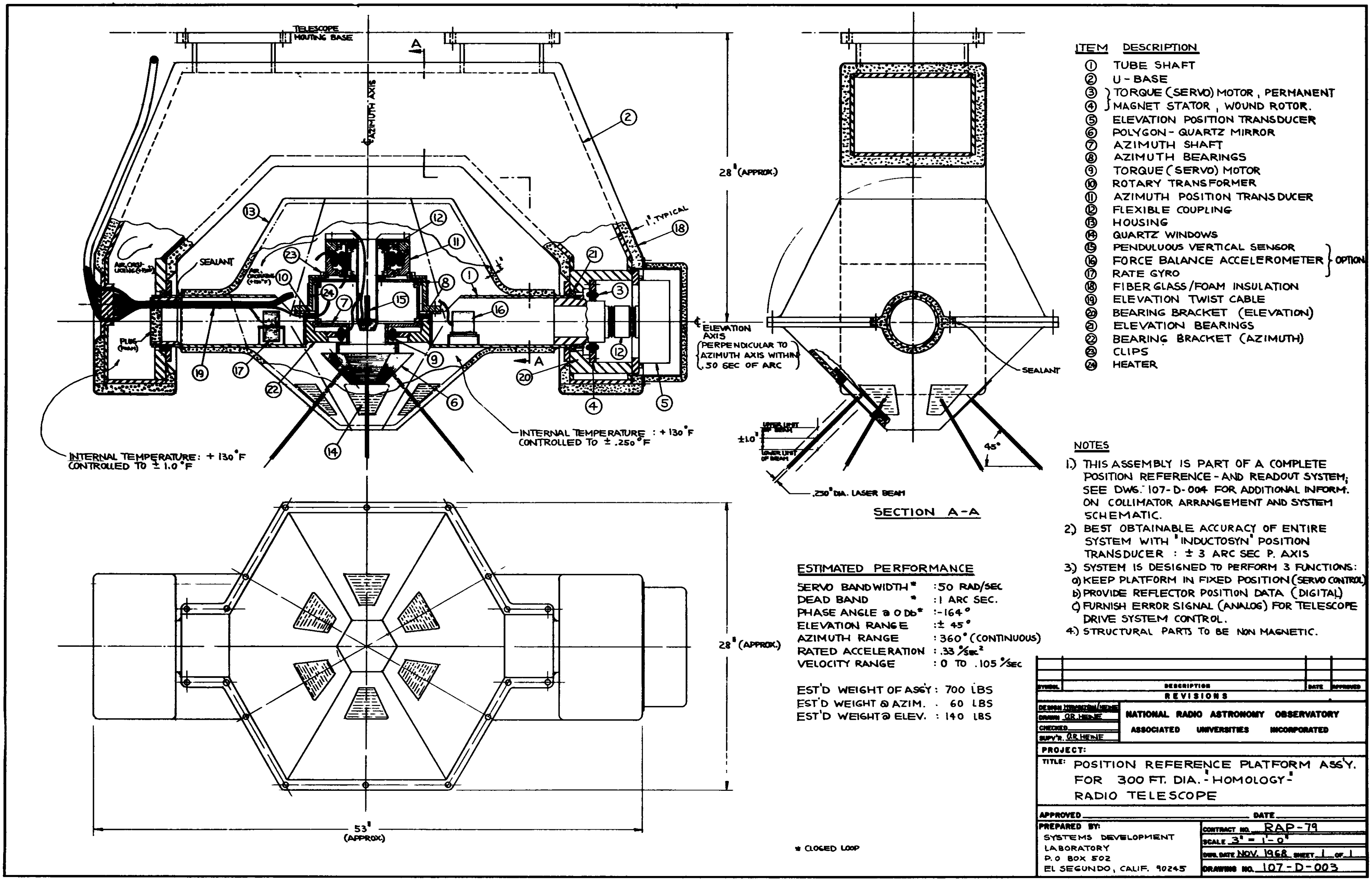

Fig. 4-30. Position reference platform assembly for 300-ft diameter homology radio telescope.

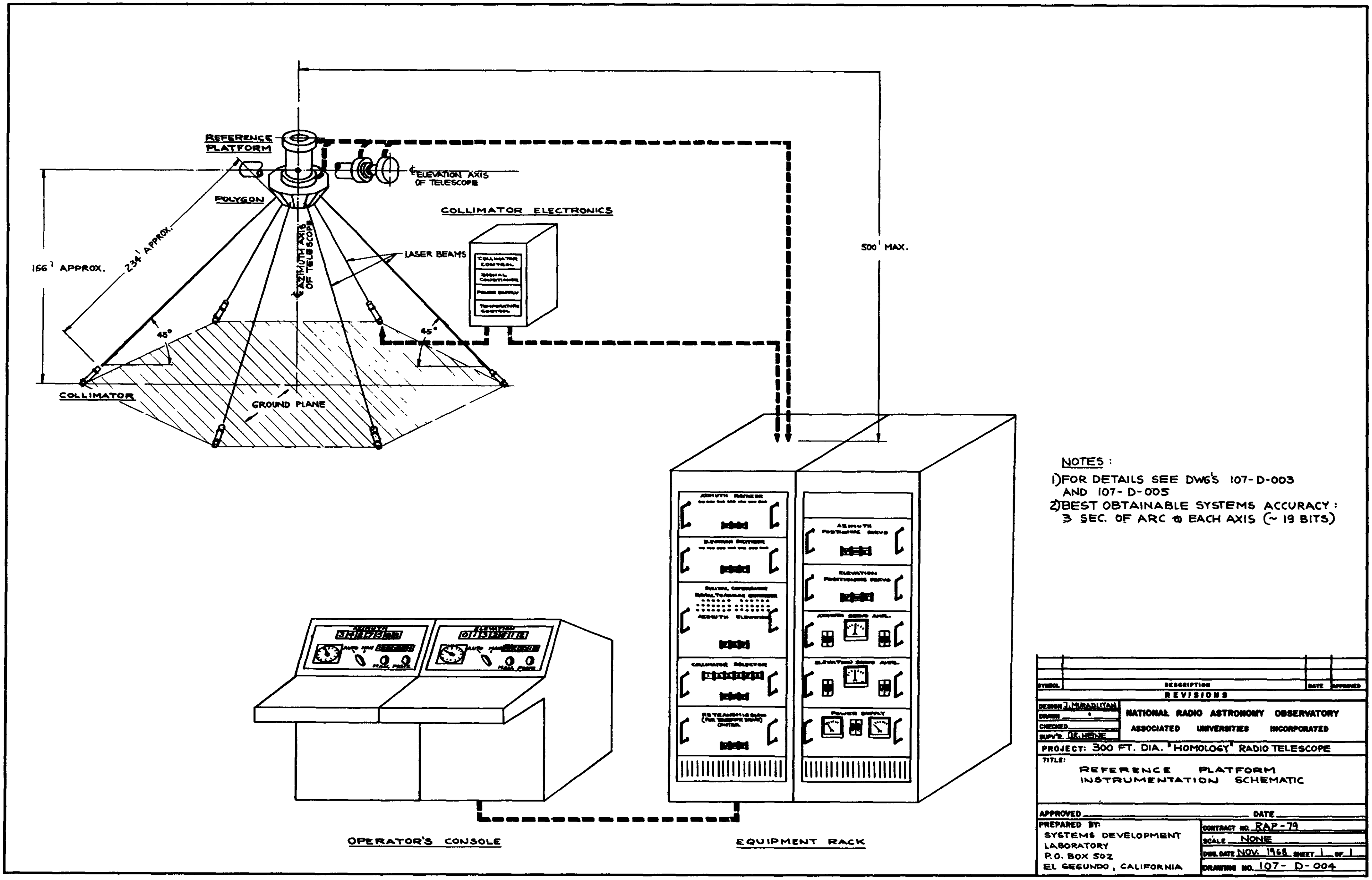

Fig. 4-31. Reference platform instrumentation schematic.

(k) Performance requirements. The position reference platform studied herein must function at maximum accuracy (3÷5 arc sec) under the following environmental conditions and external perturbations.

Environmental temperature range	:	-20° F to +120° F
Wind velocity (tracking condition)	:	18 mph, gusty
Rain or snow	:	Reduced accuracy permissible
Angular velocity (Az and El)	:	0 to 18°/min
Angular acceleration (Az and El)	:	0.330°/sec^2, max
Vertical, linear acceleration	:	0.013 cm/sec^2
Lateral, linear acceleration	:	0.060 cm/sec^2
Frequency range of perturbations	:	0 to 1.0 C.P.S.
Eccentricity of Az axis	:	± 1.0 in/360°
Heave motion at full Az rotation	:	± 1.0 in/360°
Light condition	:	Night to full daytime

3. The drive system

Both elevation and azimuth axes drive systems will utilize DC motors with tachometer feedback as prime movers. On the azimuth axis 16 drive units are required (4 on each drive truck) and 4 drive units will be required on the elevation axis.

During tracking operation one-half of the drive units will generate the required drive torque, while the other half will be used for bucking purposes in order to eliminate backlash.

When driving in stow under maximum load conditions and during slewing operation, all drive units will operate in parallel.

The azimuth axis drive system consists of sixteen 15 hp, 2500 rpm, totally enclosed, fan cooled DC motors, geared down (48,600:1) so that the maximum azimuth-axis slew speed will be about 18°/min.

The elevation axis drive system consists of four 40 hp, 1750 rpm totally enclosed, fan cooled, DC motors geared down (48,600:1). The maximum elevation axis speed will be approximately 12°/min.

The application of DC servo motors with solid state servo amplifiers appears to be best suited for the drive of the homology telescope. Other drive concepts, such as variable voltage/frequency systems, amplydyne and eddy current controls have been studied and found to be inferior or higher in cost to the DC motor system.

Since the multiple positioning servo units all have a common reference input (derived from the reference platform) one must anticipate that unequal drive torques could be generated due to the tolerances in the control components and the disturbance signals. Thus there should be a feedback circuit for correction of the torque or position differentials. Each unit will perform sometimes as a drive unit and at other times as a bucking unit, in which case the bucking unit always has a fixed ratio of the output torque of the driving unit. Because of component performance variations (due to manufacturing tolerances), the bucking ratio should be made adjustable.

The DC servo motors can accept momentary overloads up to 900% for a period of 0.5 sec. Thus the power amplifier must be projected against overload. The required interlock arrangement, drive servo interface with the reference platform, generation of the position error signal and mechanical feedback path is shown in Fig. 4-32.

Fig. 4-33 shows a block diagram for drive-bucking ratio selection and unit torque control. It shows some of the functions in the "servo circuits and interlocks" block of Fig. 4-32. The operation of Fig. 4-33 is as follows.

The error signal from the error bus is fed to the error polarity discriminator. This circuitry has two functions: (1) Provide positive and negative analog error signals on separate terminals, and (2) Provide switching signals (logic signals) indicative of positive and negative error.

The blocks No. 3 on Fig. 4-33 provide adjustable bucking signals to analog signal switching circuits (No. 4), whereas the correct signal is selected by logic signals 2c and 2d.

The comparator receives two voltage signals of which one is proportional to error and the second proportional to unit torque. These two variables can be compared because they both can be scaled in terms of servo stiffness.

The signal thus generated is fed through the servo compensation circuits and power amplifier to energize the servo motor. The torque sensor has isolated floating input but referenced output, converting motor torque to a voltage signal. Item No. 10 on Fig. 4-33 is an adjustable scaler and limit setter for the torque signal.

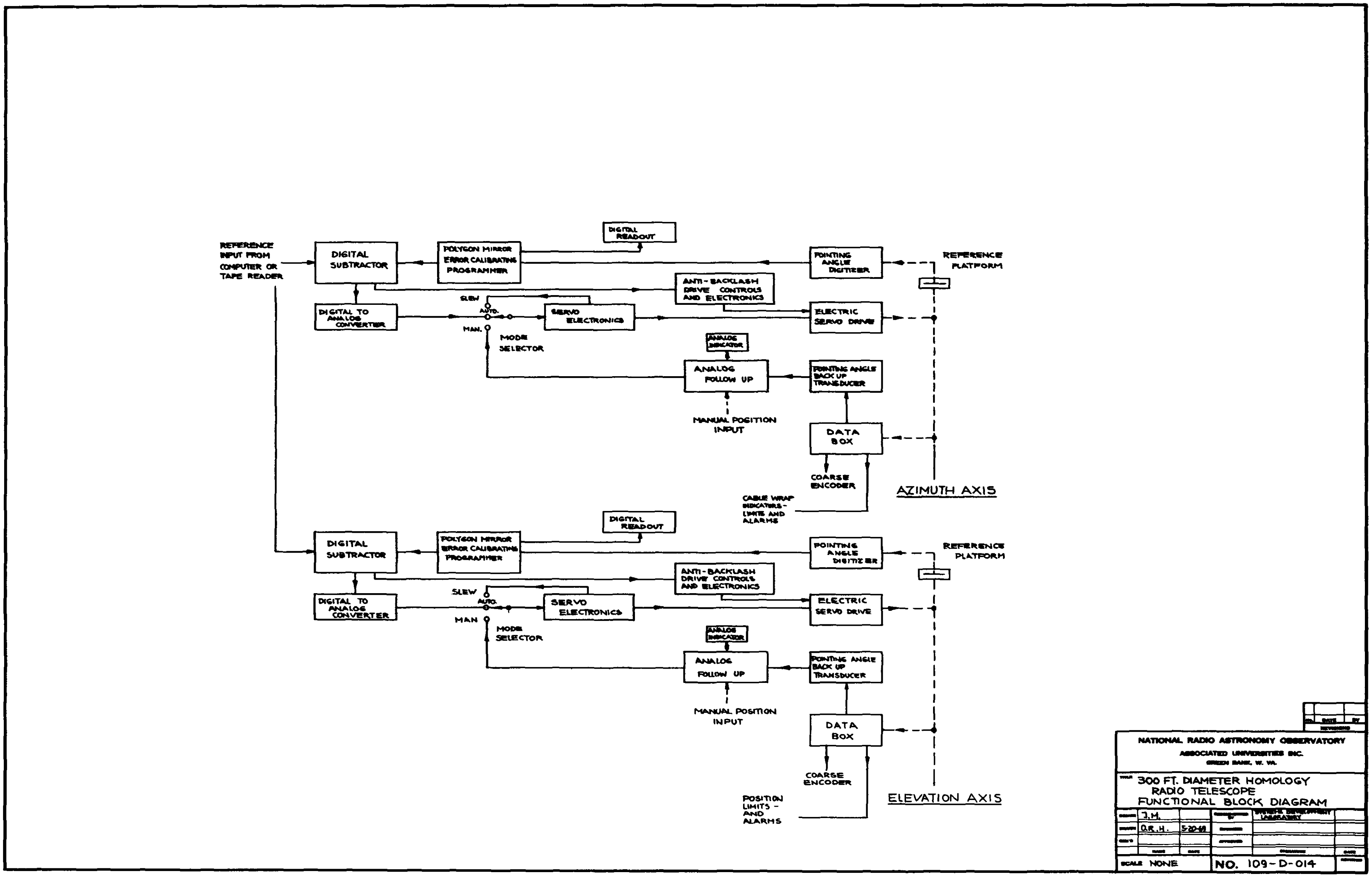

Fig. 4-32. 300-ft diameter homology radio telescope functional block diagram.

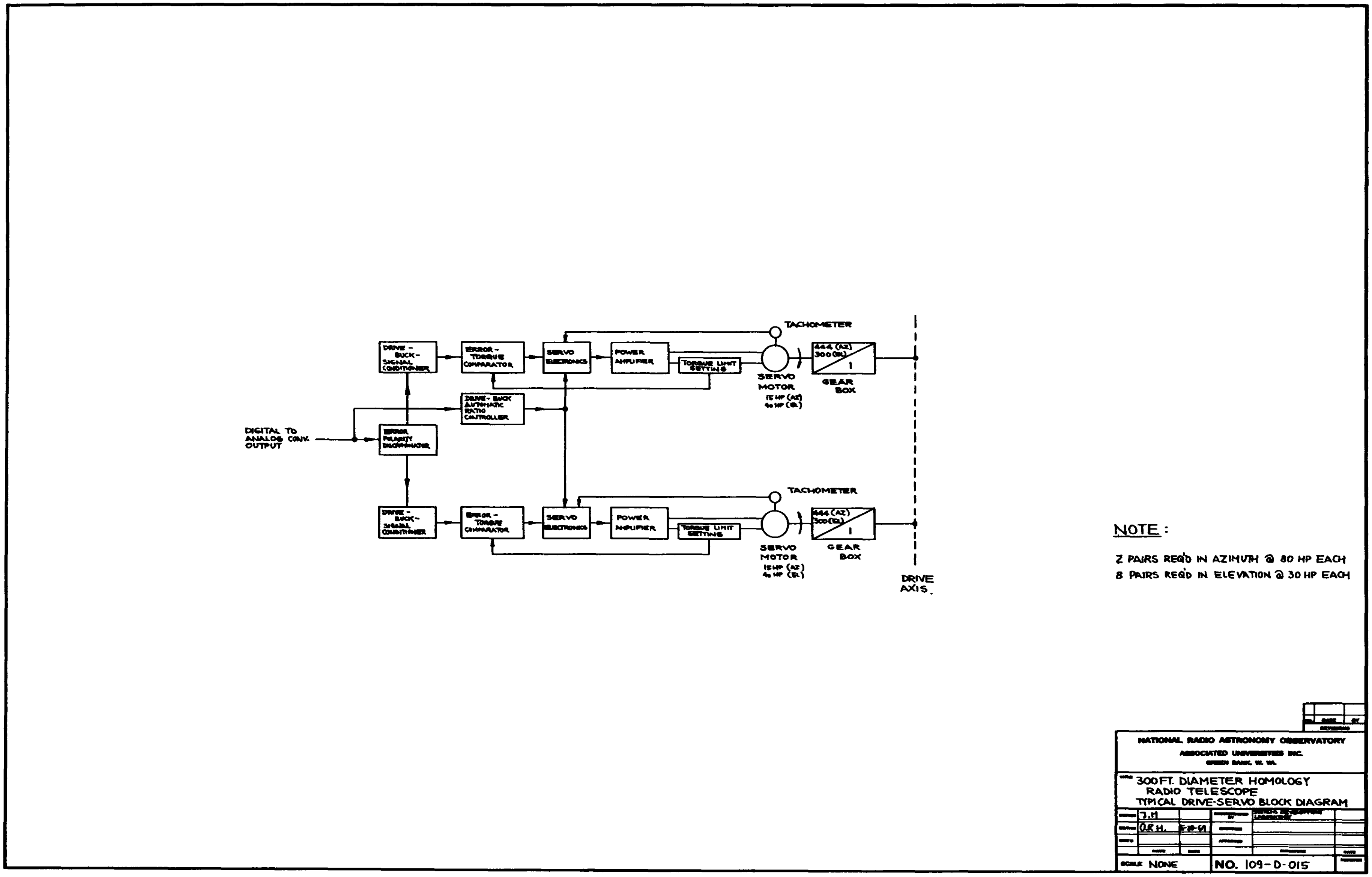

Fig. 4-33. 300-ft diameter homology radio telescope typical drive-servo block diagram.

Both azimuth and elevation drives are arranged in such a way that only tangential forces are introduced at the respective points of load transfer. In azimuth this is accomplished by floating gear train arrangements, which drive rigid axle-wheel assemblies and which are connected by means of a link to the adjacent walking beam so that the gear box is only rotationally restrained to counteract the tangential friction drive forces at the wheel radius.

In elevation the arrangement consists of an articulating drive mount which follows the drive gear contour by means of guide rollers and which is simply linked to point 6 of the tower. This arrangement eliminates torques or large vertical loads at this point since the separating forces generated by the output pinions of the gear trains engaging in the elevation drive gear are internally reacted by the guide rollers.

The drive system is unaffected by pitch radius tolerances, as the gear trains can follow the elevation gear contour without restriction, permitting dimensional tolerances of appreciable magnitude. Details of the proposed drive system are shown in Fig. 4-34.

The previously described drive systems have been analyzed in sufficient detail to predict that stable operation under the disturbances due to environmental conditions will be feasible and that a highly accurate pointing program will be attainable with the application of the optical reference system, if the lowest natural resonance of the telescope structure and drive system is maintained at a frequency of above 1.0 cycles/sec.

4. Pointing accuracy

The estimated error budget for the reference system is as follows:

Sensor error	:	0.50 arc sec	Sensor Loop
Platform servo error	:	1.00 arc sec	
Readout instrumentation error	:	1.70 arc sec	Readout Instrumentation
Cabling error		0.50 arc sec	
R.S.S. error of reference system:		2.6 arc sec	

Two types of pointing errors are introduced by the drive system: A drive servo hysteresis error and a dynamic error caused by wind gust disturbance.

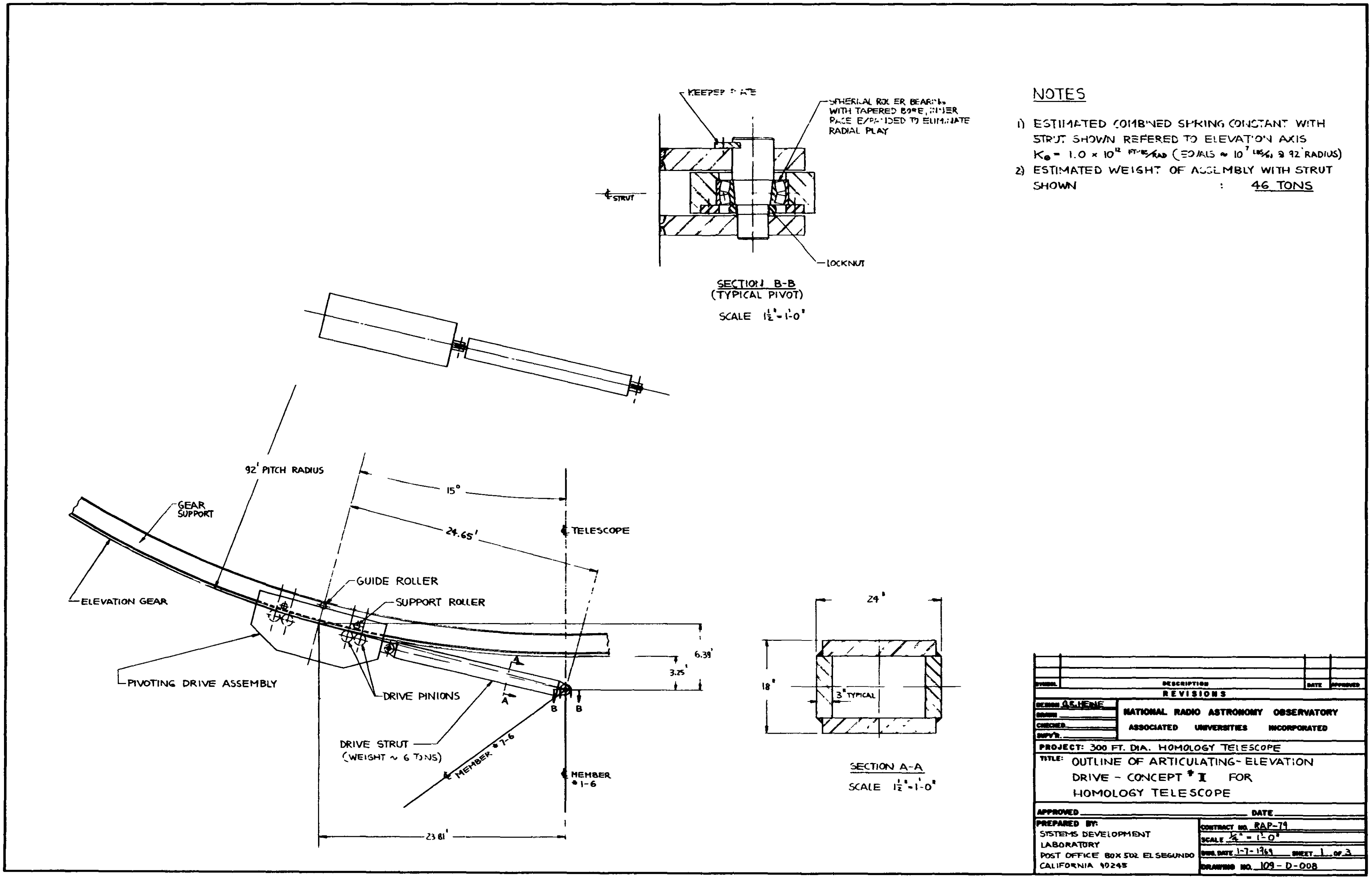

Fig. 4-34. Outline of articulating elevation drive, Concept No. II, for homology telescope.

Servo hysteresis error	:	1.9 arc sec
Dynamic error	:	0.8 arc sec
R.S.S. error of drive system	:	2.0 arc sec
Estimated pointing accuracy of drive and control system	:	3.2 arc sec

REFERENCES

4-1 Naval Research Laboratory Report 5549, "Wind Induced Torques Measured on a Large Antenna."

I. The Control Building and Service Tower

The Control Building for the Homology Antenna as shown on Fig. 4-35, in addition to providing offices, control console room, electronic equipment rooms and the required mechanical and electrical support facilities, serves as the base for the service tower. This combination facility will be located in the Northern section of the telescope to avoid interference with the radio beam of the antenna. Access to the focal room of the antenna is provided by a door in the south face of the Service Room which matches a door in the end of the focal point structure of the antenna. An enclosed elevator within the tower structure traveling from the basement to the Service Room will be large enough to transport all feeds and equipment to the focal point. Testing and service equipment as well as spare feeds will be located in the Service Room so that most maintenance and servicing as well as feed changes may be performed with a minimum of equipment shifting as well as a minimum down-time. This Service Room will be temperature controlled for feed testing and will have provisions for temperature stabilization of feeds prior to their installation in the antenna.

The Control Building itself will be air conditioned and in the basement will provide electrical facilities such as frequency control equipment, switchgear, and transformers. The main floor will contain 2 electronic equipment rooms, 2 offices, the control room containing control console and computer, and a small service shop.

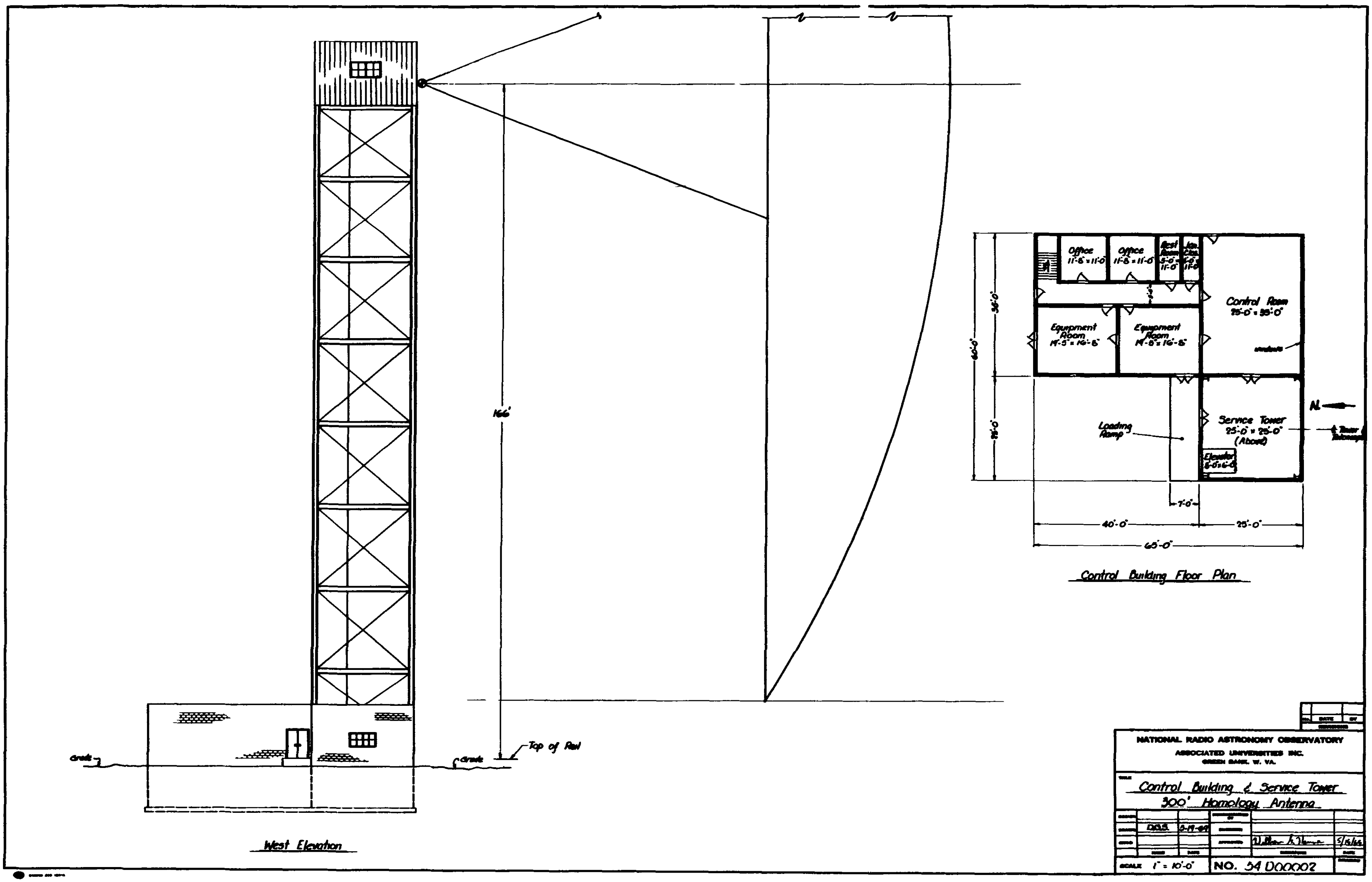

Fig. 4-35 Outline of Control Building & Service Tower

Chapter 5

THE PERFORMANCE

A. Survival Conditions and Wind

Wind data and their statistical treatment are given in Ref. 5-1. Recent wind data show that for 75% of the time wind velocity at Green Bank is below 18 mph. In order to be on the safe side, a wind survival velocity of 85 mph was adopted for the design, a condition that will occur statistically only once in 200 years. So,

$$v_{obs} = 18 \text{ mph, } 3/4 \text{ of the time} \tag{5-1}$$

and

$$v_{sv} = 85 \text{ mph.} \tag{5-2}$$

Both values, eqs. (5-1) and (5-2), refer to a height of 150 ft above the ground. The highest possible snow load is

$$P_{sv} = 20 \text{ lb/ft}^2 \text{ of snow or ice} \tag{5-3}$$

which corresponds to a solid layer of ice 4 in thick, or about 2 ft of snow. Since one must be able to dump the snow, it is assumed that the full load of eq. (5-3) may occur in any elevation angle. Since eq. (5-2) gives a higher overall load than eq. (5-3), the homology program uses only eq. (5-3), which must be satisfied for any elevation angle; it iterates only to those homology solutions where every single bar is stable in the survival condition. After a solution is obtained, x and y directions are exchanged and eq. (5-3) is applied again, as an approximation of a heavy storm in any horizontal direction. Thus, the present structure is stable under the conditions of eq. (5-3) in any horizontal or vertical direction.

The azimuth drive will operate the telescope in winds up to 50 mph.

B. Lowest Dynamical Mode

The design of the servo system is dependent on the dynamical behavior of the telescope.

The dynamical response of the telescope system to wind-induced perturbations was described in Chapter 4. The lowest dynamical mode of the combined system is

$$f = 1.20 \text{ cps} \tag{5-4}$$

including the effects of single long member, dish structure, suspension, drive and gear units, towers, trucks, rails and ground. The servo bandwidth is chosen as $b = f/3$ or

$$b = 0.40 \text{ cps.} \tag{5-5}$$

The critical wavelength of perturbations then is $1/b = 2.5$ sec. Slower perturbations will be eliminated by the servo system, while faster ones remain as pointing errors. In order to be on the safe side, a critical wavelength of 3.0 sec will be used in the following analysis.

C. The rms Surface Deformation

Surface deformations and pointing errors from wind and thermal effects are treated in Ref. 5-2, using measurements and experiments on thermal behavior from Ref. 5-3 and some recent high-resolution wind statistics.

White protective paint is used as on the 140-ft telescope, which gives a difference between sunshine and shadow of $\Delta T \leq 5°$ C on sunny calm days ($v < 5$ mph). The thermal time lag of heavy members during fast changes of ambient air temperature gives $\Delta T \leq 6.1°$ C per inch of wall thickness for the fastest daily change on three-fourths of all calm days. In Ref. 5-3, it was concluded that the six heavy cone members of the telescope should be made from open shapes (not pipes) which reduces the time-lag by a factor of 2.

Table 5-1 shows the various contributions to the rms surface deviation from the best-fit paraboloid of revolution. In detail, we have:

1. Difference between flat plate and paraboloid.

If the paraboloid goes through the three corners of the plate, the plate centers are too high by about 0.709 in. For finding the rms deviation from the best-fit paraboloid, this item must be combined with the next one.

2. Deviation from flatness.

A test has been performed with two rectangular plates, made from 1/8 in aluminum sheets as they come from the mill. After clamping the three sides onto aluminum channels 3/2 in deep, the maximum deviation at the plate center from a plane defined by the three corners was about $\Delta z_m = 0.025$ in for both plates. One plate was welded to the ribs and gave a completely useless deformation after cooling. The other plate was riveted to the ribs and gave a maximum center deviation of 0.032 in (the ribs were straight within 0.005 in). This accuracy is good enough for our purpose, and it was achieved without any selection before, or trimming after, the cutting and riveting. Originally it was decided to specify a maximum deviation of $\Delta z_m = \pm\ 0.050$ in of the plate center from the corner plane. Adding up this item with all other deformations resulted in a $\lambda = 2$ cm telescope. A comparison of all items showed that items 1 and 2 were by far the largest contributions under most observing conditions.

It thus was decided to go one step further, specifying

$$0 \leq z_m \leq 0.120 \text{ in} \qquad (5\text{-}6)$$

which means that one-half of all plates must be turned around before the exact cutting and the riveting. The average $\overline{\Delta z_m}$ then will be about 0.050 in for all plates, and the limits $0.030 \leq z_m \leq 0.075$ shall be adopted. Under this assumption, and adding 0.005 in for the rms difference between the levels of the six leaf springs in Fig. 4-3, as well as adding 0.010 in for the rms amplitude of shorter waves in the plate, one finds that the rms deviation of the riveted plates, from a best fit paraboloid of revolution is

$$\text{rms}\ (\Delta z_p) = 0.014 \text{ in} = 0.356 \text{ mm} \qquad (5\text{-}7)$$

for the combined effect of using flat plates, deviations from flatness and manufacturing tolerance of the adjuster.

3. Sag of plate and ribs.

The center sag of the plate, of side length ℓ and thickness h, was calculated for dead load q (1.70 lb/ft^2) as

$$\Delta z_m = \frac{\ell^4}{162\ E\ h^3} = 0.00722 \text{ in} = 0.184 \text{ mm} \tag{5-8}$$

and the center sag of the rib was found as

$$\Delta z_m = \frac{W\ \ell^3}{E\ I} = 0.00161 \text{ in.} \tag{5-9}$$

Eqs. (5-8) and (5-9) add up linearly to $\Delta z_m = 0.0088$ in.

This calculation is true if gravity is perpendicular to the plate. Actually, the plates sag by different amounts, in proportion to the cosine of the angle between their normal and gravity, and this angle depends on the position of the plate within the surface and on the elevation angle of the telescope. However, the centers of the plates sag in a nearly homologous way; they define a new paraboloid of revolution, with negligible deviations of less than 1/500 of Δz_m. With respect to the sag of all plates, the best-fit paraboloid of revolution is thus defined by the average sag, $\overline{\Delta z}$; it has a parallel translation of $\overline{\Delta z}$, and a change of focal length of $df = -0.53\ \overline{\Delta z}$. Only the deviations (within each plate) from this paraboloid matter.

In general, an integration yields for triangular objects with a constant radius of curvature

$$\text{rms } (\Delta z - \overline{\Delta z}) = 0.193\ \Delta z_m . \tag{5-10}$$

The dead load sag then yields for the riveted plate

$$\text{rms } (\Delta z_p) = 0.193 \times 0.00883 = 0.00171 \text{ in} = 0.043 \text{ mm} \tag{5-11}$$

It should be mentioned that the stiffness for a distributed load on the riveted plate was checked experimentally and was found to be a few percent higher than calculated.

4. Wind on plates and ribs.

With an 18 mph wind the pressure is 0.83 lb/ft^2. A face-on wind then gives a central deformation of

$$\Delta z_m = 0.00409 \text{ in} = 0.104 \text{ mm} \tag{5-12}$$

or, with eq. (5-10)

$$\text{rms } (\Delta z_p) = 0.00079 \text{ in} = 0.020 \text{ mm}. \tag{5-13}$$

If ϕ is the angle between the plate normal and gravity, the combined deformation from gravity and wind is 0.043 cos ϕ + 0.020 sin ϕ, from eqs. (5-11) and (5-13). For a frontal wind direction the maximum total deformation occurs when tau ϕ = 0.020/0.043, and for this worst case both contributions eqs. (5-11) and (5-13) add up quadratically to 0.048 mm. Thus, the worst combination of wind and dead load gives

$$\text{rms } (\Delta z_p) = 0.00189 \text{ in} = 0.048 \text{ mm}. \tag{5-14}$$

5. Sag of panels.

The panel of Fig. 4-1 was investigated with the STRUDL program, including welded joints. The maximum sag, occurring at point 6, is

$$\Delta z_m = 0.028 \text{ in} = 0.711 \text{ mm}, \tag{5-15}$$

the average sag is $\overline{\Delta z}$ = 0.0214 in, and the rms deviation from the average is

$$\text{rms } (\Delta z_p) = 0.00624 \text{ in} = 0.159 \text{ mm}. \tag{5-16}$$

These values are true if gravity is perpendicular to the panel surface. The calculations which were done for the plates are also applied to the panels. A new best-fit paraboloid of revolution is defined by the average panel sag. Within each panel, the deviation from the average eq. (5-16) then is also the deviation from the best-fit paraboloid, if all panels would sag by the same amount under perpendicular gravity. This can easily be achieved by making the smaller central panels less thick than the larger outer panels. The thickness should be in proportion to the square of the size.

6. Wind on panels.

From the STRUDL analysis, we find for an 18 mph face-on wind a maximum deformation at point 6 of

$$\Delta z_m = 0.0070 \text{ in} = 0.178 \text{ mm} \tag{5-17}$$

and the deviation from the average is

$$\text{rms } (\Delta z_p) = 0.00156 \text{ in} = 0.040 \text{ mm.} \tag{5-18}$$

This must be added quadratically to eq. (5-16).

7. External loads on panels.

Since the panel stiffness contributes to the dish stiffness, the panels take up loads which vary with elevation angle. From the stress analysis of the homology program we find loads up to 15 kip with an rms of 7.8 kip. If two holding points are pressed toward each other with 7.8 kip, this load is distributed into two panels. And if the panel of Fig. 4-1 is pressed with 3.9 kip at point 51, the STRUDL analysis yields a maximum deformation (at points 14 and 19) of

$$\Delta z_m = 0.0035 \text{ in} = 0.089 \text{ mm.} \tag{5-19}$$

Since the panels deform differently from each other depending on their external loads, one cannot subtract an average deformation and thus the rms of the deformation itself (from design) is used:

$$\text{rms } (\Delta z) = 0.00149 \text{ in} = 0.038 \text{ mm.} \tag{5-20}$$

8. Standard pipes.

The present structure was iterated with the homology program to

ΔH = 0.003 in. After replacing all calculated bar areas by the closest Steel Manual values, the rms deviation from homology increased to 0.0158 in in one case, and for 0.0095 in in a second case. In order to be on the safe side, the larger

$$\Delta H = 0.0158 \text{ in} = 0.402 \text{ mm}, \tag{5-21}$$

is adopted, for a tilt from zenith to horizon. Further improvement may be possible.

9. Surface adjustment.

Unless a better method is found, a number of about 400 surface points will be used as "key points", measured from the apex with theodolite and tape. The remaining adjustment points will be measured by their deviation from straight lines between these key points.

Some theodolites on the market claim an accuracy of $\pm$ 1 arc sec. For the present estimate, an rms error of $\pm$ 1.5 arc sec is adopted. At the rim of the telescope, this gives Δz = 0.0131 in = 0.333 mm. For the average Δz over the dish, two-thirds of that value is adopted, or Δz = 0.0088 in = 0.222 mm for the rms error of the key points. It is further assumed that the rms measuring error, when going from the key points to the normal points, is 0.20 mm = 0.0079 in. For the normal points then, the rms error adds up to

$$\text{rms } (\Delta z) = 0.0118 \text{ in} = 0.299 \text{ mm} \tag{5-22}$$

10. Wind on whole telescope

In Ref. 5-2, the surface is divided into three equal parts 100 ft apart, with different gusts acting on them. The high-resolution wind statistics shows that the pressure difference, responsible for the non-rigid deformation of a 300-ft telescope, is $0.415/\sqrt{2}$ = 0.294 of the total pressure for winds of 18 mph. Without subtracting a best-fit paraboloid, one obtains

$$\text{rms } (\Delta z) = 0.0135 \text{ in} = 0.343 \text{ mm}. \tag{5-23}$$

11. <u>Thermal deformations</u>.

Thermal deformations are also treated in Ref. 5-2. The deformation of the feed legs gives a negligible gain decrease ($\leq$ 1%) gain decrease, and we can neglect it. The aluminum plates have a floating mount and do not contribute to the deformation. The only strong contribution comes from the cone members:

$$\text{rms } (\Delta z) = 0.0062 \; \Delta T \text{ (inch)} \quad (\Delta T \text{ in } ^\circ\text{C}) \tag{5-24}$$

For sunny calm days ($v < 5$ mph), $\Delta T = 5°$ C, and for all other conditions $\Delta T = 1.5°$ C (wind, ambient air temperature change, nights). Thus

$$\text{rms } (\Delta z) \quad \begin{cases} 0.0310 \text{ in} = 0.788 \text{ mm, sunny and calm;} \\ 0.0093 \text{ in} = 0.236 \text{ mm, other condition.} \end{cases} \tag{5-25}$$

Table 5-1 lists 15 different causes for deformation. They are combined in four groups: First, all items that are independent of observing conditions; second, all items that depend on elevation tilt; third, wind deformations; and fourth, thermal deformations. All four groups give about the same values which shows that the design is close to optimum.

The final summary for the shortest wavelength,

$$\lambda = 16 \times \text{rms } (\Delta z), \tag{5-26}$$

is given in Fig. 5-1 as a function of elevation tilt for winds below 10 mph, and in Fig. 5-2 as a function of wind velocity for 60° zenith distance. From these results it is concluded that the shortest wavelength of observation is

$$\lambda = \begin{cases} 1.5 \text{ cm, on calm sunny days;} \\ 1.0 \text{ cm, for all other times.} \end{cases} \tag{5-27}$$

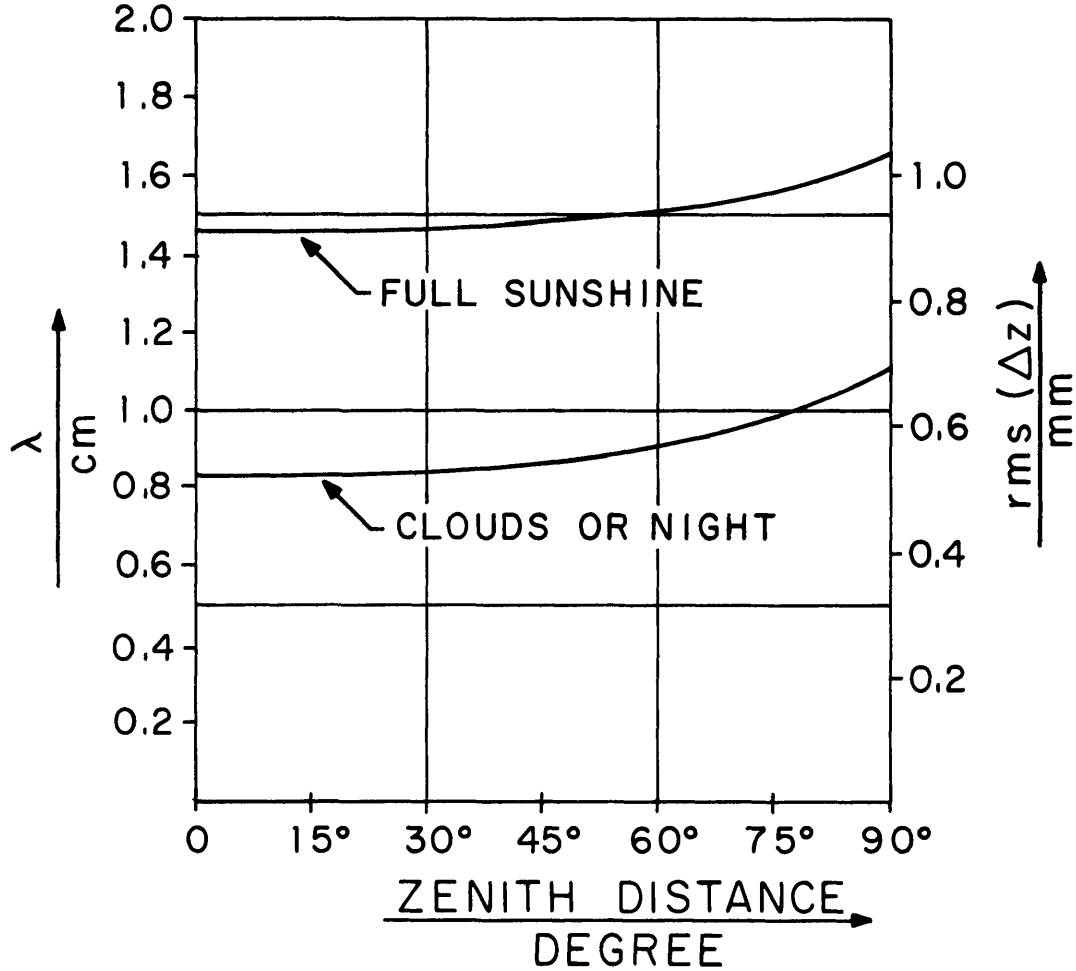

Fig. 5-1. The shortest observational wavelength as a function of elevation tilt for low winds ($\leq$ 10 mph). rms (Δz) = deviation from best-fit paraboloid; λ = 16 x rms (Δz) = shortest wavelength.

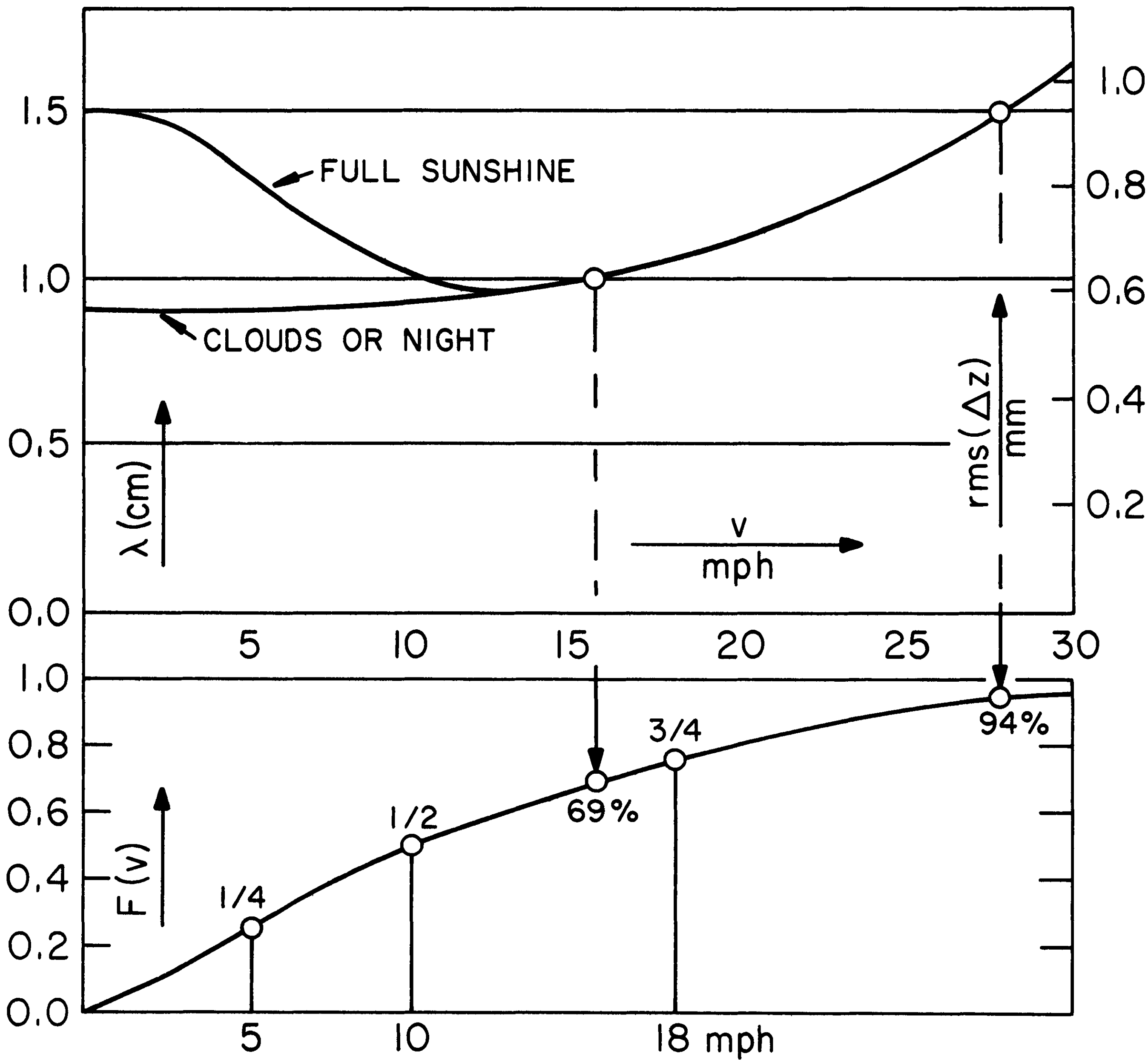

Fig. 5-2. Shortest wavelength λ as a function of wind velocity v, for a zenith distance of $\zeta = 60°$. $F(v) = \int_0^v f(v)dv$ = cumulative wind distribution. For 94% of all time, $\lambda \leq 1.5$ cm; for 69% of all nights, $\lambda \leq 1.0$ cm.

Table 5-1

The rms Surface Deviation

No.	Item	Δz_m mm	rms(Δz) mm	Combined rms(Δz) mm	
1	Parabola/flat plate	1.801	0.356	0.465	Telescope, at zenith, no wind, $\Delta T = 0$.
2	Dev. from flatness	1.270			
3	Shorter bulges	0.254			
4	Adjuster level	0.127			
5	Adjustment accuracy	0.533	0.299		
6	Dev. from homology, ΔH	0.186	0.076	0.437	For tilt of 90°; otherwise $\sim(1-\cos \zeta)$.
7	Use of standard pipes, ΔH	0.912	0.402		
8	Sag of plate	0.184	0.043		
9	Sag of ribs	0.041			
10	Sag of panels	0.711	0.159		
11	Ext. load, panels	0.089	0.038		
12	Wind on plate + ribs	0.104	0.020	0.347	for 18 mph; otherwise $\sim v^2$
13	Wind on panels	0.178	0.040		
14	Wind on telescope		0.343		
15	Thermal def. $\Delta T = 5.0°$ C		0.788	0.788	sunny, calm $\sim\Delta T$
	$\Delta T = 1.5°$ C		0.236	0.236	other condition

12. <u>Further improvement</u>.

The use of small, flat surface plates gives one additional advantage: The surface accuracy may be improved later, making observations down to $\lambda = 5.8$ mm possible during calm nights.

Only two items of Table 5-1 are important during calm nights, (1) the deviation of the actual plate surface from the best-fit paraboloid, and (2) the replacement of the calculated bar areas by standard pipes. Only two trials have been made for item (2). The first gave $\Delta H = 0.402$ mm which was adopted in Table 5-1; a second trial gave $\Delta H = 0.241$ mm, and further trials may also yield more favorable values for the deflection of the surface plates.

Let us therefore assume that a plate deflection of 0.200 mm is achieved in a final design and that a few years from now a better method is developed for measuring the telescope surface, yielding an rms error of 0.2 mm (instead of 0.299 mm). Let us further assume that the rms temperature difference at night is $\Delta T = 1.0°$ C (instead of 1.5° C), which is quite possible. Under these conditions, any improvement of the surface plates becomes highly desirable, and an easy solution is evident. A single aluminum channel can be riveted onto the present ribs across the back side of the plate, and one adjustment screw can be added which changes the distance between the plate center and this channel. With a proper template, the adjustment can be done very fast.

For calculating the remaining rms deviation, it is assumed that the plate ribs do not bend during the adjustment and that any connection between plate edge and plate center is a straight line (the actual shape is more favorable). The plate center should then be adjusted to a level of 1.16 mm $[1 + (r/2f)^2]^{-3/2}$ below the plane defined by the plate corners, where r is the distance of the plate from the focal axis, and f is the focal length. The resulting rms deviation between all surface plates and the best-fit paraboloid of revolution then is calculated to be 0.202 mm. The following values are added quadratically: 0.200 mm for measuring and adjusting the telescope, 0.127 mm for the adjuster level, and 0.157 mm for thermal deformations with $\Delta T = 1.0°$C. Item (7) of Table 5-1 is changed from 0.402 to 0.200 mm, while items (8) through (11) are left unchanged. The total surface deviation then is

$$\text{rms}\ (\Delta z) = \begin{cases} 0.349\ \text{mm, for}\ \zeta = 0,\ \text{or} \\ 0.375\ \text{mm, for}\ \zeta = 60°,\ \text{where}\ \zeta = \text{zenith distance} \end{cases} \tag{5-29}$$

The shortest wavelength of observation becomes

$$\lambda = \begin{cases} 5.6\ \text{mm, for}\ \zeta = 0, \\ 6.0\ \text{mm, for}\ \zeta = 60°,\ \text{if we take}\ \lambda = 16\ \Delta z(\text{rms}). \end{cases} \tag{5-30}$$

This improvement of the plates may be done either during the telescope construction where it can be accomplished with the least expense, or after construction when the improvement can be weighed against actual telescope performance.

D. The Pointing Error

The pointing error is treated in detail in Ref. 5-2. The optical pointing system eliminates the thermal and stow wind deformations between the center of the dish structure and the ground. Furthermore, it eliminates the need for an accurate azimuth tracer.

The servo bandwidth adopted in eq. (5-6) means that deformations slower than 3 sec are eliminated while faster ones still give pointing errors. For the following estimate a sharp cutoff at 3 sec is assumed. (This might be optimistic and for that reason a safety factor of $\sqrt{2}$ was left when the statistics of pressure differences were applied in Ref. 5-2.) Three seconds is a full wavelength of the longest remaining deformation, and so the longest one-sided deformation is of duration

$$\tau = 1.5 \text{ sec.} \tag{5-31}$$

From the NRAO wind measurements one finds that the rms pressure difference between adjacent time averages of duration τ is the fraction

$$P(\tau) = 0.375 \tag{5-32}$$

of the average pressure. Furthermore, gusts of 1.5 sec duration have a size of only 1.5 sec x 18 mph = 40 ft, and a telescope of 300 ft diameter then is hit simultaneously by 57 gusts which are uncorrelated if all longer gusts are estimated. The computer analysis yields the stiffness of dish and towers and the resulting pointing error is entered into Table 5-2.

The contribution of the feed support legs to the thermal pointing error would be rather high (12.6 arc sec for sunshine). It was suggested in Ref. 5-4 to blow ambient air at 56 μ/sec through the chords of the feed legs (4 in diameter pipes), which reduces the temperature difference from 5° C to 2° C for sunshine, and from 1.5° C to 0.6° C for all other times. The resulting pointing errors are shown in Table 5-2. It should be mentioned that the thermal errors that affect the feed legs and, separately, the backup structure tend to give pointing errors of opposite sign.

Table 5-2

Pointing Errors

Source	Item	rms($\Delta\zeta$) arc sec	Combined arc sec
Wind (18 mph)	towers	1.29	2.83
	dish	1.37	
	feed legs + cabin	1.02	
Thermal (sunshine)	backup structure	6.20	6.20
	feed legs	5.02	
Thermal (other)	backup structure	1.86	1.86
	feed legs	1.51	
Instrumental	--		3.2

The instrumental pointing error includes the optical readout, servo drive system, drive units and platform as described in Chapter 4.

The total pointing error is given in Table 5-6 for two conditions: (1) For sunny, calm days where 6.2 arc sec thermal and 3.2 arc sec instrumental pointing errors are added quadratically; (2) for all other times, wind and thermal errors are not added up, since one either has a wind of 18 mph or temperature differences, but not both. Thus, the maximum was taken, adding quadratically 2.83 arc sec from wind and 3.2 arc sec instrumental.

Table 5-3

Total Pointing Error

Condition	rms ($\Delta\phi$) arc sec
Sunny, Calm	7.0
Other	4.3

Finally, the pointing error $\Delta\phi$ is compared with the half-power beam width, $\beta = 1.17\ \lambda/D$. Table 5-4 shows that the ratio between the pointing error and the beam width (≈ 0.17) is slightly better than that for the NRAO 140-ft telescope at 2 cm wavelength, where the relation $\Delta\phi = 0.22\ \beta$ is a tolerable one.

Table 5-4

Wavelength λ, Beam width β, and Pointing error $\Delta\phi$

	λ cm	β arc sec	$\Delta\phi$
Sunny, calm day	1.5	39.6	7.0 arc sec = 0.177 β
Other times	1.0	26.4	4.3 arc sec = 0.163 β

REFERENCES

5-1 von Hoerner, S. 1966, "Statistics of Wind Velocities at Green Bank," Report 16.

5-2 von Hoerner, S. 1969, "Wind and Temperature Deformations of the 300-ft Homologous Telescope," Report 23.

5-3 von Hoerner, S. 1967, "Thermal Deformations of Telescopes," Report 17.

5-4 von Hoerner, S. 1969, "Reducing the Influence of Sunshine by Blowing Ambient Air Through the Feed Support Legs," Report 28.

Chapter 6

COST ESTIMATES AND TIME SCHEDULE

Cost estimates for the various elements of the 300-ft high precision telescope, as described in the previous chapters, are summarized in Table 6-1. All costs necessary for a complete antenna are included. The estimates are in 1969 dollars and do not include any price escalation.

Estimates of cost have been arrived at (1) by approaching firms qualified to perform portions of the work and securing estimates on this portion, (2) by securing current prices on manufactured items, such as gear boxes, gears, axles, bearings, and motors and controls, (3) from prices previously experienced on similar items with escalation to current date, and (4) by estimates prepared by experienced engineers and estimators. All estimates are believed to be accurate to within $\pm$ 10%. Some contingency should be provided, however, to allow for the uncertainties of the estimates, incompleteness of the detail design, and vagaries of the market at the time of procurement. This is provided at a rate of 10% on the whole project, as shown in Table 6-1. The estimate further assumes the site for the instrument to be at Green Bank, West Virginia. No amount is provided for site procurement, access roads, and major power line extension to the site, as these are all available at Green Bank. Price escalation should be anticipated when funding is available.

An estimated time schedule for design and construction is shown in Fig. 6-1. As seen from the schedule, total time for completion is estimated to be about four and one-half years from the time funding is available.

An estimated commitment schedule, based on the above cost and time estimates, is shown in Table 6-2.

Operation of the completed antenna at Green Bank is expected to increase NRAO operating costs by an estimated $250,000 per year initially. The estimated operating costs are relatively small because the various support facilities and equipment already exist at Green Bank and would require little or no expansion by the addition of another large antenna.

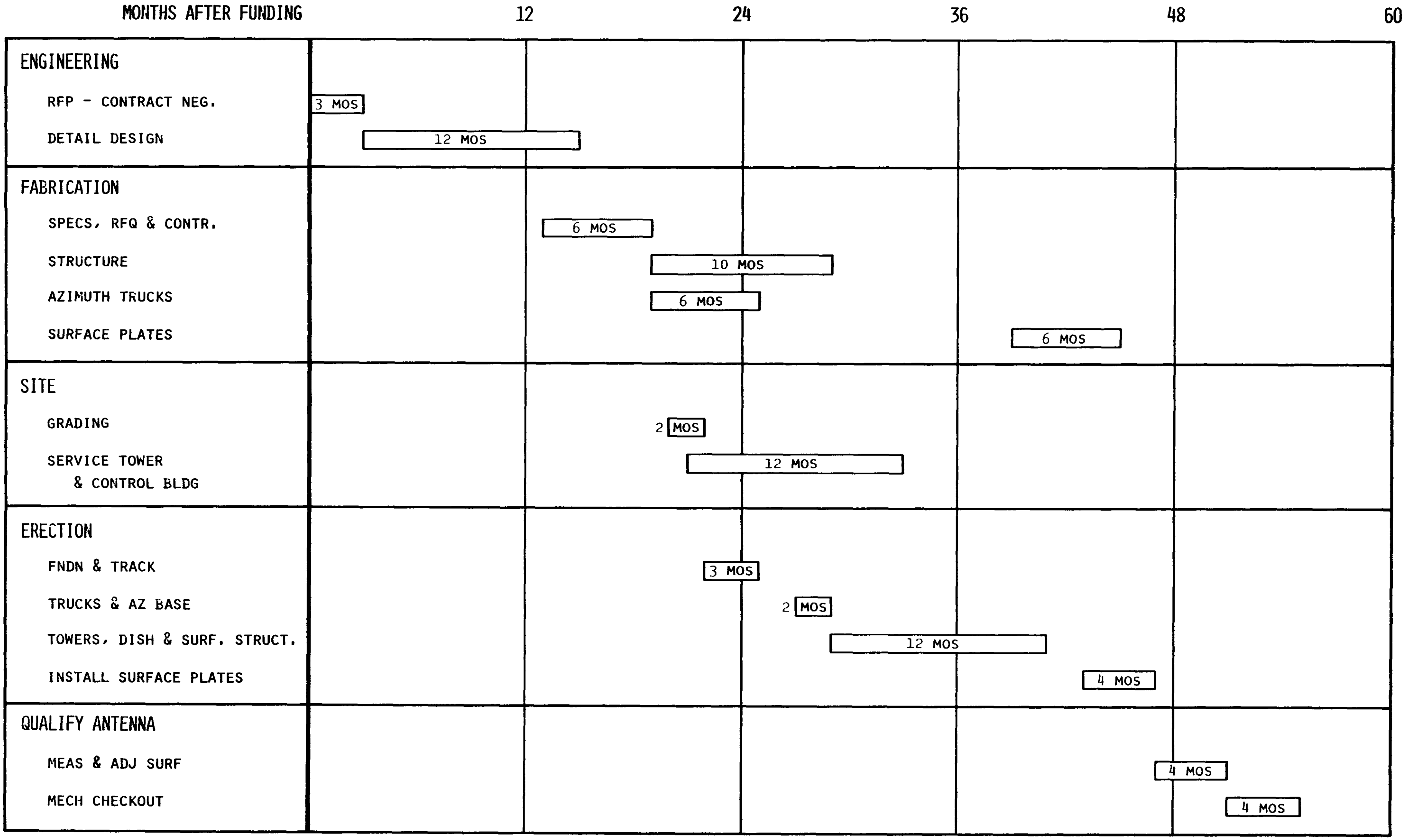

Fig. 6-1. Design and construction schedule, 300-ft high-precision telescope.

Table 6-1

Cost Estimates
(1969 Dollars)

May 16, 1969

	k$	
Reflector and tower structure	4,140	
Surface panels	700	
Azimuth trucks	300	
Pintle bearing	60	
Elevation bearings	100	
Elevation gear and gear trains	190	
Foundation and track	120	
Feed mount	50	
Optical position reference system	350	
Control system (servo)	300	
Control computer	100	
Total basic telescope construction		6,410
Telescope cabling (including snubbers)	100	
Service tower	110	
Building (3000 ft^2)	120	
Power	75	
Water; Sewer	30	
Site preparation	35	
Total ancillaries		470
Adjusting surface panels	150	
Engineering (20,000 man hours)	300	
Computer analysis	100	
Startup, checkout, test, etc.	100	
Total engineering		650
Total complete telescope		7,530
10% contingency		750
GRAND TOTAL		8,280

Table 6-2

Commitment Schedule
(less escalation)

Year	Commitment (millions)
1	$0.450
2	7.100
3	0.455
4	-0-
5	0.275
	$8.280

Chapter 7

COST AND PERFORMANCE FOR VARIOUS TELESCOPE DIAMETERS

A scaling method based on the proposed 300-ft design and which leaves the survival stability constant for all diameters D has been derived. All items of Cost C, surface deformation Δz, and pointing error $\Delta\theta$ have been investigated in order to find with which power of D they increase.

Since it turns out that the cost per telescope area increases only very slowly with D, while the cost per observable radio source even decreases somewhat, the present 300-ft design may serve as a model for future larger telescopes.

A. Method of Scaling

Many single bars of the present design come close to their stability limit in survival conditions and the scaling of bar areas should be done in such a way that the survival stability stays constant.

1. Telescope structure

$$\begin{aligned} \Lambda &= \ell/r = \text{slenderness ratio of single pipe;} \\ S_\Lambda &= \text{maximum allowed stress;} \\ S_s &= \text{stress from survival loads;} \\ S_g &= \text{stress from dead loads;} \\ k &= S_g/S_s; \end{aligned} \tag{7-1}$$

and

$$\begin{aligned} Q &= (S_s + S_g)/S_\Lambda = (1 + k)\, S_s/S_\Lambda = \text{stress ratio;} \\ d &= D/300 \text{ ft} = \text{scaling factor.} \end{aligned} \tag{7-2}$$

The bar areas then shall be scaled according to

$$A \sim D^\alpha \tag{7-3}$$

and that

$$Q = \text{constant} \tag{7-4}$$

A-1 bars shall be standard steel pipes, whose $r \sim A^{2/3}$ yields a good fit to the tables of the Steel Manual, thus

$$\Lambda \sim D/A^{2/3} \sim D^{1-2\alpha/3} \tag{7-5}$$

An inspection of the 300-ft design shows that all bars with $Q \geq 0.70$ have $\Lambda \geq 100$, where $S_\Lambda \sim \Lambda^{-2}$; thus

$$S_\Lambda \sim D^{(4\alpha/3)-2} \ . \tag{7-6}$$

Furthermore, since the survival forces go with D^2,

$$S_s \sim D^2/A \sim D^{2-\alpha}; \tag{7-7}$$

and since the dead load goes with $W \sim AD$,

$$S_g \sim W/A \sim D \ . \tag{7-8}$$

The demand of Q = constant then yields

$$(1 + k\, d^{\alpha-1})d^{4-7\alpha/3} = 1 + k, \tag{7-9}$$

and for $d \approx 1$ finally

$$\alpha = \frac{12 + 9k}{7 + 4k} \ . \tag{7-10}$$

Inspection of the 300-ft design shows that all bars with $Q \geq 0.70$ have $0.20 \leq k \leq 0.35$, yielding $1.769 \leq \alpha \leq 1.803$. The following value then is adopted:

$$\alpha = 1.80 \text{ for all telescope bars.} \tag{7-11}$$

2. Tower Structure

The highest stresses in the tower members are due to lateral survival loads (85 mph wind), where $F \sim D^2$. The main chords are very heavy, $\Lambda \leq 40$, where S_Λ increases only slowly with decreasing Λ. For simplicity S_Λ = const. is used. The demand Q = const then leads to

$$A \sim D \text{ for all tower bars.} \tag{7-12}$$

3. <u>Other items</u>.

It is decided to use the same type of surface plates for all D, but to vary the length ℓ of the plates as $\ell \sim D$, which means keeping a constant number of plates.

Drive motors, gears and bearings are scaled in proportion to the weight above them, and the cost of foundations and tracks, service tower and cables is scaled in proportion to D.

The console system, optical pointing system, computer, feed mount, building, site development, and engineering are items which are assumed to be independent of D.

B. <u>Application to Various Diameters</u>

1. <u>The cost</u>.

All items of the cost estimate are listed in Table 7-1, with the power γ of D as used for the scaling.

Table 7-2 contains the different groups of γ, with their 300-ft cost. The resulting costs for varwous D are given in Table 7-4, together with the shortest wavelength and the pointing error. All results are plotted in Figs. 7-1 and 7-2. A contingency of 10% is always included in the cost.

The cost/lb of steel is kept constant in the scaling. The cost/lb of the erection goes up with increasing D because all parts must be lifted to greater height, but the cost/lb of the manufacturing decreases because the number of single pieces stays constant while their weight increases with $D^{2.8}$ for the dish and D^3 for the towers. Manufacturing is much more expensive than erection, and both effects will about cancel.

Table 7-2

Price Groups Regarding γ, from Table 7-1

γ	300-ft price M$
3.0	1.52
2.9	0.46
2.8	2.75
2.0	0.84
1.0	0.33
0	1.63
Total	7.53

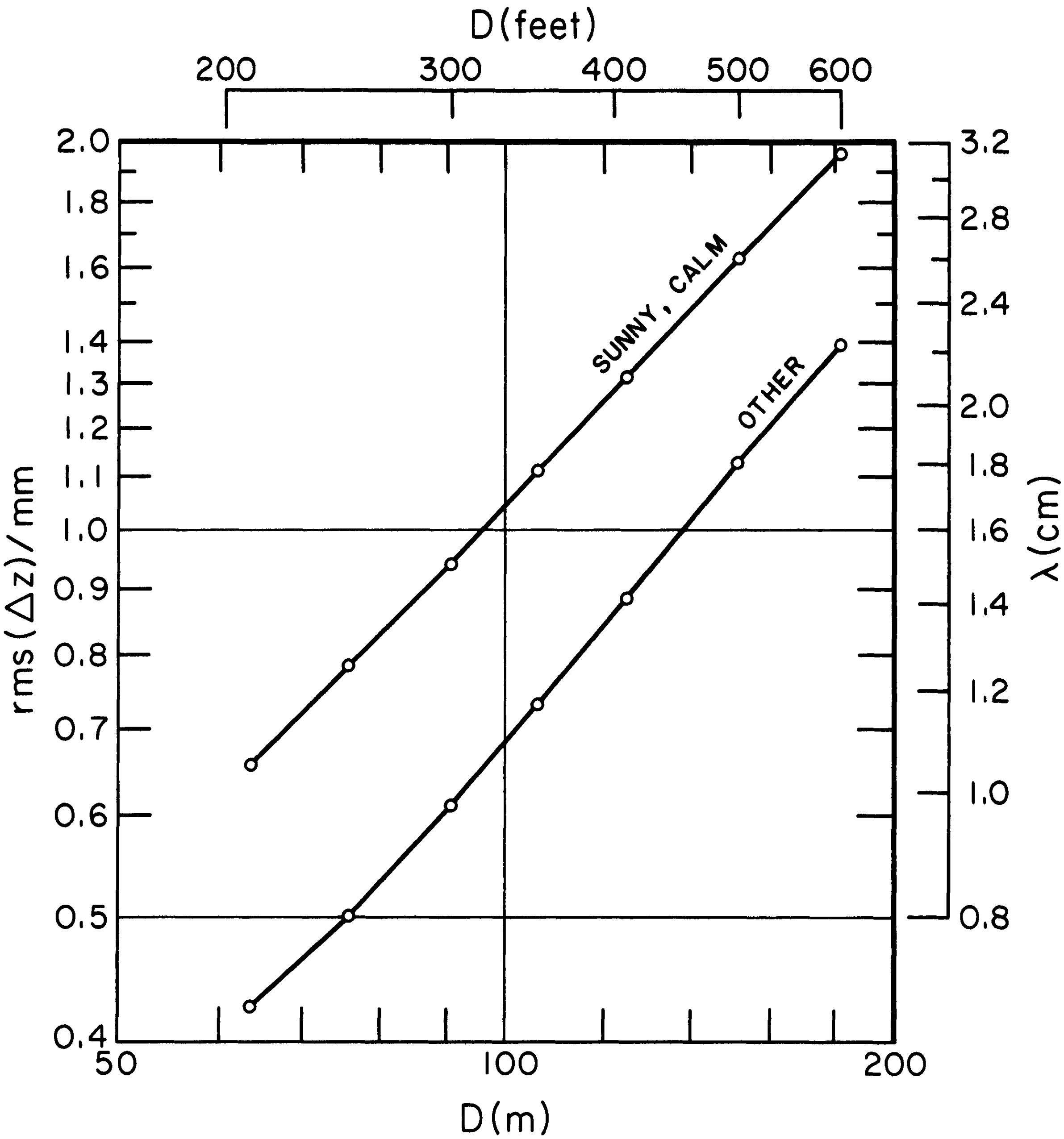

Fig. 7-1. Shortest wavelength λ as function of diameter D. λ = 16 rms (Δz). Δz = surface deviation from best-fit paraboloid.

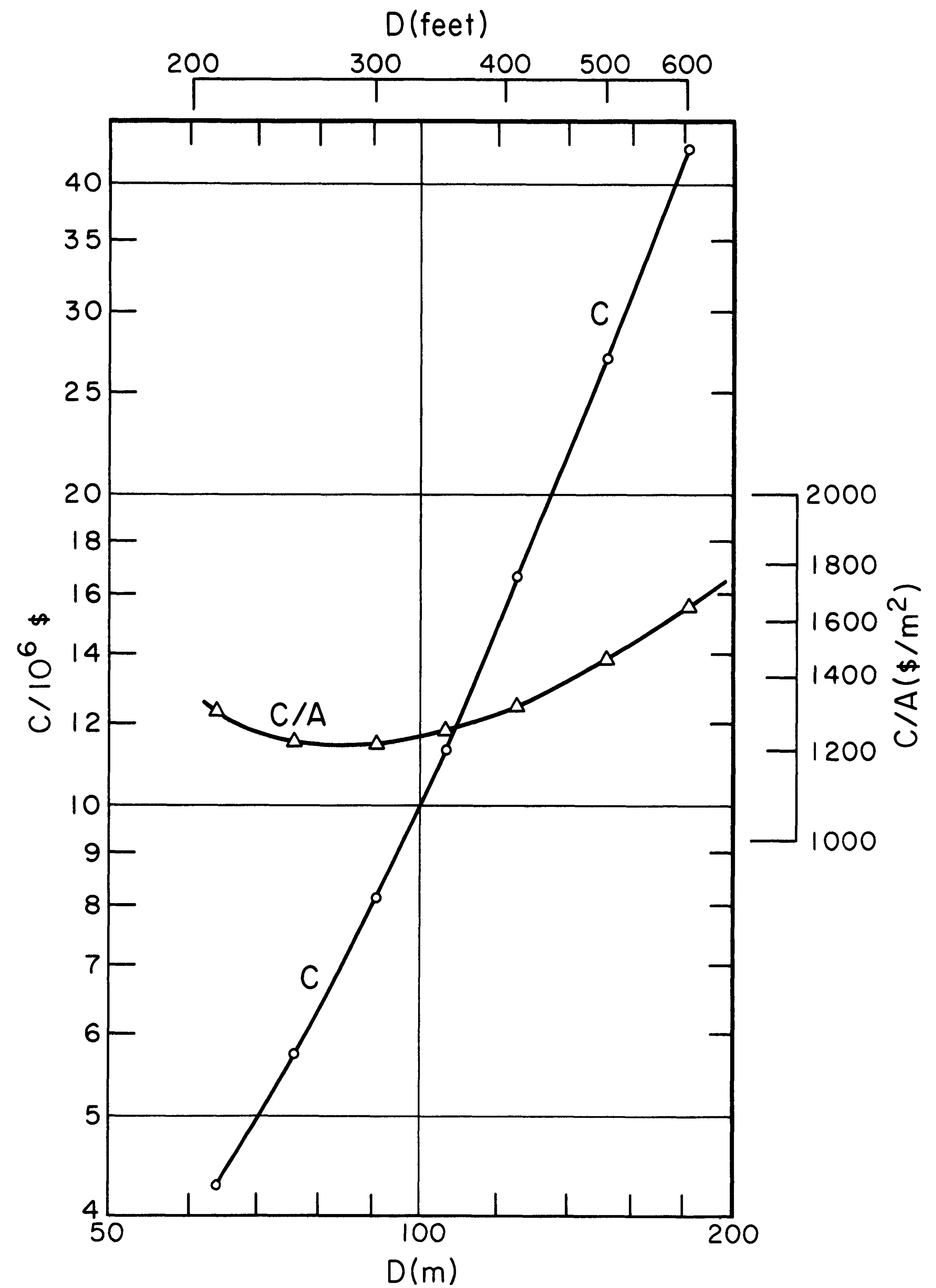

Fig. 7-2. Cost C, and cost per area C/A, as functions of telescope diameter D.

Table 7-1

Scaling the Price (γ defined by $P \sim D^{\gamma}$)

Item	300-ft price M$	Subtotals M$	γ
Aluminum surface, studs	0.70		2.0
Dish structure	2.62		2.8
Tower structure	1.52		3.0
Track assemblies	0.30		2.9
Foundations + tracks	0.12		1.0
Elevation bearings	0.10		2.8
Pintle bearing	0.06		2.0
Elevation gear	0.03		2.8
Azimuth gear	0.16		2.9
Feed mount	0.05		0
Surface adjustment	0.15		0
		5.81	
Optical pointing (7 beacons, platform, encoders, servo)	0.35		0
Drive system (amplifiers, console)	0.30		0
Computer	0.10		0
		0.75	
Cabling, catwalks, small items	0.10		1.0
Service tower	0.11		1.0
		0.21	
Building (3000 ft^2)	0.12		0
Power + transformer	0.08		1
Water, sewer, road	0.03		0
Site preparation	0.03		0
Engineering	0.50		0
		0.76	
Total		7.53	
Add 10% contingency		8.28	

2. The shortest wavelength

All gravitational deformations are proportional to D^2, and all thermal deformations are proportional to D, and both are independent of the bar areas A. If the size of the surface plates is scaled as $\ell \sim D$, then the first three items of Table 7-3 vary in proportion to D. If the adjustment is done with constant angular accuracy, then the linear accuracy is also in proportion to D.

The wind force goes with D^2, and the wind deformation thus with D^2/A. Since $A \sim D^{1.8}$ for the dish, the wind deformation is

$$\Delta z \sim D^{1.2} \tag{7-13}$$

Table 7-3

Scaling of the rms Surface Deviation from the Best-fit Paraboloid
(γ defined by rms $(\Delta z) \sim D^{\gamma}$)

	300-ft rms (Δz) mm	γ
Parabola/flat plate Dev. from flatness Shorter bulges Adjustment accuracy	0.447	1.0
Adjuster level	0.127	0
Dev. from homology, ΔH Use of standard pipes Sag of plates Sag of ribs Sag of panels Ext. load, panels	0.219	2.0
Wind on plate + ribs Wind on panels Wind on telescope structure	0.241	1.2
Thermal def. $\Delta T = 5.0°$ C	0.788	1.0
Thermal def. $\Delta T = 1.5°$ C	0.236	1.0

Table 7-3 shows all items considered from Table 5-1. For all gravitational deformations, it is assumed that the telescope is adjusted at zenith and then tilted down by 60°. For the wind deformations, v = 15 mph is used; the wind is below this value for two-thirds of all time at Green Bank. The results of the scaling are shown in Table 7-4 and Fig. 7-1.

3. <u>The pointing error</u>.

The thermal pointing error is independent of D and A. The instrumental pointing error (including optical reading, servo and drive system) amounts to 3.2 arc sec for the present design and is also independent of D and A.

Table 7-4

Cost and Performance for Various Diameters D

λ = 16 x rms (Δz) = shortest wavelength
β = 1.17 λ/D = half-power beam width;
$\Delta\theta$ = pointing error

D Ft	M$	C/Area $/ft^2	Sunny, calm days			All other times		
			λ cm	β arc sec	$\Delta\theta$ arc sec	λ cm	β arc sec	$\Delta\theta$ arc sec
210	4.28	123.4	1.05	44.5	6.98	0.68	25.7	4.0
250	5.71	115.8	1.25	42.8	"	0.80	25.4	4.1
300	8.14	115.0	1.50	42.3	"	0.98	25.9	4.3
350	11.41	118.1	1.77	41.9	"	1.17	26.5	4.4
410	16.51	195.0	2.10	41.7	"	1.42	27.4	4.6
500	27.21	137.9	2.60	41.6	"	1.80	28.7	4.7
600	43.80	154.9	3.15	41.7	"	2.22	30.0	4.9

The wind-induced pointing error depends on τ, the duration of the longest (one-sided) wind deformation which is not omitted by the optical pointing system. For D = 300 ft, τ = 1.5 sec. In general, with stiffness K $\sim$ A/D and weight W $\sim$ DA,

$$\tau \sim \sqrt{W/K} \sim D. \quad (7\text{-}14)$$

The wind-induced pointing error is treated as in Chapter 5, § D, using $v = 18$ mph. The three contributions of Table 5-2 are scaled as follows:

$$\text{towers,} \quad \Delta\theta \sim P(\tau) \; ; \tag{7-15}$$

$$\text{dish,} \quad \Delta\theta \sim D^{0.2} \, P(D/v) \, P(\tau) \; ; \tag{7-16}$$

$$\text{feed structure,} \quad \Delta\theta = \text{const.} \tag{7-17}$$

The errors from towers and dish are added linearly, and the sum is added quadratically to the error from the feed structure. The resulting wind-induced pointing error ranges from 2.5 arc sec for D = 210-ft, over 2.8 arc sec for 300 ft, to 3.7 arc sec for 600 ft. It is always larger than the thermal one (1.9 arc sec) for nights and windy days. Since both do not occur simultaneously, only the wind-induced error is taken into account. It is added quadratically to the instrumental error of 3.2 arc sec. The result is shown in the last column of Table 7-4. This pointing error is almost a constant fraction of the beam width for all D considered:

$$\Delta\theta = (0.160 \pm 0.003 \text{ max}) \, \beta. \tag{7-18}$$

Actually, the wind induced pointing errors from towers and dish have small time scales ($\leq \tau$) and are averaged out for long integration times. The remaining constant error from the feed structure (1.0 arc sec) is then smaller than the thermal error, thus only the thermal one (1.9) is added quadratically to the instrumental error (3.2 arc sec), resulting in

$$\Delta\theta = 3.70 \text{ arc sec, for all D.} \tag{7-19}$$

C. The Number of Observable Sources.

One of several ways of measuring the efficiency of a radio telescope is to calculate the number of observable radio sources and to compare it with the cost of the telescope. If a telescope observes about 80% of the total sky, which is about 10 steradian, then the total number of observable sources is $n = 10$ N.

Table 7-5 shows the results. The last two columns give the relative cost, in dollars per source, which is also plotted in Fig. 7-3. The curve C/n_2 moves up again for larger diameters, because of a beginning resolution limit which effects n_2 earlier than n_m.

Table 7-5

The Number of Observable Radio Sources and the Cost Per Source

n_m = maximum number of observable sources

n_2 = number of sources, observable through factor 2 in wavelength

D	R_m	n_2	C/n_m	C/n_2
feet	10^5	10^5	$/source	$/source
210	2.50	2.1	17.2	20.4
250	3.8	3.1	15.0	18.4
300	6.1	5.0	13.2	16.3
350	9.2	7.6	12.4	15.0
410	13.8	11.3	12.0	14.6
500	23.2	18.2	11.7	14.9
600	37.6	23.0	11.6	19.0

D. Discussion

The scaling is done in a way that the survival stability is not changed. Fig. 7-1 shows that the shortest wavelength then increases about as

$$\lambda \sim D^{1.15} \qquad (7\text{-}20)$$

and the cost increases about as

$$P \sim D^{2.34} \qquad (7\text{-}21)$$

for $250 \leq D \leq 600$ ft.

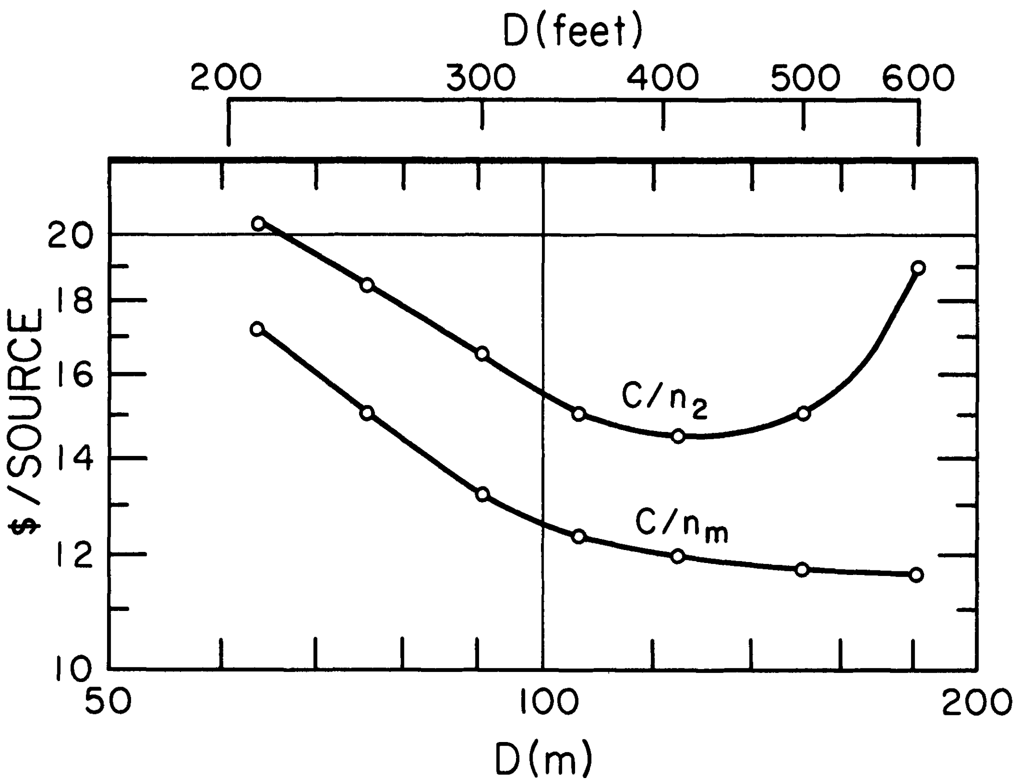

Fig. 7-3. Cost per observable radio source, as a function of telescope diameter, n_m = maximum number of observable sources; n_2 = number of sources, observable through a factor 2 in wavelength.

The economy of the telescopes can be measured in two ways. First, Fig. 7-2 shows that the cost per telescope area, in dollars per unit area stays almost constant for $D \leq 400$ ft and increases only very slowly for larger diameters. For the whole range of $210 \leq D \leq 600$ ft,

$$C/A = \text{const.} \pm 15\% \text{ max.} \tag{7-22}$$

This means that a large homologous telescope is almost as economical as a small one, regarding the cost per area.

Second, Fig. 7-3 shows that a large homologous telescope (at least up to 500 ft) is even slightly more economical than a small one, regarding the cost per observable radio source.

Both these results together then mean that an actually built 300-ft telescope, although extremely useful in itself, may well be considered as a model for future much larger telescopes.